

## Vehicle-to-Grid for Reliable Frequency Regulation

Présentée le 3 juin 2022

Collège du management de la technologie  
Chaire analyse de risque et optimisation  
Programme doctoral en management de la technologie

pour l'obtention du grade de Docteur ès Sciences

par

**Dirk LAUINGER**

Acceptée sur proposition du jury

Prof. T. A. Weber, président du jury  
Prof. D. Kuhn, Dr F. R. Vuille, directeurs de thèse  
Prof. A. Sun, rapporteur  
Prof. D. Wozabal, rapporteur  
Prof. C. Jones, rapporteur



Plans based on average assumptions are wrong on average.  
— Sam L. Savage, *The Flaw of Averages*, 2009.

Für meine Eltern, für Nils, and to 菲菲 ...

# Acknowledgements

Electric vehicles and electric power grids are complex technical, economic and legal systems. Throughout my PhD, my advisors Daniel Kuhn and François Vuille have given me the freedom to explore the diverse facets of these systems and guided me in translating their most important characteristics into mathematical optimization problems. Daniel has shown me how to achieve simplicity in research and teaching. François has taught me to engage with stakeholders outside academia's ivory tower. I am intensely grateful.

The Institut VEDECOM not only funded my thesis but also provided me with many thought-provoking questions. I am particularly thankful to François Colet, Nadège Faul, Wilco Burghout, Emilia Suomalainen, and Jaâfar Berrada.

I thank my jury members Andy Sun, David Wozabal, Colin Jones and president Thomas Weber, who have carefully read and discussed my thesis.

I also thank the Master students with whom I had the chance to collaborate: Samuel Majerus, Fernando Aguilar, Yann Martinson, Nikolai Orgland, Jangwon Park, and Diane Remmy.

Thanks to my advisors from EPFL and VEDECOM, I was able to meet Willett Kempton, Yannick Perez, Paul Codani, Olivier Borne, Andrew Thompson, Evangelos Vrettos, Damien Sainflou and David Allard, whom I thank for intriguing and insightful discussions. Anna Demeo, Mike Jacobs, Willy Osborn, Paul Pimentel, Dan Doyle, Warren Adams, Richard Andre, and Angie Grant have helped me understand the electricity and mobility system on the Vineyard.

Gretchen Bakke's book "*The Grid: The Fraying Wires between Americans and our Energy Future*" has inspired me to view electric power grids as technical and cultural systems; so did my Master's program in *Energy Management and Sustainability*, which was created by Maher Kayal and Franco Vigliotti. Through this program, I was able to intern with a public works and services department in the UAE, to follow a minor in area and cultural studies, and to pursue a self-directed Master's project on the optimization of residential energy systems under the guidance of Jan Van herle, Daniel Kuhn, and Priscilla Caliandro, which laid the basis for my PhD thesis. Daniel Müller has encouraged me to reflect on the role of infrastructures in the material and energy turnover of contemporary and possible future societies.

My colleagues Napat, Soroosh, Çağıl, Viet, Kilian, Trevor, Bahar, Tobias, Wouter, Yves, Mengmeng, Tianshu, Roland, Yann, Florian, Piero, Michaël and Vincent have filled my work days with joy and laughter. I remember Kilian for his talent to find the right words for any occasion.

## Acknowledgements

---

Trevor helped me navigate everyday PhD life. Bahar has been my confidant and shared the ups and downs of teaching with me. Mengmeng and Tianshu translated the abstract of my thesis into Mandarin. Rachel m'impressionne avec son énergie, sa discipline et sa résilience. Yara has helped me analyze how teaching duties are distributed among PhD students.

The administrative assistants Amandine, Carole and Anne-Sandra as well as the doctoral school, Céline and Mélody, guided me through the formal steps of the PhD.

At home, my colocs Manu, Michele, Alex, Amandine, Laura and my neighbors Greg and Dori made sure that I was never lonely. Avec Manu, j'ai développé une amitié profonde autour des longues discussions de tout et de rien, des projets d'apiculture et de jardinage, rendus possibles par la famille D'Agostino, et des projets un peu fou, comme le SwissTrainChallenge. My friends Justin, Wiebke, Alessandro, Peter, Thomas, Firmin, Priscilla, Manuel, Giorgio and Cecilia were there when I needed a break from or a discussion about the ups and downs of PhD life. Ho incontrato Wiebke and Alessandro à travers la Schweizerische Studienstiftung, which supported me throughout my studies in widening my personal and intellectual horizon. Nichts von alldem wäre ohne die ständige Unterstützung meiner Familie möglich gewesen. Nur dank dieser Geborgenheit bin ich überhaupt erst soweit gekommen einen PhD anzufangen und nur dank ihr konnte ich ihn zu Ende bringen. Ganz besonders danke ich also meinen Eltern und Nils, meinem Bruder.

Finally, I thank Michelle for all her love and for encouraging me to follow my own path without losing myself. Together, we have crossed two PhDs. I look forward to the next chapter.

*Morges, 14 February 2022*

Dirk Lauinger

# Abstract

Future low-carbon societies will need to store vast amounts of electricity to stabilize electricity grids and to power electric vehicles. Vehicle-to-grid allows vehicle owners and grid operators to share the costs of electricity storage by making the batteries of electric vehicles available to the grid. In practice, vehicle owners decide when to reserve their cars for driving and when to make them available for grid services. Vehicle aggregators then decide how to commit the vehicles to grid services.

For vehicle-to-grid to succeed, both vehicle owners and grid operators must be able to trust aggregators, *i.e.*, vehicles should be available for driving and for grid services when the aggregators promise they will be. In this thesis, we solve a decision-making problem that ensures reliable commitments by vehicle aggregators for a particular grid service known as primary frequency regulation, considered one of the most profitable applications of vehicle-to-grid. Mathematically, we first formulate a robust optimization problem with functional uncertainties that maximizes the expected profit from selling primary frequency regulation to grid operators and guarantees that vehicle owners can meet their market commitments for all frequency deviation trajectories in an uncertainty set that encodes applicable European Union regulations. Functional uncertainties ensure that vehicle owners and grid operators can trust the decisions of aggregators at all times. Faithfully modeling the energy conversion losses during battery charging and discharging renders the optimization problem nonconvex. By exploiting a total unimodularity property of the proposed uncertainty sets and an exact linear decision rule reformulation, we prove that the nonconvex robust optimization problem with functional uncertainties is equivalent to a tractable linear program. Somewhat counterintuitively, the underlying deterministic problem for a known frequency deviation trajectory does not reduce to a linear program but results in a large-scale mixed-integer linear program, even if time is discretized. We believe that we have thus discovered the first practically interesting class of optimization problems that become dramatically easier through robustification.

Through extensive numerical experiments using real-world data, we quantify the economic value of vehicle-to-grid and elucidate the financial incentives of vehicle owners, aggregators, equipment manufacturers, and regulators. In particular, we find that the prevailing penalties for non-delivery of promised regulation power are too low to incentivize aggregators to honor their promises toward grid operators.

## Abstract

---

For general electricity storage devices, we then solve a simplified version of the decision-making problem analytically to understand how the optimal frequency regulation commitments depend on the roundtrip efficiency of the storage device, the dispersion of the frequency deviations, and the EU delivery guarantee. We show how the marginal cost of frequency regulation decreases with roundtrip efficiency and increases with frequency deviation dispersion. For energy-constrained storage devices, we find that the profits from frequency regulation are inversely proportional to the length of time for which storage operators commit regulation power. Establishing an intra-day market for frequency regulation would thus make electricity storage devices more competitive with other regulation providers, such as thermal power plants.

**Keywords:** Vehicle-to-Grid, Frequency Regulation, Electricity Storage, Electricity Markets, Energy Economics, Robust Optimization, Functional Uncertainties, Operations Research.

# Vehicle-to-Grid pour un réglage fréquence fiable

Les futures sociétés à bas taux de carbone devront pouvoir stocker des quantités importantes d'électricité pour équilibrer les réseaux électriques et pour alimenter les véhicules électriques. La technologie *vehicle-to-grid* permet aux propriétaires de véhicules électriques et aux gestionnaires de réseaux de partager les coûts de stockage de l'électricité en mettant les batteries de ces véhicules à disposition pour les besoins de stockage du réseau. En pratique, les propriétaires de véhicules planifient les créneaux horaires pour lesquels leur voiture peut-être à disposition du réseau. Les agrégateurs de véhicules électriques décident ensuite comment engager ces véhicules pour les services de réseau.

Le *vehicle-to-grid* aura du succès uniquement si les propriétaires de véhicules et les gestionnaires de réseaux peuvent faire confiance aux agrégateurs, à savoir que les véhicules doivent pouvoir être disponibles pour la mobilité d'une part et pour les services de réseau d'autre part quand les agrégateurs le promettent. Dans cette thèse de doctorat, nous résolvons un problème de prise de décision qui garantit des engagements fiables de la part des agrégateurs pour le service réseau connu sous le nom de « réglage fréquence primaire », considéré comme l'une des applications les plus favorables du *vehicle-to-grid*. Mathématiquement, nous formulons d'abord un problème d'optimisation robuste avec des incertitudes fonctionnelles qui maximise le bénéfice attendu de la vente du réglage primaire aux opérateurs de réseau tout en garantissant que les propriétaires de véhicules peuvent respecter leurs engagements de marché pour toutes les trajectoires de déviation de fréquence dans un ensemble d'incertitudes qui correspond aux réglementations applicables de l'Union européenne. Les incertitudes fonctionnelles garantissent que les propriétaires de véhicules et les gestionnaires de réseau peuvent faire confiance aux décisions des agrégateurs à tout moment. La modélisation fidèle des pertes de conversion d'énergie lors des cycles de charge et de décharge des batteries rend le problème d'optimisation non-convexe. En exploitant une propriété d'unimodularité totale de l'ensemble d'incertitudes proposé et une reformulation exacte par une règle de décision linéaire, nous prouvons que le problème d'optimisation robuste non-convexe avec des incertitudes fonctionnelles est équivalent à un programme linéaire efficacement soluble. De manière un peu contre-intuitive, le problème déterministe sous-jacent pour une trajectoire de déviation de fréquence connue ne se réduit pas à un programme linéaire mais plutôt à un programme linéaire mixte en nombres entiers à grande échelle, même si le temps est



discrétisé. Nous pensons avoir ainsi découvert la première classe de problèmes d'optimisation intéressants sur le plan pratique qui deviennent considérablement plus faciles à résoudre grâce à une robustification.

Basé sur des expériences numériques approfondies utilisant des données du monde réel, nous quantifions la valeur économique du vehicle-to-grid et discutons les incitations économiques des propriétaires de véhicules, des agrégateurs, des fabricants d'équipements et des régulateurs. En particulier, nous constatons que les pénalités en vigueur dans l'UE pour la non-livraison de la puissance de réglage promise sont trop faibles pour inciter les agrégateurs à honorer leurs promesses envers les gestionnaires de réseaux.

Pour des dispositifs généraux de stockage d'électricité, nous résolvons ensuite une version simplifiée du problème de décision de manière analytique afin de comprendre comment les engagements optimaux de réglage de fréquence dépendent du rendement du dispositif de stockage, de la dispersion des déviations de fréquence et de la garantie de livraison de l'Union européenne. Nous montrons comment le coût marginal du réglage de fréquence diminue avec le rendement et augmente avec la dispersion des déviations de fréquence. Pour les dispositifs de stockage limités par leur capacité à stocker de l'énergie, nous constatons que les bénéfices du réglage de fréquence sont inversement proportionnels à la durée pour laquelle la puissance de réglage doit être engagée. L'établissement d'un marché intra-journalier pour le réglage de fréquence rendrait donc les dispositifs de stockage d'électricité plus compétitifs par rapport aux autres fournisseurs, tels que les centrales thermiques.

**Mots-clés :** Vehicle-to-Grid, Réglage fréquence, Marché de l'électricité, Stockage d'électricité, Economie de l'énergie, Optimisation robuste, Incertitudes fonctionnelles, Recherche opérationnelle.

# Vehicle-to-Grid zur zuverlässigen Frequenzregelung

Künftige, kohlenstoffarme Gesellschaften werden grosse Mengen Strom speichern müssen, um Stromnetze zu stabilisieren und um Elektrofahrzeuge anzutreiben. Vehicle-to-Grid ermöglicht es Fahrzeugbesitzern und Netzbetreibern die Kosten der Stromspeicherung zu teilen, indem Batterien von Elektrofahrzeugen den Netzen zur Verfügung gestellt werden. In der Praxis entscheiden die Fahrzeugbesitzer, wann sie ihre Autos für Fahrten reservieren und wann sie sie für Netzdienstleistungen zur Verfügung stellen. Fahrzeug-Aggregatoren entscheiden dann, wie sie die Fahrzeuge für Netzdienstleistungen einsetzen.

Damit Vehicle-to-Grid erfolgreich ist, müssen sowohl die Fahrzeugbesitzer als auch die Netzbetreiber den Aggregatoren vertrauen können. Das heißt, die Fahrzeuge sollten zum Fahren und für Netzdienste zur Verfügung stehen, wenn die Aggregatoren dies versprechen. In dieser Dissertation lösen wir ein Entscheidungsproblem, das sicherstellt, dass Zusagen von Fahrzeug-Aggregatoren für eine bestimmte Netzdienstleistung, die Primärregelleistung, verlässlich sind. Diese gilt als eine der profitabelsten Anwendungen von Vehicle-to-Grid. Mathematisch formulieren wir zunächst ein robustes Optimierungsproblem mit funktionalen Unsicherheiten, das den zu erwartenden Gewinn aus dem Verkauf primärer Regelleistung an Netzbetreiber maximiert. Damit können Fahrzeugbesitzer ihre Marktverpflichtungen für alle Frequenzabweichungs-Trajektorien in einer Unsicherheitsmenge erfüllen, welche den geltenden Vorschriften der Europäischen Union entspricht. Funktionale Unsicherheiten stellen sicher, dass Fahrzeugeigentümer und Netzbetreiber den Entscheidungen der Aggregatoren zu jeder Zeit vertrauen können. Die getreue Modellierung der Energieumwandlungsverluste während des Ladens und Entladens der Batterien führt zu einem nichtkonvexen Optimierungsproblem. Unter Ausnutzung einer totalen Unimodularitätseigenschaft der vorgeschlagenen Unsicherheitsmenge und einer exakten linearen Entscheidungsregel-Reformulierung beweisen wir, dass das nichtkonvexe, robuste Optimierungsproblem mit funktionalen Unsicherheiten äquivalent zu einem effizient-lösbarem linearen Programm ist. Überraschenderweise lässt sich das zugrundeliegende deterministische Problem für eine bekannte Frequenzabweichungstrajektorie nicht auf ein lineares Programm reduzieren, sondern führt zu einem großen, gemischt-ganzzahligen, linearen Programm selbst in diskreter Zeit. Wir denken, dass wir damit die erste Klasse von praxisrelevanten Optimierungsproblemen entdeckt haben, die durch Robustifizierung dramatisch einfacher werden.

Mittels umfangreicher numerischer Experimente mit realen Daten bestimmen wir den wirtschaftlichen Wert von Vehicle-to-Grid und diskutieren die finanziellen Anreize von Fahrzeugbesitzern, Aggregatoren, Geräteherstellern und Regulierungsbehörden. Insbesondere stellen wir fest, dass die derzeitigen Strafen für die Nichtlieferung der versprochenen Regelleistung zu gering sind, um Aggregatoren dazu zu bewegen, ihre Versprechen gegenüber Netzbetreibern einzuhalten.

Für allgemeine Stromspeicher lösen wir dann eine vereinfachte Version des Entscheidungsproblems analytisch, um zu verstehen, wie die optimalen Regelleistungsmengen von dem Wirkungsgrad des Speichers, der Streuung der Frequenzabweichungen und der EU-Liefergarantie abhängen. Wir zeigen, dass die Grenzkosten der Frequenzregelung mit steigendem Wirkungsgrad sinken und mit steigender Streuung der Frequenzabweichungen steigen. Für energiebeschränkte Speicher stellen wir fest, dass die Gewinne aus der Frequenzregelung umgekehrt proportional zu der Zeitspanne sind, für welche Regelleistung bereit gestellt wird. Die Schaffung eines untätigen Marktes für die Frequenzregelung würde somit die Wettbewerbsfähigkeit von Stromspeichern gegenüber anderen Anbietern von Regelenergie, wie z. B. Wärmekraftwerke, erhöhen.

**Stichwörter:** Vehicle-to-Grid, Regelleistung, Stromspeicher, Strommärkte, Energiewirtschaft, Robuste Optimierung, Funktionale Unsicherheiten, Operations Research.

# 车网互联背景下电网的可靠调频

未来的低碳社会将需要储存大量的电能以使电网运行更加稳定，并为电动汽车提供动力。车网互联允许车主和电网运营商共享汽车的电池、通过电动汽车反向向电网充电的形式来分担电力储存的成本。在实践当中，车主可以选择何时将他们的汽车用于出行，又或者何时用其服务于电网。与此同时，车辆聚合商将决定是否批准该车辆向电网提供服务。

车网互联的成功，必须以车主和电网运营商能够信任聚合商为前提：即服役车辆应该在聚合商允许的情况下方可用于出行或电网服务。在这篇博士论文中，我们解决了一个决策问题——如何确保车辆聚合商的承诺对于电网的一次调频服务有效并可靠，这被认为是车网互联的最有前景的应用之一。从数学角度出发，我们首先制定了一个具有泛函不确定性的鲁棒优化问题——最大化向电网运营商提供一次调频服务的预期利润，并保证车主能够在编码适用的欧盟法规的不确定性集合中的所有频率偏差轨迹中履行其向市场作出的承诺。泛函不确定性确保车辆所有者和电网运营商在任何时候都能信任集合商的决定。然而，直接模拟电池充电和放电过程中的能量转换损失会导致优化问题非凸。通过运用我们提出的不确定性集的完全单模性属性和精确的线性决策规划重构，我们证明了具有功能不确定性的非凸性鲁棒优化问题等同于一个可操作的线性规划问题。出人意料的是，即使时间被离散化，已知频率偏差轨迹的下层确定性问题并没有简化为线性规划问题，而是变成了大规模的混合整数线性规划问题。因此，相信我们发现了一类实际应用有价值的、并可通过鲁棒简化的优化问题。

在基于现实世界实际数据的大规模数值实验后，我们量化了车网互联的经济效益，并阐明了车主、聚合商、设备制造商和监管机构的财务激励。特别是，我们发现目前对不交付所承诺调节电力的惩罚太低，这将无法激励聚合商履行对电网运营商的承诺。

对于一般的电能存储设备，我们随后找到了一个简化版的决策问题的解析解，以了解最佳的频率调节如何取决于存储设备的充放电效率、频率偏差的离散程度和欧盟的交付保证。我们证明了调频的边际成本如何随着充放电效率的提高而降低，并随着频率偏差的离散程度而提高。对于能量受限的存储设备，我们发现频率调整的利润与存储运营商投入调节功率的时间长度成反比。因此，建立一个日内的频率调节市场将使电能储存设备与其他调节提供者（如火力发电厂）相比更具竞争力。

关键词。车网互联（Vehicle-to-Grid），频率调节，电能储存，电力市场，能源经济学，稳健优化，函数不确定性，运筹学。



# Contents

<b>Acknowledgements</b>	<b>i</b>
<b>Abstract (English/Français/Deutsch/Chinese)</b>	<b>iii</b>
<b>Introduction</b>	<b>1</b>
<b>1 A Review of the State-of-Research on Vehicle-to-Grid:</b>	
<b>Progress and Barriers to Deployment</b>	<b>7</b>
1.1 Introduction . . . . .	8
1.2 Technology Development . . . . .	9
1.3 Economic Prospects and Barriers . . . . .	12
1.4 Conclusion . . . . .	16
<b>2 Reliable Frequency Regulation through Vehicle-to-Grid:</b>	
<b>Encoding Legislation with Robust Constraints</b>	<b>19</b>
2.1 Introduction . . . . .	19
2.2 Problem Description . . . . .	25
2.3 Time Discretization . . . . .	30
2.4 Linear Programming Reformulation . . . . .	34
2.5 Multi-Stage Extensions . . . . .	37
2.6 Numerical Experiments . . . . .	38
2.6.1 Model Parametrization . . . . .	38
2.6.2 Backtesting Procedure and Baseline Strategy . . . . .	40
2.6.3 Futility of Solving a Multi-Stage Model . . . . .	41
2.6.4 Experiments: Set-up, Results and Discussion . . . . .	42
2.7 Conclusions . . . . .	46
<b>Appendices</b>	<b>49</b>
2.A Problem Data and Model Parameters . . . . .	49
2.B Additional Experiments and Results . . . . .	50
2.C Proofs . . . . .	51
<b>3 The Economics of Frequency Regulation through Electricity Storage:</b>	
<b>An Analytical Solution</b>	<b>67</b>
3.1 Introduction . . . . .	67

## Contents

---

3.2 Problem Description . . . . .	69
3.3 Reduction to a Deterministic Optimization Problem . . . . .	72
3.4 Candidate Solutions . . . . .	77
3.5 Analytical Solution . . . . .	79
3.6 Applications . . . . .	82
3.6.1 Model Parametrization . . . . .	82
3.6.2 Marginal Cost and Maximum Regulation Bid . . . . .	85
3.6.3 Economics . . . . .	88
3.7 Conclusions . . . . .	91
<b>Appendices</b>	<b>93</b>
3.A Additional Figures . . . . .	93
3.B Proofs . . . . .	94
<b>Conclusions and Perspectives</b>	<b>105</b>
<b>Bibliography</b>	<b>107</b>
<b>Curriculum Vitae</b>	<b>115</b>

# Introduction

In November 1896 when America's first large-scale power plant at Niagara Falls began transmitting electricity to the city of Buffalo about 20 miles away, the electricity came in the form of alternating current. The reason was that "*unlike direct current, alternating current can travel*" (Bakke, 2016, p. 48). Most electricity grids today still rely on alternating current although modern power electronics allow direct current to travel even farther than alternating current. The frequency of the alternating current indicates the balance between electricity supply and demand. Whenever there is too much supply, electricity generators spin faster and the frequency rises. Similarly, whenever there is too little supply, generators spin slower and the frequency falls. If the generators do not run close to their nominal speed, they shut down to protect themselves from damage. In order to ensure a reliable electricity grid and to prevent blackouts, the frequency must be close to its nominal value of 50Hz in Europe and most of Asia and 60Hz in North America at all points in time. This gives rise to the need for *primary frequency regulation*, also known as frequency containment reserves, which is a power reserve that grid operators purchase to balance electricity supply and demand in real-time. Regulation providers measure the instantaneous frequency deviation and adjust their power consumption from the grid by an amount equal to the normalized deviation times the amount of reserve power promised to and paid for by grid operators.

Traditionally, this reserve power has been provided by centralized power plants, which were often fired by fossil fuels. Today, as we transition toward low-carbon societies, wind and solar power plants are replacing fossil-based power plants. Electricity generation is therefore becoming increasingly weather-dependent. So is electricity consumption, as heating is increasingly electrified through heat pumps. The further we move into the energy transition, the more electricity supply and demand will be variable and less predictable. This shall increase the need for real-time balancing and thus the need for frequency regulation.

Electricity storage is envisioned to fulfill part of the increased need for regulation power (European Network of Transmission System Operators for Gas and Electricity, 2021). Currently, lithium-ion batteries are one of the best storage technologies to cover the future need for frequency regulation because they can be deployed anywhere, as opposed to hydropower, and because they have fast dynamics (World Energy Council, 2020). Primary frequency regulation, in particular, is a promising application for lithium-ion batteries. In fact, as the grid frequency usually fluctuates rapidly around its nominal value, batteries providing frequency regulation



only experience small deviations in their state-of-charge, which limits battery degradation (Uddin et al., 2018; Thompson, 2018). At the moment, however, lithium-ion batteries are still too expensive to be deployed at scale for frequency regulation, although their prices have been declining rapidly (Ziegler and Trancik, 2021).

In parallel with the transition toward renewable energy technologies, we are also transitioning toward electric vehicles. In fact, many cities restrict or plan to restrict the use of internal combustion engine vehicles to reduce urban air pollution and meet CO<sub>2</sub> emissions targets. On average, privately owned cars are a vastly underutilized resource as they are parked 95 percent of the time (Kempton and Tomić, 2005a). Since many of them will be electric in the future, their batteries could be made available to electricity grids when the cars sit idle. This could be beneficial to both vehicle owners, which stand to make a profit, and to society at large, which stands to gain safer electricity grids and a decreased reliance on battery imports that may otherwise be needed for electricity storage.

The idea of putting electric vehicle batteries to use for electricity grids is called “*vehicle-to-grid*” (V2G) and was conceived by Kempton and Letendre (1997). Brooks (2002) built the first working prototype of an electric vehicle delivering frequency regulation. Since then, there have been about 100 pilot projects, but there has been virtually no commercial deployment of vehicle-to-grid yet.

In **Chapter 1**, we investigate the reasons for which vehicle-to-grid has not been deployed on a larger scale yet. We find that the barriers are not technological but rather socio-economic in nature. Specifically, the costs of vehicle-to-grid are too high compared to the revenues under current market conditions and vehicle owners are sceptical because they are concerned about battery degradation and about restricting the access to their cars for only moderate pay-offs. In the following chapters, we explore under which conditions vehicle-to-grid can become profitable in the future.

Among the various services that vehicle-to-grid can provide to electricity grids, primary frequency regulation is often considered to be most promising as it limits battery degradation (Kempton and Tomić, 2005a; Noel et al., 2019). Grid operators, however, might doubt whether they can rely on electric vehicles for primary frequency regulation because they are used to operate stationary assets rather than mobile assets (Réseau de transport d’électricité, 2017b). In practice, the intermediary between vehicle owners and grid operators is the aggregator, who will pool hundreds of electric vehicles into so-called “*virtual power plants*” and engage these in power regulation markets. In doing so, aggregators make promises to both vehicle owners and grid operators. For vehicle-to-grid to be successful both groups must be able to trust aggregators. This means that grid operators should get the regulation power they were promised and vehicle owners should be able to drive when they were promised they would be able to. Aggregators must thus provide certainty in the face of two sources of uncertainty, which are future vehicle usage for driving and future deviations in the grid frequency. There are several ways of dealing with the uncertain vehicle usage for driving in

the literature (Guille, 2009; Vandael et al., 2013, 2020). We find, however, that uncertain future frequency deviations have not been addressed satisfactorily yet, especially given applicable EU regulations that prescribe what frequency deviation trajectories aggregators must be able to cover to participate in primary frequency regulation (European Commission, 2017). In the following chapters, we assume for simplicity that vehicles will be available for grid services when drivers say they are. In practice, this will not always be the case and aggregators would reserve some margin, which depends on the number of vehicles they pool.

In **Chapter 2**, we solve a decision-making problem that ensures reliable commitments of electric vehicles by aggregators for primary frequency regulation. Mathematically, we formulate a robust optimization problem with functional uncertainties that maximizes the expected profit from selling frequency regulation while guaranteeing that regulation power can be delivered for all frequency deviation trajectories in an uncertainty set that encodes applicable EU regulations. Functional uncertainties ensure that the delivery of regulation power is guaranteed at all times. Faithfully modeling the energy conversion losses during charging and discharging renders the optimization problem nonconvex. By exploiting a total unimodularity property of the proposed uncertainty set and an exact linear decision rule reformulation, we prove that this nonconvex robust optimization problem with functional uncertainties is equivalent to a tractable linear program. Surprisingly, the underlying deterministic problem for a known frequency deviation trajectory does not reduce to a linear program but results in a large-scale mixed-integer linear program, even if time is discretized. We believe that we have thus discovered the first practically interesting class of optimization problems that become dramatically easier through robustification. We point out that the decision-making problem also captures stationary electricity storage devices, which can be modeled as electric vehicles that never drive.

Two parameters constrain the amount of regulation power electric vehicles can provide: the maximum charging and discharging power and the energy storage capacity. In the literature, the charging and discharging capacity is often thought to be the most limiting factor (Kempton and Tomić, 2005a; Borne, 2019). In contrast, by faithfully accounting for the EU delivery guarantee, we find that it is actually often the energy storage capacity that is limiting the amount of regulation power that electric vehicles can provide. This has two implications. First, vehicle owners may reserve their cars for driving for up to 9 hours per day without reducing the profits from frequency regulation. In fact, up to a point, vehicle owners can always sell the same amount of regulation energy by selling more regulation power in a shorter time if necessary. Second, the amount of regulation power that electric vehicles can provide depends on how grid operators interpret EU regulations. In fact, the European Commission specifies that frequency regulation providers must be able to deliver all the power they promise between about 10% and 20% of the time. It is up to grid operators to choose a percentage within that range. If they choose 10% rather than 20%, this means that electric vehicles can provide double the regulation power for a fixed amount of regulation energy.

Whenever aggregators are not able to provide the regulation power they promised, they need to

pay a fine. In our case study, we find that current fines are too low to incentivize aggregators to make promises they can hold. In other words, crime pays under current EU market regulations. The profits from frequency regulation are 2.5 times higher when aggregators ignore the EU regulations and pay the fines instead. Even so, we find yearly operating profits of just 300 € per year and vehicle. It is quite likely that this is too low to convince equipment manufacturers and aggregators to invest in vehicle-to-grid, especially given that vehicle owners will also want a share of the profits when participating in vehicle-to-grid. In short, crime pays but possibly not enough.

Until now, we have considered fixed ranges for the regulatory parameters, namely the percentage and duration of time for which promised regulation power must be delivered and committed, respectively. From now on, we consider them variable, which makes sense because they are the result of political negotiations and thus subject to change in the future. Specifically, we wonder whether it is profitable at all to provide primary frequency regulation through electricity storage, not limited to electric vehicles, and how the profitability depends on regulatory parameters, on the roundtrip efficiency of the storage device, and on the dispersion of frequency deviations.

In **Chapter 3**, we derive an analytical solution for a simplified version of the decision-making problem in Chapter 2, which only considers stationary storage devices. The decision-making problem applies to storage operators that can sell regulation power and buy or sell electricity on retail or wholesale markets. Mathematically, we formulate again a nonconvex robust optimization problem and treat future frequency deviation trajectories as functional uncertainties. This time, we constrain the expected terminal state-of-charge to be equal to some target, which should allow storage operators to not only make good decisions for the present but also for the future. We show that, thanks to the expected state-of-charge constraint, the amount of electricity bought on the market is an implicit function of the regulation power sold to the grid operator. The decision-making problem thus reduces to a one-dimensional problem, which we show to be convex for all storage devices with realistic roundtrip efficiencies.

The implicit function quantifies the amount of power that needs to be purchased to cover the expected energy loss that results from providing frequency regulation. In fact, although the average frequency deviation vanishes, the average flow of regulation power that exits the storage device is nonnegative and does not necessarily vanish. We show that the expected energy loss is nonincreasing in the roundtrip efficiency and nondecreasing in the dispersion of the frequency deviations. The higher the market price of electricity, the more costly the losses. Since retail market prices can be a multiple of wholesale market prices, providing frequency regulation through storage devices is more profitable when storage operators have access to wholesale markets.

For energy-constrained storage devices, we find that the profits from frequency regulation over the lifetime of the storage devices are roughly inversely proportional to both regulatory parameters, the percentage and the duration of time for which promised regulation power

must be committed and delivered, respectively. The percentage of time relates to the safety of the electricity grid, but the duration of time does not. In fact, grid operators could establish an intra-day market for frequency regulation, which would make electricity storage devices more competitive with other regulation providers, such as thermal power plants. A priori, the creation of such a market does not have a direct negative effect on the safety of electricity grids. To the contrary, electricity grids may become more reliable if it is profitable for more electricity storage devices to participate in frequency regulation.

Based on a case-study of the French regulation market, we find that stationary lithium-ion batteries will not become sufficiently low-cost in the near future to be profitable for primary frequency. Given that the European Commission (2018, 2020) and the European Network of Transmission System Operators for Gas and Electricity (2021) estimate that Europe will need up to 100GW of installed battery power by the year 2040 to realize her climate ambitions, we conclude that it may be necessary to create regulatory conditions that allow batteries, mobile or stationary, to compete with other flexibility providers on frequency regulation and electricity markets.

For a three minute presentation of Chapters 1 and 2 aimed at a general audience please visit [https://go.epfl.ch/mt180s\\_dirk\\_lauinger](https://go.epfl.ch/mt180s_dirk_lauinger).

**Statement of Originality.** I hereby certify that this thesis is the product of my own work with some assistance from my advisors Prof. Daniel Kuhn and Dr. François Vuille. Chapter 1 is based on a conference paper (Lauinger et al., 2017) and Chapter 2 is based on a preprint (Lauinger et al., 2022). Mengmeng Li and Tianshu Yang have helped to write the Chinese abstract.



# 1 A Review of the State-of-Research on Vehicle-to-Grid: Progress and Barriers to Deployment

Each car, never exploited, gives to the grid according to its ability while remaining available to the grid to take from according to its need. Together, all our cars keep our common electrical system strong. And the grid, with their help, can at long last balance itself.

— Gretchen A. Bakke, *The Grid*, 2016.

A bidirectional power transfer between electric vehicles and the electricity grid, commonly referred to as vehicle-to-grid, offers the possibility to pair fluctuating electricity supply and demand with the fluctuating availability of electric vehicles parked at charging stations. Vehicle-to-grid is envisioned as an option for balancing electricity grids, in particular in regions aiming at a high penetration of intermittent renewable energy and a high penetration of electric vehicles. Vehicle-to-grid could lower the need for stationary electricity storage or idle backup power plants by capitalizing on the existing batteries of electric vehicles. In fact, privately owned vehicles sit idle most of the time and, if electric, could provide services to electricity grids during this time. Given this apparent benefit, it may appear surprising that vehicle-to-grid has not yet been deployed on a wide scale. We investigate this apparent discrepancy by reviewing the status of research on vehicle-to-grid and the status of technical development and deployment. We assess the barriers to vehicle-to-grid deployment by identifying the main open research questions from a technical and economic perspective. We find that the technological barriers have mostly been overcome. There is still room for improvement on reliable aggregation, operating strategies that limit battery degradation, battery chemistries, and secure communication between vehicle owners and grid operators. The economic barriers, however, have not been overcome yet. In particular, the cost of vehicle-to-grid is often too high compared to the revenues under current electricity market conditions, it is not settled under which business and aggregation model vehicle-to-grid can capture most economic value, and electric vehicle owners may be concerned about battery degradation and about restricting the access to their cars for only moderate pay-offs.

## **1.1 Introduction**

Vehicle-to-Grid is the idea of establishing a bidirectional power transfer between the electricity grid and electric vehicles. Since the introduction of the concept by Kempton and Letendre (1997), vehicle-to-grid has been said to pave the way into a future with a high penetration of electric vehicles and of power from intermittent renewable sources (Kempton and Tomić, 2005b). When electric vehicles are connected to charging stations, they could offer several services to the electricity grid such as active power regulation, reactive power support, load balancing, and current harmonic filtering. Furthermore, in electricity grids with a high penetration of decentralized electricity generation, vehicle-to-grid could reduce electricity transport losses by increasing local consumption (Lehtola and Zahedi, 2016).

These benefits are not specific to vehicle-to-grid, but true of demand response in general. In a demand response scheme, electricity consumers are given an incentive to adapt their electricity consumption to the needs of electricity grid operators (United States Department of Energy, 2006). Electric vehicle owners, for example, may give grid operators some control about when and how to charge their vehicles, which is sometimes referred to as grid-to-vehicle or unidirectional vehicle-to-grid (Yilmaz and Krein, 2013). Compared to controlled electric vehicle charging, vehicle-to-grid, as a form of both demand response and electricity storage, offers a higher dispatch flexibility. In addition, vehicle-to-grid is expected to have lower investment costs than other forms of electricity storage as it makes use of batteries that have been purchased for driving, but sit idle 96% of the time for an average personal vehicle (Kempton and Tomić, 2005b).

Although the technical feasibility of vehicle-to-grid for individual vehicles has already been demonstrated by AC Propulsion Inc. in the year 2002 (Brooks, 2002), the technology has not reached full commercial status to date. In the wake of the Fukushima nuclear disaster, Japan started a pilot project in the year 2012 with 4,000 bidirectional charging stations that allow electric vehicles to supply power to individual homes but not to the grid at large. In the same year, the United States Air Force installed 15 bidirectional charging stations to provide first backup power to their military bases and then frequency regulation and reserve power to the grid at large (Marnay et al., 2013). The Air Force project is one of the few projects that provide grid services commercially. In fact, according to the online platform V2G-Hub<sup>I</sup>, out of 96 vehicle-to-grid projects that have been implemented to date, only 8 projects provide services commercially. Excluding the Japanese pilot project with 4,000 bidirectional charging stations, the remaining 95 vehicle-to-grid projects have 22 bidirectional charging stations on average. In 2018, Everoze and EVConsult (2018) report that about half of all vehicle-to-grid projects were located in Europe, mostly in the United Kingdom, the Netherlands, France, and Germany, with Renault-Mitsubishi-Nissan providing the electric vehicles and Nuvve providing the aggregation platform for 65% and 30% of all projects. The vehicle-to-grid services that are most often provided are load shifting and frequency regulation with 48% and 32% of all projects, respectively. While virtually all projects have technical elements, social aspects such

---

<sup>I</sup>[www.v2g-hub.com](http://www.v2g-hub.com)

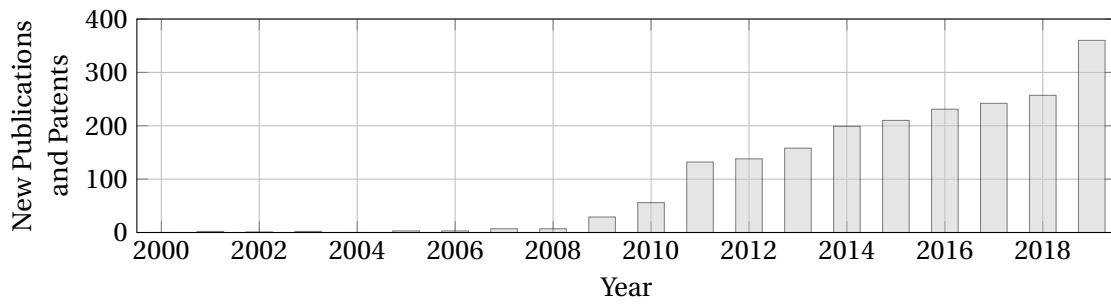


Figure 1.1: Publications and patents titled “*vehicle-to-grid*” in Google Scholar.

as user acceptance and behavior are often overlooked. The same holds true for academic publications (Sovacool et al., 2018).

After seminal articles by Kempton and Tomić (2005a,b), the research interest in vehicle-to-grid accelerated in the year 2009, increased slowly but steadily from 132 new publications and patents in the year 2011 to 257 new publications and patents in the year 2018, and accelerated again in the year 2019 to reach a total of 360 new publications and patents titled “*vehicle-to-grid*” and indexed in Google Scholar (Figure 1.1).

Through a meta-review of 17 review articles on vehicle-to-grid, we analyze the status of research and development and investigate the reasons for which vehicle-to-grid has not been deployed on a wider scale yet, in spite of its apparent benefits. Finally, we discuss and conclude upon the economic merits of vehicle-to-grid.

## 1.2 Technology Development

According to Yilmaz and Krein (2013) the six components of a vehicle-to-grid system are “1) *energy resources and an electric utility*; 2) *an independent system operator and aggregator*; 3) *charging infrastructure and locations*; 4) *two-way electrical energy flow and communication between each EV and ISO or aggregator*; 5) *on-board and off-board electrical metering and control*; and 6) *the EV itself with its battery charger and management*.” By “*independent system operators*”, Yilmaz and Krein mean operators of high voltage electricity grids. In Europe, such operators are typically called “*transmission system operators*”. We refer to them as “*grid operators*”.

The need for demand response, and thus also the need for vehicle-to-grid, in a given area depends on three factors: (i) the generation mix of the utility company, (ii) the maximum level and the intermittency of the electric load, and (iii) the grid infrastructure (Palensky and Dietrich, 2011). Electric utilities thus determine the framework conditions for vehicle-to-grid. In general, the higher the peak load and the more intermittent the electricity supply and demand, the higher the needs for demand response and electricity storage. Weak electricity grids further aggravate these needs.



## A Review of the State-of-Research on Vehicle-to-Grid: Progress and Barriers to Deployment

---

In the following, we address the remaining five components described by Yilmaz and Krein, starting with grid operators and aggregators.

Grid operators are responsible for balancing electricity demand and supply. They would dispatch electric vehicle batteries in electricity markets. Every market transaction must exceed a certain threshold to be accepted by grid operators, *e.g.*, 2MW for the capacity market in the United Kingdom (Gough et al., 2017), which corresponds to about 200 electric vehicles. The aggregation of many electric vehicles into virtual power plants is needed for vehicle-to-grid to meet these thresholds. The aggregation of small power plants or electric loads, such as heat-pumps, into virtual power plants has been researched at least since the year 1997 (Awerbuch and Preston, 1997; Pudjianto et al., 2007) and has become a “*relatively well established industry*” (Gough et al., 2017). The challenge lies in adapting existing aggregation concepts to electric vehicles given the uncertainty surrounding the number of parked and grid-connected vehicles and the total energy and power that vehicle owners may commit to deliver to the grid at any one time. To this end, Guille and Gross (2009) proposed a highly cited aggregation framework. In the meantime, current research has expanded beyond implementing aggregation on a purely technical level, to the contract parameters that aggregators and electric vehicle owners should negotiate with each other (Broneske and Wozabal, 2017). It is particularly important that aggregators are able to deliver the grid services they promise to grid operators. This is especially so for primary frequency regulation, which Kempton and Tomić (2005a) and Noel et al. (2019) consider one of the most profitable grid that vehicle-to-grid can offer. In fact, primary frequency regulation is used to stabilize electricity networks after disturbances (Rebours et al., 2007). Its provision must therefore be highly reliable. Europe’s largest grid operator, Réseau de transport d’électricité (2017b), questions the reliability of vehicle-to-grid. The European Commission (2017) has defined a delivery guarantee to address this concern. In Chapter 2, we present an optimization problem that faithfully accounts for the delivery guarantee and show that it can be solved efficiently. In Chapter 3, we derive an analytical solution for the optimization problem under a simplified delivery guarantee.

Bidirectional chargers for electric vehicles span a wide range of power levels, from about 1kW for home chargers to over 100kW for commercial fast charger. If managed poorly, fast chargers might locally overload the electricity grid, which would increase voltage deviations and decrease the lifetime of voltage transformers (Yilmaz and Krein, 2013). In the last several years, the standardization of the charging infrastructure and the development of smart vehicle-to-grid chargers has received considerable attention. Ozansoy et al. (2017) observed that there are American, European, and Japanese charging infrastructure standards, for example, for the shape of charging plugs. Ozansoy et al. expected that an international standard would be agreed upon by the end of the year 2017 and hoped that this would accelerate electric vehicle deployment. Today, four years later, there are still at least five different plug types in use.<sup>II</sup> Smart chargers coordinate the charging behaviour of individual vehicles so as to maximize the services offered to the electricity grid, while minimizing the battery degradation caused by

---

<sup>II</sup>[https://www.mobilityhouse.com/int\\_en/knowledge-center/charging-cable-and-plug-types](https://www.mobilityhouse.com/int_en/knowledge-center/charging-cable-and-plug-types)

these services. Determining optimal charging strategies is a field of active research.

Since the year 2015, wireless connectivity of new cars is required by European Union standards for automatic crash notification (Mwasliu et al., 2014). Ozansoy et al. (2017) point to the need for interoperable communication standards to manage transactions between electric vehicles and grid operators. Concerns about cybersecurity have been raised in this context (Mwasliu et al., 2014). Implementing some form of communication between electric vehicles, aggregators, electric utilities, and grid operators, is expected to be a lesser barrier than securing and standardizing the communication. As mentioned in the introduction, the technical feasibility of establishing a bidirectional power and communication flow between an electric vehicle and a (simulated) grid operator has been demonstrated back in the year 2002 (Brooks, 2002).

Based on our literature review, the metering of the electricity exchanged between electric vehicles and the electricity grid does not seem to be of particular concern to the deployment of V2G anymore. Gough et al. (2017) do not mention it in their publication about the techno-economic feasibility of vehicle-to-grid. Ozansoy et al. (2017) point out that the interplay of the electricity meter with the other system components requires substantial communication and coordination, but they do not question the technical feasibility of constructing such a meter.

For a while, vehicle-to-grid induced battery degradation seemed like the main technical barrier to vehicle-to-grid deployment, possibly severe enough to discourage any deployment (Peterson et al., 2010). More recently, it has become clear that the impact of vehicle-to-grid on battery lifetime ranges from severe to insignificant and depends on the operating conditions of the battery, such as temperature and variations in state-of-charge (Uddin et al., 2018). For example, based on computer simulations, Wang et al. (2016) have shown that providing grid services does indeed degrade the battery, but that the degradation depends on the nature and the extent of the grid services. For the particular grid services of frequency regulation and peak load shaving, battery degradation is negligible if grid services are offered for less than 2 hours per day. For other grid services, battery degradation is insignificant compared to natural wear and tear if the services are provided only during the days of greatest needs, about 20 days per year in Wang et al.'s study. One year later, based on degradation experiments, Dubarry et al. (2017) found vehicle-to-grid to cause severe battery degradation, while Uddin et al. (2017) found that vehicle-to-grid may even prolong battery lifetime. The authors of both studies later explained that they reached different conclusions about the impact of vehicle-to-grid on battery lifetime because they had made different assumptions about the operating conditions of the battery under vehicle-to-grid (Uddin et al., 2018). As a rule of thumb, Thompson (2018) recommends that the state-of-charge of common lithium-ion electric vehicle batteries should be maintained between 20% and 80% to limit battery degradation. Sweda et al. (2017) follow this rule when optimizing charging policies of electric vehicles. Beyond minimizing battery degradation through strategic charging and discharging strategies, further research is conducted on the batteries themselves to increase their energy density and to lower their cost (Ziegler and Trancik, 2021). Such batteries may favor the deployment of electric vehicles and thereby increase the potential applications of vehicle-to-grid.

## **A Review of the State-of-Research on Vehicle-to-Grid: Progress and Barriers to Deployment**

---

In their seminal work, Kempton and Tomić (2005a) did not only consider battery electric vehicles for vehicle-to-grid, but also plug-in hybrid and fuel cell vehicles. Today, it seems questionable whether plug-in hybrids and fuel cell vehicles will participate in vehicle-to-grid. On the one hand, plug-in hybrids are seen as a transition technology that should be gradually replaced by full electric vehicles until the year 2050, at least in the European Union (European Network of Transmission System Operators for Gas and Electricity, 2021, p. 17), especially if global warming is to be limited to 1.5K (European Commission, 2018, p. 119). On the other hand, once hydrogen and fuel cell vehicles become widely available, Andrey et al. (2020) foresee that electrolyzers needed for the supply of hydrogen will take part in demand response and not the fuel cell vehicles themselves.

To conclude on the state of technology development, vehicle-to-grid can be implemented from a purely technical point of view, however, reliable aggregation and potential battery degradation are the principal remaining issues that would hinder mass deployment should demand for vehicle-to-grid rise. More research is needed on (i) reliable aggregation, (ii) charging and discharging strategies that limit battery degradation, (iii) battery chemistries, and on (iv) securing the communication between vehicle owners, aggregators, and grid operators.

In Yilmaz and Krein (2013)'s words, controlled unidirectional charging of electric vehicles for demand response *"is a logical first step [towards vehicle-to-grid deployment] because it limits hardware requirements, simplifies interconnection issues, and tends to reduce battery degradation"*. As we will see in Chapter 2 at the example of frequency regulation, unidirectional charging achieves these benefits by greatly limiting the amount of power that can be made available for grid services. For frequency regulation, the profits earned through controlled unidirectional charging are negligible. For other grid services, such as peak shaving, it is not clear yet whether they will be sufficiently high to offset communication and aggregation costs.

### **1.3 Economic Prospects and Barriers**

Based on our meta-review, three socio-economic barriers currently prevent vehicle-to-grid deployment: (i) the cost of vehicle-to-grid is often too high in comparison to revenue from demand response under current electricity market conditions (Gough et al., 2017); (ii) it is not settled under which business and aggregation model vehicle-to-grid can capture most economic value (Broneske and Wozabal, 2017); (iii) electric vehicle owners may be concerned about the loss of driving range and vehicle availability when they engaged in vehicle-to-grid (Parsons et al., 2014; Geske and Schumann, 2018).

The United States Department of Energy defines demand response as *"changes in electric usage by end-use customers from their normal consumption patterns in response to changes in the price of electricity over time, or to incentive payments designed to induce lower electricity use at times of high wholesale market prices or when system reliability is jeopardized"* (United States Department of Energy, 2006, p. IX). In other words, demand response helps to balance electricity supply and demand. Depending on the time scale over which electricity is balanced,

demand response is referred to more specifically as peak shaving (corresponding to periods of “*high wholesale market prices*”) or as ancillary services (corresponding to time instants during which “*system reliability is jeopardized*”). Most of the literature sees the delivery of control energy for frequency and voltage regulation in the ancillary services market as the most promising economic opportunity for vehicle-to-grid. This is because grid operators purchase control energy as an insurance against extreme but rare electricity supply and demand mismatch scenario. In practice, grid operators only need a small amount of the control energy they purchased to balance supply and demand. On average, control energy providers thus only need to deliver a small fraction of the control energy they sell to grid operators, which limits battery usage and degradation (Kempton and Tomić, 2005a). Gough et al. (2017) find that participating in both the peak power and the ancillary services markets may prove most profitable for vehicle-to-grid in the United Kingdom. By offering these services, demand response stabilizes the grid and potentially reduces the need for infrastructure upgrades—an aspect that is rarely analysed in the literature we reviewed.

The need for balancing electricity supply and demand depends on the intermittency of electricity generation and consumption. It is amplified when electricity networks come close to their thermal limits. In this case, demand response is used to locally and temporarily reduce the power flows through the networks. The rise of electric vehicles and of intermittent renewable energy, in particular wind and solar, is likely to increase the need for demand response. Numerous studies have shown that a high penetration of electric vehicles, which are not charged in a coordinated fashion, increases the peak load (Habib et al., 2015). Since a higher peak loads are likely to lead to a lower system reliability, electric vehicle deployment may indeed increase the need for demand response. Should vehicle-to-grid be competitive with other demand-response technologies, this need could at least partially be covered by the electric vehicles themselves. To assess the competitiveness of vehicle-to-grid, Mwasliu et al. (2014) call for “*more research and analysis [...] to justify the adoption of the [vehicle-to-grid] framework over other energy storage systems.*” At the moment, however, the economic prospects of “*other energy storage systems*”, such as stationary batteries and hydrogen storage, are still under investigation themselves (Malhotra et al., 2016; Victoria et al., 2019). In Chapter 3, we address this gap by investigating the economics of providing frequency regulation with various storage technologies. In particular, we quantify the marginal costs stemming from charging and discharging losses.

In addition to battery degradation and operating costs, the costs of vehicle-to-grid consist of investments in bidirectional charging infrastructure and of transaction costs for aggregating electric vehicles. Although Gough et al. (2017) expect the costs of charging stations to follow a similar decline as the costs of photovoltaic systems have followed in the past, the exact nature of the costs for charging stations is not clear yet, which leads to additional uncertainty about the profitability of vehicle-to-grid. In their seminal paper, Kempton and Tomić (2005a) explain that vehicle-to-grid requires wiring upgrades from 6.6kW to between 10kW and 15kW in residential dwellings to be most profitable. A higher line capacity, so their reasoning, provides more options for individual vehicles to participate in power markets. It also increases the

## **A Review of the State-of-Research on Vehicle-to-Grid: Progress and Barriers to Deployment**

---

overall system cost and reduces the overall charging time. After reviewing the literature, it is not clear to us whether vehicle owners will connect their cars to chargers for shorter periods of time if they can charge them faster and what the consequences for vehicle aggregators might be. If vehicle owners do connect their cars for shorter periods of time, we expect that aggregators have to pool more vehicles to offer the same amount of grid services, which increases their transaction costs. For the example of electric loads, Nursimulu (2016) shows that transaction costs have a significant impact on the economic viability of demand response. The same may be true for electric vehicles, although we have not found any detailed study of vehicle-to-grid transaction costs in the literature. Aggregators incur such costs when recruiting electric vehicles for participation in vehicle-to-grid. The costs depend on the minimum amount of power aggregators need to be able to offer to participate in electricity markets, on the minimum duration over which they must be able to provide power, and on the reliability with which power should be delivered. All three points are subject to regulations governing electricity grid operators which are set, for example, by the European Commission (2017). Transaction costs for vehicle-to-grid may be higher than for other demand response technologies. In fact, electric vehicle owners might be more difficult to convince than, *e.g.*, heat pumps owners to enlist in demand response because a potential loss of car availability and battery lifetime might be considered a higher burden than a mere drop in room temperature.

Based on the above, three necessary conditions for vehicle-to-grid deployment can be identified: (i) electric vehicle penetration needs to be sufficiently high for aggregators to be able to pool hundreds to thousands of electric vehicles, (ii) there must be a need for electricity storage, and (iii) the cost of vehicle-to-grid must be low enough to compete with other storage technologies. We discuss these three conditions below.

The International Energy Agency (2021) reports that the global passenger electric vehicle stock, including plug-in hybrid electric vehicles, has grown rapidly during the last decade, from about 20,000 vehicles in the year 2010 to over 10 million vehicles in the year 2020 (see Figure 1.2). Nevertheless, the share of electric vehicles in the global passenger vehicle fleet is, at about 1%, still small. In addition, according to Eurostat (2021) half of the passenger electric vehicle fleet in the European Union in the year 2019 consisted of plug-in hybrid electric vehicles, which usually have smaller batteries than full battery electric vehicles. We will see in Chapters 2 and 3 at the example of frequency regulation that small batteries sizes significantly limit the amount of grid services that electric vehicles can provide. Full battery electric vehicles therefore seem most promising for vehicle-to-grid applications. The European Network of Transmission System Operators for Gas and Electricity (2021) estimates that such vehicles will account for between 10% and 20% of the European passenger vehicle fleet by the year 2030 and for between 70% and 90% by the year 2050. Norway has already reached a penetration of 12% by the end of the year 2020 (Statistics Norway, 2021). The European Network of Transmission System Operators for Gas and Electricity (2021) also estimates that Europe will need between 75GW and 100GW of installed battery power by the year 2040 to balance electricity supply and demand. All this power could in theory be provided by 10 million electric vehicles, which corresponds to 4% of the about 250 million passenger vehicles currently registered in the

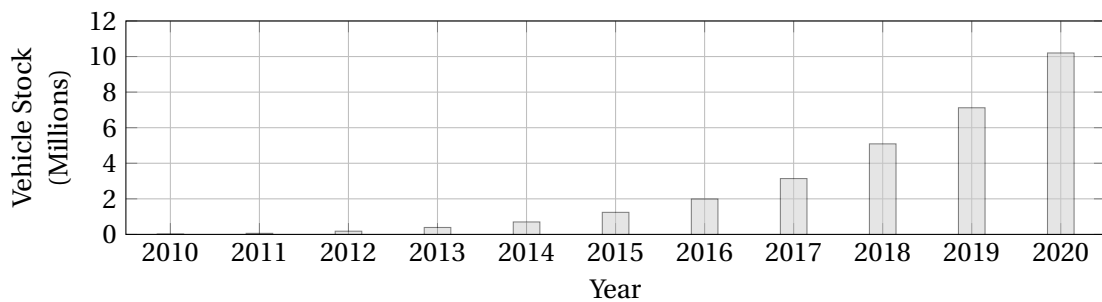


Figure 1.2: Global passenger electric vehicle stock including plug-in hybrid electric vehicles.

European Union. In practice, not all vehicle owners will want to participate in vehicle-to-grid, and not all of those who will participate, will be connected to a bidirectional charging station at the same time. Nevertheless, these figures show that the electric vehicle fleet will be sufficiently large for aggregators to be able to pool enough vehicles to offer grid services, even in the near future.

Since the European Network of Transmission System Operators for Gas and Electricity (2021) foresees that electricity storage will be needed to balance electricity supply and demand, one may suspect that the prices for balancing power will rise in the future. Higher prices for primary frequency regulation, one specific form of balancing power, would be of particular interest for vehicle-to-grid operators. In fact, primary frequency regulation is often considered as one of the most profitable services that vehicle-to-grid could provide because it is thought to cause very little battery degradation (Kempton and Tomić, 2005a; Noel et al., 2019). From the year 2017 to the year 2020, however, the prices for primary frequency regulation have declined in both France and Germany, two major European electricity markets. In Germany, in particular, they declined by more than 50%, whereas the decline in France was less pronounced (see Figure 2.A.1). The German Federal Network Agency and the German Federal Cartel Office suspect that the decline is due to increased competition on the primary frequency regulation market (Bundesnetzagentur and Bundeskartellamt, 2021, p. 204). In fact, since 19 June 2019 the electricity grid operators of Austria, Belgium, the Netherlands, France, Germany, Slovenia, Switzerland, and West Denmark procure frequency regulation power in a common market. In summary, it seems likely that there will be a need, which may include frequency regulation, for electricity storage in the future. At the moment, however, the need for additional storage seems limited, at least as far as frequency regulation is concerned.

Concerning the competitiveness of vehicle-to-grid with other storage technologies, Beer et al. (2012) showed that removing batteries from electric vehicles *“at an early stage of their lifecycle creates considerable economic value”*. In their case, the removed batteries were to be used for stationary storage in a commercial microgrid in California. More recently, Thorne et al. (2021) estimate that in Norway alone there will be end-of-life batteries with a capacity of about 0.6GWh and 2.1GWh available for second-life applications and recycling in the years 2025 and 2030, respectively. We therefore raise the question whether second-life batteries will

## A Review of the State-of-Research on Vehicle-to-Grid: Progress and Barriers to Deployment

---

directly compete with vehicle-to-grid. In fact, depending on how much vehicle-to-grid deployment lags electric vehicle deployment, there may be an abundance of second-life electric vehicle batteries for stationary storage, before vehicle-to-grid has the chance to establish itself as a technology. The number of second-life batteries will depend on the fraction of batteries that is recycled into new electric vehicles batteries and the fraction that is reused in stationary applications. The European Parliament currently debates regulations that mandate a minimum recycled content in new batteries (Halleux, 2021). Such a mandate may decrease the competition from second-life batteries. This competition will also depend on the respective costs of vehicle-to-grid and second-life batteries when they will be mature technologies, for which no robust data is available yet. Although important, the question regarding the competitiveness of these two technologies remains open.

Finally, we are concerned about market gaming. In reaction to Enron's gaming of the California electricity market in the years 2000 and 2001, which caused blackouts affecting several hundred thousand customers, the then-Chairman of the California Power Authority S. David Freeman testified to the United States Senate (2002): *"There is one fundamental lesson we must learn from this experience: electricity is really different from everything else. It cannot be stored, it cannot be seen, and we cannot do without it, which makes opportunities to take advantage of a deregulated market endless. It is a public good that must be protected from private abuse. If Murphy's Law were written for a market approach to electricity, then the law would state 'any system that can be gamed, will be gamed, and at the worst possible time.' And a market approach for electricity is inherently gameable. Never again can we allow private interests to create artificial or even real shortages and to be in control."* For vehicle-to-grid, the question at hand is whether aggregators could make profits by intentionally stressing electricity grids and then offering help to relieve the very same stress?

### 1.4 Conclusion

Based on a meta-review of 17 review articles, we find that the technical feasibility of vehicle-to-grid has already been demonstrated in the year 2002 for individual vehicles with first aggregation functions. The main technological challenges that remain today are battery degradation, smart (dis-)charging, and reliable aggregation of electric vehicles offering grid services.

The economic merits of vehicle-to-grid are uncertain and the revenues that can be generated often not high enough to justify deployment under prevailing electricity market conditions. This may change in the future with the deployment of electric vehicles and intermittent energy sources creating a larger need for demand response. The question at hand is whether the potentially low investment costs of vehicle-to-grid can more than compensate for the uncertain and potentially high aggregation and operating costs when competing with other storage technologies. Specifically, how will vehicle-to-grid compete with second-life electric vehicle batteries that may be used for stationary storage?

The fundamental motivation behind vehicle-to-grid is to take advantage of the underutilization of passenger vehicles. However, autonomous vehicles and car sharing schemes may increase the utilization of passenger vehicles significantly. To judge the prospects of vehicle-to-grid, it thus seems important to reflect on the evolution of both the absolute number and the utilization of electric vehicles. Beyond judging the economic viability of vehicle-to-grid, these reflections should inform the planning of the infrastructure required for vehicle-to-grid. Finally, the options for vehicle-to-grid aggregators to “game” electricity markets should be investigated.

Considering the uncertainty surrounding the economic viability of vehicle-to-grid and the limited need for demand response, it is not surprising that the technology is still at the pilot stage. First applications are military bases, where vehicle-to-grid is used to ensure a reliable supply of electricity during black-outs, with limited consideration for the economic viability of everyday operations. Furthermore, aggregation is easier, because all vehicles are owned and operated by the same entity. In fact, after military bases, commercial fleets might be a good starting point for civilian vehicle-to-grid deployment.

Despite the challenges on the long road to deployment, vehicle-to-grid is a dream worth pursuing. If it becomes real, then *“we could have more green power, fewer polluting backup power plants, and no robocalls asking us to switch off the AC on the summer’s hottest days”* (Bakke, 2016, p. 244).





## 2 Reliable Frequency Regulation through Vehicle-to-Grid: Encoding Legislation with Robust Constraints

The grid, then, is built as much from law as from steel, it runs as much on investment strategies as on coal, it produces profits as much as free electrons.  
— Gretchen A. Bakke, *The Grid*, 2016.

Vehicle-to-grid increases the low utilization rate of privately owned electric vehicles by making their batteries available to electricity grids. We formulate a robust optimization problem that maximizes a vehicle owner’s expected profit from selling primary frequency regulation to the grid and guarantees that market commitments are met at all times for all frequency deviation trajectories in a functional uncertainty set that encodes applicable legislation. Faithfully modeling the energy conversion losses during battery charging and discharging renders this optimization problem non-convex. By exploiting a total unimodularity property of the uncertainty set and an exact linear decision rule reformulation, we prove that this non-convex robust optimization problem with functional uncertainties is equivalent to a tractable linear program. Through extensive numerical experiments using real-world data, we quantify the economic value of vehicle-to-grid and elucidate the financial incentives of vehicle owners, aggregators, equipment manufacturers, and regulators. We find that the prevailing penalties for non-delivery of promised regulation power are too low to incentivize vehicle owners to honor their promises toward grid operators.

### 2.1 Introduction

Replacing internal combustion engine vehicles with electric vehicles reduces urban air pollution and mitigates climate change if electricity is generated from renewable sources (Sperling, 1994). In general, privately owned vehicles are a vastly underutilized resource. Vehicle usage data collected by the US Federal Highway Administration (2017) shows that on an average day over 90% of all privately owned vehicles are parked at any one time—even during peak

## Reliable Frequency Regulation through Vehicle-to-Grid: Encoding Legislation with Robust Constraints

---

rush hour. Since electricity grids require storage capacity to integrate increasing amounts of intermittent wind and solar power, electric vehicle owners could capitalize on their batteries by offering storage to the electricity grid when their vehicles are parked. Kempton and Letendre (1997) term this idea *vehicle-to-grid*.

Réseau de transport d'électricité (RTE), Europe's largest transmission system operator, expects to need an additional flexible generation and electricity storage capacity of 10GW to 20GW by 2035. This corresponds to 7.5% to 15% of the total French electricity generation capacity in 2017 (RTE 2017b; 2017c). If electric vehicles were to provide some of this flexibility, then the vehicles and the electricity grid could share the costs of electric vehicle batteries. Kempton and Tomić (2005a) and Noel et al. (2019) have identified *primary frequency regulation*<sup>1</sup> as one of the most profitable flexibility services for vehicle-to-grid. Electric vehicles that provide this service must maintain a continuous power flow to the vehicle battery that is proportional to the deviation of the instantaneous grid frequency from its nominal value (*e.g.*, 50Hz in Europe). As primary frequency regulation is the first flexibility service used to stabilize the electricity network after disturbances (Rebours et al., 2007), its provision must be highly reliable. However, RTE questions the reliability of vehicle-to-grid (RTE 2017b). The European Commission (2017) has recently addressed this concern by defining a minimum level of reliability that electric vehicles and other providers of frequency regulation must guarantee. Specifically, it demands that providers must be able to deliver regulation power for all frequency deviation trajectories with certain characteristics.

Adopting the perspective of a vehicle owner, we formulate an optimization model for determining the bidding strategy on the regulation market that maximizes the expected profit from selling primary frequency regulation to the transmission system operator under the reliability constraints imposed by the European Commission. These constraints must hold *robustly* for all frequency deviation trajectories in an uncertainty set consistent with applicable legislation. As these trajectories constitute continuous-time functions, we are confronted with a robust optimization problem with functional uncertainties. Moreover, the impossibility of simultaneously charging and discharging the battery—which amounts to dissipating energy through conversion losses and could be profitable when the battery is full and there is a reward for down-regulation (see, *e.g.*, (Taylor, 2015, p. 84))—renders the optimization problem non-convex. The main theoretical contribution of this paper is to show that the resulting non-convex robust optimization problem with functional uncertainties is equivalent to a tractable linear program. Specifically, this paper makes the following methodological contributions to robust optimization (see Ben-Tal et al. (2009) for a textbook introduction).

- We introduce new *uncertainty sets in function spaces* that capture those frequency deviation trajectories for which regulation providers must be able to deliver all promised regulation power. These uncertainty sets are reminiscent of the *budget uncertainty sets* by Bertsimas and Sim (2004) in finite-dimensional spaces, and their construction is

---

<sup>1</sup>Primary frequency regulation is also known as primary frequency control and as frequency containment reserves.

inspired by EU legislation.

- By leveraging a *total unimodularity property* of the proposed uncertainty sets and an *exact linear decision rule reformulation*, we prove that the worst-case frequency deviation scenarios in all (convex or non-convex) robust constraints of the vehicle owner’s optimization problem can be found by solving continuous linear programs, which can be viewed as variants of the so-called *separated continuous linear programs* introduced by Anderson et al. (1983).
- By demonstrating that all these continuous linear programs are solved by piecewise constant frequency deviation trajectories, we show that the vehicle owner’s robust optimization problem in continuous time is equivalent to a *robust optimization problem in discrete time*. In doing so, we use more direct proof techniques than Pullan (1995), who derived sufficient conditions under which the solutions of separated continuous linear programs are piecewise constant.
- The robust optimization problem obtained by time discretization is still non-convex. Using the structural properties of its (discretized) uncertainty sets and of its objective and constraint functions, however, we can prove that it is equivalent to a *linear* robust optimization problem that can be reformulated as a *tractable linear program* via standard techniques.

To our best knowledge, robust optimization models with uncertainty sets embedded in function spaces have so far only been considered in the context of robust control, where the primary goal is to develop algorithms for evaluating conservative approximations (Houska, 2011), and in the context of robust continuous linear programming, where the primary goal is to reduce robust to *non*-robust continuous linear programs, which can be addressed with existing algorithms (Ghate, 2020). In contrast, we study here a non-convex robust optimization problem with functional uncertainties that admits a lossless time discretization and can be reformulated *exactly* as a tractable linear program. Remarkably, the state-of-the-art methods for solving the deterministic counterparts of this robust optimization problem are based on methods from mixed-integer linear programming. To our best knowledge, we thus describe the first class of practically relevant mixed-integer linear programs that simplify to standard linear programs through robustification.

As the emerging linear programs are amenable to efficient numerical solution, we are able to perform extensive numerical experiments based on real-world data pertaining to the French electricity system. We define the *value of vehicle-to-grid* as the profit from selling primary frequency regulation relative to a baseline scenario in which the vehicle owner does not offer grid services. As our optimization model faithfully captures effective legislation, it enables us to quantify the true value of vehicle-to-grid. This capability is relevant for understanding the economic incentives of different stakeholders such as vehicle owners, aggregators, equipment manufacturers, and regulators. The model developed in this paper enables us to assess how the value of vehicle-to-grid depends on the penalties for non-delivery of promised regulation

## Reliable Frequency Regulation through Vehicle-to-Grid: Encoding Legislation with Robust Constraints

---

power, the size of the uncertainty set, and the vehicle's battery, charger, and mileage. We thus contribute to the growing literature on the impact of contract parameters on electricity storage (Broneske and Wozabal, 2017; Sunar and Birge, 2019). The main insights drawn from our computational experiments can be summarized as follows.

- Based on 2016–2019 data, we show that the value of vehicle-to-grid attainable with a bidding strategy that is *guaranteed* to satisfy all reliability requirements is around 100 € per year and vehicle. Earlier studies based on anticipative bidding strategies that may violate the legal requirements in practice have estimated this value to be four times higher (Codani et al., 2015; Borne, 2019).
- We find a similar value of vehicle-to-grid as Codani et al. (2015) and Borne (2019) if the vehicle owner risks financial penalties for ignoring the legal reliability requirements. This suggests that *current penalties are too low* to incentivize vehicle owners to respect the law.
- We show that the value of vehicle-to-grid saturates at daily plug times above 15 hours. Thus, maximal profits from frequency regulation can be reaped even if the vehicle is disconnected from the grid up to 9 hours per day. This means that vehicle owners still enjoy considerable flexibility as to when to drive, which could help to promote the adoption of vehicle-to-grid.

Beyond vehicle-to-grid, this paper contributes to the literature on the optimal usage of energy storage assets. The value of a storage asset is usually identified with the profit that can be generated through arbitrage by trading the stored commodity on spot or forward markets. If trading is restricted to the spot market and prices are Markovian, it is known that the asset's value is maximized by a basestock policy (Secomandi, 2010). If the commodity is also traded on forward markets, then the high dimensional models of forward curve evolution lead to intractable Markov decision processes that can be addressed with approximate dynamic programming methods (Nadarajah et al., 2015). For systems of interconnected storage assets with large capacities such as hydroelectric reservoirs, medium-term planning over several months or years is necessary. The resulting optimization problems are traditionally addressed with stochastic dynamic programming (Yeh, 1985) or stochastic dual dynamic programming (Pereira and Pinto, 1991). Alternatively, Pritchard et al. (2005) use a two-layer dynamic programming method to optimize the participation of a hydroelectric reservoir in a spot market, where the inner layer maximizes the expected revenues over a stage, which comprises several trading intervals, for a fixed mean and variance of water release over the stage, while the outer layer optimizes the mean and variance of water release over the stages. More recently, Löhn-dorf et al. (2013) combine ideas from stochastic dual dynamic programming and approximate dynamic programming for optimizing the forward trading decisions of hydro storage systems.

Unlike traditional centralized storage assets, decentralized storage assets such as electric vehicles are usually connected to distribution rather than transmission grids. This means that

they face retail and not wholesale electricity prices. While wholesale prices are determined by market mechanisms and thus stochastic, retail prices are often regulated and thus deterministic. Another major difference is that it may take several days to fully charge or discharge centralized storage assets such as hydropower plants, whereas the batteries of electric vehicles can be fully charged and discharged in just a few hours. A daily planning horizon is therefore sufficient for optimizing their usage. In addition, typical vehicle owners can anticipate their driving needs at most one day in advance. One can thus solve the storage management problem in a receding horizon fashion.

The state-of-charge of a vehicle battery depends non-linearly on the power in- and outflows, which leads to non-convex optimization models. If the battery is merely used for arbitrage and market prices are non-negative, then these optimization models admit exact convex relaxations. Conversely, if the battery is used for frequency regulation or if market prices can fall below zero, then a non-convex constraint is needed to prevent the models from dissipating energy by simultaneously charging and discharging the battery (Zhou et al., 2016). If energy conversion losses are negligible and the battery state-of-charge is thus linear in the power flows, then one can model the provision of frequency regulation through adjustable uncertainty sets. Such an approach has been proposed by Zhang et al. (2017) for frequency regulation with building appliances. A stochastic dynamic programming scheme for optimizing the charging and discharging policy of an electric vehicle with linear battery dynamics is proposed by Donadee and Ilić (2014). If energy conversion losses are significant, however, one may still approximate the state-of-charge by a linear decision rule of the uncertain frequency deviations (Warrington et al., 2013). Sortomme and El-Sharkawi (2012) study a similar model under the assumption of perfect foresight.

In practice, several hundreds or thousands of electric vehicles must be aggregated to be able to bid enough reserve power to qualify for participation in the frequency regulation market. Guille and Gross (2009), Han et al. (2010), Wenzel et al. (2018) and Zhang et al. (2021) develop frameworks for controlling the batteries of aggregated vehicles, while the design of contracts between aggregators and vehicle owners is examined by Han et al. (2011) and Broneske and Wozabal (2017). The policy implications for the market entry of electric vehicle aggregators are investigated by Borne et al. (2018). Yet the study of vehicle-to-grid schemes for individual vehicles remains relevant because they constitute important building blocks for aggregation schemes and because they still pose many challenges—especially when it comes to faithfully modeling all major sources of uncertainty.

The model developed in this paper is most closely related to the discrete-time robust optimization models by Yao et al. (2017) and Namor et al. (2019), which capture the uncertainty of the frequency deviations through simplicial uncertainty sets that cover all empirical frequency deviation scenarios. However, these uncertainty sets may fail to include unseen future frequency deviation scenarios and are inconsistent with applicable EU legislation. While Yao et al. (2017) disregard energy conversion losses, Namor et al. (2019) account for them heuristically and test the resulting charging and discharging policies experimentally on a real battery. Heuristics

## Reliable Frequency Regulation through Vehicle-to-Grid: Encoding Legislation with Robust Constraints

---

are also common in pilot projects that demonstrate the use of vehicle-to-grid for frequency regulation (Vandael et al., 2013, 2020).

The model proposed in this paper relies on three simplifying assumptions that we justify below.

Our first key assumption is that the provision of frequency regulation has no negative impact on battery lifetime—even though the fear of battery degradation has been identified as a major obstacle to the widespread adoption of vehicle-to-grid (Lauinger et al., 2017). To justify this assumption, we point out that the impact of vehicle-to-grid on battery longevity is not yet well understood. In fact, Dubarry et al. (2017) claim that such degradation is severe, while Uddin et al. (2017) claim that vehicle-to-grid may actually extend battery lifetime. In (Uddin et al., 2018), the authors of these two studies reconcile their contradictory findings by concluding that the impact of vehicle-to-grid depends on the operating conditions of the battery, such as its temperature and variations in its state-of-charge. We further justify our no-degradation assumption by restricting the battery state-of-charge to lie within 20% and 80% of the nominal battery capacity. Thompson (2018) suggests these restrictions as a rule of thumb for extending the lifetime of common lithium-ion batteries, and Sweda et al. (2017) adopt similar rules to optimize recharging policies of electric vehicles. Models that account for battery degradation are studied by He et al. (2016) and Carpentier et al. (2019).

Our second key assumption is that vehicle owners can specify time and energy windows for their driving needs one day in advance. This assumption makes sense for commuters who adhere to predictable daily routines, for example.

The third key assumption is that the vehicle owners are price takers who influence neither the market prices nor the grid frequency. This assumption is reasonable because one vehicle may cover at most several kilowatts of the 700 megawatts required for frequency regulation in France. A model of a regulation provider influencing the grid frequency is described by Mercier et al. (2009).

The paper proceeds as follows. Section 2.2 formulates the vehicle owner’s decision problem for a single day as a non-convex robust program with functional uncertainties. In Sections 2.3 and 2.4 we show that this problem can be reformulated equivalently as a non-convex robust program with vectorial uncertainties and even as a tractable linear program, respectively. Section 2.5 formulates a decision problem that looks several days into the future and shows that the resulting multistage model is still equivalent to a linear program. Numerical experiments are discussed in Section 2.6, and policy insights are distilled in Section 2.7. All proofs are relegated to Appendix 2.C.

**Notation.** All random variables are designated by tilde signs. Their realizations are denoted by the same symbols without tildes. Vectors and matrices are denoted by lowercase and uppercase boldface letters, respectively. For any  $z \in \mathbb{R}$ , we define  $[z]^+ = \max\{z, 0\}$  and  $[z]^- =$

$\max\{-z, 0\}$  such that  $z = [z]^+ - [z]^-$ . The intersection of a set  $\mathcal{A} \subseteq \mathbb{R}^d$  with  $\mathbb{R}_+^d$  is denoted by  $\mathcal{A}^+$ . For any closed intervals  $\mathcal{T}, \mathcal{U} \subseteq \mathbb{R}$ , we define  $\mathcal{L}(\mathcal{T}, \mathcal{U})$  as the space of all Riemann integrable functions  $f : \mathcal{T} \rightarrow \mathcal{U}$ , and we denote the intersection of a set  $\mathcal{B} \subseteq \mathcal{L}(\mathcal{T}, \mathbb{R})$  with  $\mathcal{L}(\mathcal{T}, \mathbb{R}_+)$  as  $\mathcal{B}^+$ .

## 2.2 Problem Description

Consider an electric vehicle whose state at any time  $t$  is characterized by the amount of energy  $y(t)$  stored in its battery and the instantaneous power consumption for driving  $d(t)$ . We require that  $y(t)$  is never smaller than  $\underline{y}$  and never larger than  $\bar{y}$ . To mitigate battery degradation, we set these limits to 20% and 80% of the nominal battery capacity, respectively. The battery interacts with the power grid through a bidirectional charger with charging efficiency  $\eta^+ \in (0, 1]$  and discharging efficiency  $\eta^- \in (0, 1]$ , where an efficiency of 1 corresponds to a lossless energy conversion between the grid and the battery. The charger is further characterized by its maximum power consumption  $\bar{y}^+(t)$  from the grid and its maximum power provision to the grid  $\bar{y}^-(t)$ . The power the battery can charge or discharge is therefore limited by  $\eta^+ \bar{y}^+(t)$  and  $\frac{1}{\eta^-} \bar{y}^-(t)$ , respectively. Note that  $\bar{y}^+(t)$  and  $\bar{y}^-(t)$  depend on the charger to which the vehicle is connected at time  $t$ . When the vehicle is not connected to any charger, *e.g.*, when it is driving, then both  $\bar{y}^+(t)$  and  $\bar{y}^-(t)$  must vanish. A stationary battery can be modeled by setting  $d(t) = 0$  and keeping  $\bar{y}^+(t)$  and  $\bar{y}^-(t)$  constant for all  $t$ .

In order to charge the battery at time  $t$ , the vehicle owner may buy power  $x^b(t)$  from the local utility at a known time-varying price  $p^b(t)$  as is the case under dynamic pricing schemes or day/night tariffs. In addition, she may also use the vehicle battery to earn extra revenue by providing primary frequency regulation, which can be viewed as an insurance bought by the transmission system operator (TSO) to balance unforeseen mismatches of electricity demand and supply in real time (Glover et al., 2010). If there is more supply than demand, the frequency of the power grid rises. Conversely, if there is more demand than supply, the frequency falls. A battery owner offering regulation power  $x^r(t)$  at time  $t$  is obliged to change her nominal power consumption  $x^b(t)$  from the grid by  $\delta(t)x^r(t)$ , where  $\delta(t)$  quantifies the normalized deviation of the instantaneous grid frequency  $f(t)$  from its nominal value  $f_0$  (Gestionnaire du Réseau de Transport d'Electricité, 2009). Formally, we have

$$\delta(t) = \begin{cases} +1 & \text{if } f(t) > f_0 + \Delta f, \\ \frac{f(t) - f_0}{\Delta f} & \text{if } f_0 - \Delta f \leq f(t) \leq f_0 + \Delta f, \\ -1 & \text{if } f(t) < f_0 - \Delta f, \end{cases}$$

where  $\Delta f > 0$  is a threshold beyond which all promised regulation power must be delivered.

The TSO contracts frequency regulation as an insurance over a prescribed planning horizon of length  $T$ , *e.g.*, one day. The planning horizon is subdivided into trading intervals  $\mathcal{T}_k = [(k-1)\Delta t, k\Delta t)$  for all  $k \in \mathcal{K} = \{1, \dots, K\}$ , where  $K = \frac{T}{\Delta t} \in \mathbb{N}$ . In the French electricity market, for example, the length  $\Delta t$  of a trading interval is 30 minutes. The TSO requests the vehicle



## Reliable Frequency Regulation through Vehicle-to-Grid: Encoding Legislation with Robust Constraints

---

owner to announce the market decisions  $x^b(t)$  and  $x^r(t)$  before the beginning of the planning horizon, *e.g.*, one day ahead at noon (Réseau de transport d'électricité, 2017a). These decisions need to be piecewise constant over the trading intervals. The TSO compensates the vehicle owner for the frequency regulation  $x^r(t)$  made available at the *availability price*  $p^a(t)$  and charges her for the increase  $\delta(t)x^r(t)$  in her power consumption at the *delivery price*  $p^d(t)$ . Note that this charge becomes negative (*i.e.*, it becomes a remuneration) if  $\delta(t)$  is negative. In summary, the vehicle owner's total cost over the planning horizon  $\mathcal{T} = [0, T]$  amounts to

$$\int_0^T p^b(t)x^b(t) - \left(p^a(t) - \delta(t)p^d(t)\right)x^r(t) dt.$$

The impact of providing frequency regulation on the battery state-of-charge depends on how the vehicle owner adjusts the power consumed from and the power injected into the grid to achieve the desired net power consumption  $x^b(t) + \delta(t)x^r(t)$ . The most energy-efficient way is to avoid unnecessary energy conversion losses resulting from simultaneously charging and discharging. Sometimes, however, such losses can be attractive, for example if the battery is almost full and receives a request for down-regulation ( $\delta(t) > 0$ ). Zhou et al. (2016) show that energy losses can also be attractive when electricity prices are negative. Since common chargers are not able to simultaneously charge and discharge, we forbid this option and set the charging rate to

$$y^+ \left( x^b(t), x^r(t), \delta(t) \right) = \left[ x^b(t) + \delta(t)x^r(t) \right]^+ \quad (2.1a)$$

and the discharging rate to

$$y^- \left( x^b(t), x^r(t), \delta(t) \right) = \left[ x^b(t) + \delta(t)x^r(t) \right]^-. \quad (2.1b)$$

**Remark 2.1.** When operating a vehicle fleet, some vehicles could charge while others discharge, which suggests that the regulation profits achievable with  $n$  vehicles may exceed the regulation profit of a single vehicle multiplied by  $n$ . In this paper, we focus on the case  $n = 1$ .  $\square$

The power exchanged with the grid and the power needed for driving determine the battery state-of-charge at any time  $t$  via the integral equation

$$y \left( x^b, x^r, \delta, y_0, t \right) = y_0 + \int_0^t \eta^+ y^+ \left( x^b(t'), x^r(t'), \delta(t') \right) - \frac{y^- \left( x^b(t'), x^r(t'), \delta(t') \right)}{\eta^-} - d(t') dt', \quad (2.2)$$

where  $y_0$  represents the state-of-charge at time 0. For later use, we establish here some basic properties of the battery state-of-charge.

**Proposition 2.1.** *Holding all other factors fixed, the battery state-of-charge  $y(x^b, x^r, \delta, y_0, t)$  is concave nondecreasing in  $x^b$ , concave in  $x^r$ , concave nondecreasing in  $\delta$ , and affine nondecreasing in  $y_0$ .*

At the time when the vehicle owner needs to choose and report the market commitments

$x^b(t)$  and  $x^r(t)$ , she has no knowledge of the uncertain future frequency deviations  $\delta(t)$  and the delivery prices  $p^d(t)$  at time  $t \in \mathcal{T}$ . In addition, she has no means to predict the battery state-of-charge  $y_0$  at the beginning of the planning horizon, which depends on market commitments chosen on the previous day and on the uncertain frequency deviations to be revealed until time 0. By contrast, the availability prices  $p^a(t)$  for  $t \in \mathcal{T}$  can be assumed to be known at the planning time. In practice, these prices are determined by an auction. As the vehicle owner bids an offer curve expressing  $x^r(t)$  as a function of  $p^a(t)$  for any  $t \in \mathcal{T}$ , it is as if the availability prices were known upfront.<sup>II</sup> Next, we describe the information that is available about the uncertain problem parameters  $\delta$ ,  $p^d$ , and  $y_0$ .

We first discuss the uncertainty in the frequency deviations, which limits the amount of reserve power that can be sold on the market. Indeed, the vehicle owner must ensure that the battery state-of-charge will never drop below  $\underline{y}$  or exceed  $\bar{y}$  when the TSO requests down-regulation ( $\delta(t) < 0$ ) or up-regulation ( $\delta(t) > 0$ ), respectively, for a prescribed set of conceivable frequency deviation scenarios. Otherwise, the vehicle owner may not be able to honor her market commitments, in which case the TSO may charge a penalty or even ban her from the market.

The TSO defines under what conditions regulation providers must be able to deliver the promised regulation power, keeping in mind that extreme frequency deviations are uncommon. Indeed, between 2015 and 2018 the frequency deviation  $\delta(t)$  has never attained its theoretical maximum of 1 or its theoretical minimum of  $-1$  in the French market.<sup>III</sup> In the following, we thus assume that the vehicle owner needs to guarantee the delivery of regulation power *only* for frequency deviation scenarios within the uncertainty set

$$\mathcal{D} = \left\{ \delta \in \mathcal{L}(\mathcal{T}, [-1, 1]) : \int_{[t-\Gamma]^+}^t |\delta(t')| dt' \leq \gamma \quad \forall t \in \mathcal{T} \right\}$$

parametrized by the duration  $\Gamma \in \mathbb{R}_+$  of a *regulation cycle* and the duration  $\gamma \in \mathbb{R}_+$  of an *activation period*. Throughout this paper, we assume that  $0 < \gamma \leq \Gamma \leq T$ . By focusing on frequency deviation scenarios in  $\mathcal{D}$ , one stipulates that consecutive extreme frequency deviations  $\delta(t) \in \{-1, 1\}$  can occur at most over one activation period within each regulation cycle. The *activation ratio*  $\gamma/\Gamma$  can thus be interpreted as the percentage of time during which the vehicle owner must be able to deliver all committed reserve power.

**Remark 2.2.** Note that the uncertainty set  $\mathcal{D}$  grows with  $\gamma$  and shrinks with  $\Gamma$ . □

Besides displaying favorable computational properties, the uncertainty set  $\mathcal{D}$  has conceptual appeal because it formalizes the delivery guarantee rules prescribed by the European Commission (2017). These rules stipulate that the “*minimum activation period to be ensured by [frequency regulation] providers [is not to be] greater than 30 or smaller than 15 minutes.*” This guideline prompts us to set  $\gamma = 30$  minutes. The EU further demands that regulation providers “*shall ensure the recovery of [their] energy reservoirs as soon as possible, within 2 hours after the*

<sup>II</sup>The bidding process is described at [https://www.entsoe.eu/network\\_codes/eb/fcr/](https://www.entsoe.eu/network_codes/eb/fcr/).

<sup>III</sup>The French TSO publicizes frequency measurements at <http://clients.rte-france.com/>.

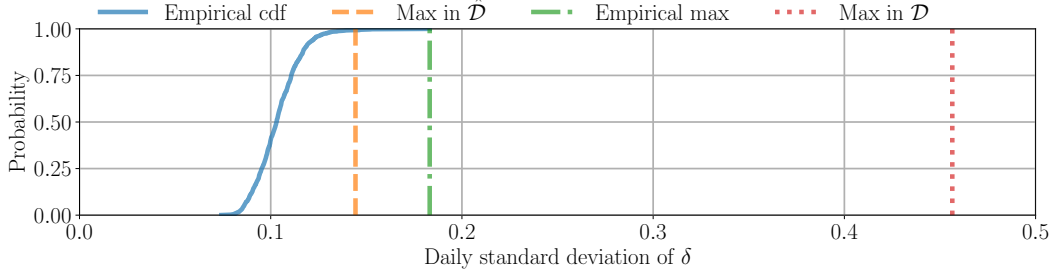


Figure 2.1: Empirical cumulative distribution function (cdf) of the daily standard deviation of  $\delta$  and the maximum standard deviation of any scenario in  $\hat{\mathcal{D}}$  or in  $\mathcal{D}$ .

*end of the alert state.*” This means that, although there may be several activation periods of 30 minutes within any 2.5 hour interval, the regulation provider only has to cover one of them. Thus, we set  $\Gamma = 2.5$  hours.

In the following, we compare the empirical distribution of the daily variance of  $\delta$  between the years 2017 and 2019 with the maximum variance that can be achieved by any hypothetical frequency deviation scenario  $\delta \in \mathcal{D}$  for a planning horizon of one day. By slight abuse of notation, we define the variance of a frequency deviation scenario  $\delta$  with respect to zero as  $\text{Var}(\delta) = \frac{1}{T} \int_0^T \delta(t)^2 dt$ . This is justified because the TSO protects the system against *unforeseen* demand and supply fluctuations, which means that the frequency deviations should be unbiased and thus vanish on average. Indeed, the empirical frequency deviations have an average of  $5.98 \cdot 10^{-4}$ .

**Proposition 2.2.** *If  $\delta \in \mathcal{D}$ , then  $\text{Var}(\delta) \leq \lceil T/\Gamma \rceil \gamma / T$ .*

Figure 2.1 shows that if  $T = 1$  day,  $\gamma = 30$  minutes, and  $\Gamma = 2.5$  hours, then the maximum standard deviation of any  $\delta \in \mathcal{D}$  exceeds the maximum empirical standard deviation by a factor of 2.5. Thus,  $\mathcal{D}$  contains extreme frequency deviation scenarios with unrealistically high variance.

The optimization model developed below not only involves the conservative uncertainty set  $\mathcal{D}$  compatible with the guidelines of the European Commission but also a smaller uncertainty set

$$\hat{\mathcal{D}} = \left\{ \delta \in \mathcal{L}(\mathcal{T}, [-1, 1]) : \int_{[t-\hat{\Gamma}]^+}^t |\delta(t')| dt' \leq \hat{\gamma} \forall t \in \mathcal{T} \right\}$$

parametrized by  $\hat{\Gamma} \geq \Gamma$  and  $\hat{\gamma} \leq \gamma$ . This uncertainty set contains only frequency deviation scenarios that are likely to materialize under normal operating conditions. Note that  $\hat{\mathcal{D}}$  is obtained from  $\mathcal{D}$  by inflating  $\Gamma$  to  $\hat{\Gamma}$  and shrinking  $\gamma$  to  $\hat{\gamma}$ . By Remark 2.2, we may thus conclude that  $\hat{\mathcal{D}}$  is indeed a subset of  $\mathcal{D}$ . While the pessimistic uncertainty set  $\mathcal{D}$  is used to enforce the stringent delivery guarantees imposed by the European Commission, the more optimistic uncertainty set  $\hat{\mathcal{D}}$  is used to model a softer reachability guarantee for the terminal state-of-

charge. In the numerical experiments we will set  $\hat{\Gamma} = T = 1$  day and  $\hat{\gamma} = \gamma = 30$  minutes. By Proposition 2.2, the variance of all frequency deviation scenarios in  $\hat{\mathcal{D}}$  is therefore bounded above by  $\Delta t/T = 1/48$ . Empirically, this threshold exceeds the variance of the frequency deviation on 99.2% of all days in the years from 2017 to 2018.

Next, we discuss the uncertainty in the initial battery state-of-charge  $y_0$ . Recall that  $y_0$  is uncertain at the time when  $x^b$  and  $x^r$  are chosen because it depends on how much regulation energy must be provided until the beginning of the planning horizon. This quantity depends itself on uncertain frequency deviations that have not yet been revealed. We assume that the vehicle owner constructs two confidence intervals  $\mathcal{Y}_0 = [\underline{y}_0, \bar{y}_0]$  and  $\hat{\mathcal{Y}}_0 = [\underline{\hat{y}}_0, \bar{\hat{y}}_0]$  for  $y_0$ , either taking into account all frequency deviations under which she must imperatively be able to deliver regulation power or only those frequency deviations that are likely to occur under normal operating conditions.

The only assumption we make about the uncertainty in the delivery price  $p^d$  is that the vehicle owner can reliably estimate the *expected* regulation price  $p^r(t) = p^a(t) + \mathbb{E}[\tilde{\delta}(t)\tilde{p}^d(t)]$ .

We are now ready to formalize the vehicle owner's decision problem for selecting the market decisions  $x^b$  and  $x^r$ . The primary objective is to minimize the expected cost

$$c(x^b, x^r) = \mathbb{E} \int_{\mathcal{T}} p^b(t)x^b(t) - \left( p^a(t) + \tilde{\delta}(t)\tilde{p}^d(t) \right) x^r(t) dt = \int_{\mathcal{T}} p^b(t)x^b(t) - p^r(t)x^r(t) dt, \quad (2.3)$$

while ensuring that  $x^b$  and  $x^r$  are robustly feasible across all frequency deviation scenarios  $\delta \in \mathcal{D}$  and initial battery states  $y_0 \in \mathcal{Y}_0$ . Mathematically, the charging rate  $y^+(x^b(t), x^r(t), \delta(t))$ , the discharging rate  $y^-(x^b(t), x^r(t), \delta(t))$ , and the battery state-of-charge  $y(x^b, x^r, \delta, t, y_0)$  must therefore satisfy the robust constraints

$$\left. \begin{aligned} y^+(x^b(t), x^r(t), \delta(t)) &\leq \bar{y}^+(t), & y(x^b, x^r, \delta, y_0, t) &\leq \bar{y}, \\ y^-(x^b(t), x^r(t), \delta(t)) &\leq \bar{y}^-(t), & y(x^b, x^r, \delta, y_0, t) &\geq \underline{y} \end{aligned} \right\} \forall t \in \mathcal{T}, \forall \delta \in \mathcal{D}, \forall y_0 \in \mathcal{Y}_0.$$

As the vehicle owner continues to use the vehicle for driving and for offering grid services after the end of the planning horizon, the battery should end up in a state that is “*conducive to satisfactory future operations*” (Yeh, 1985). Consequently, the vehicle owner aims to steer  $y(x^b, x^r, \delta, y_0, T)$  to a desirable state-of-charge  $y$ . We assume that the cost-to-go of any  $y \in [\underline{y}, \bar{y}]$  is quantified by a convex and piecewise affine value function  $\varphi(y) = \max_{n \in \mathcal{N}} \{a_n y + b_n\}$  determined by  $a_n, b_n \in \mathbb{R}$  for all  $n \in \mathcal{N} = \{1, \dots, N\}$ . In Section 2.5, we will present a principled approach to calibrate these coefficients by solving a dynamic programming problem over multiple periods of length  $T$ . As  $y_0$  and  $\delta$  are uncertain, the terminal state-of-charge is also uncertain. To trade off present versus future costs, it is therefore reasonable to minimize  $\varphi(y(x^b, x^r, \delta, y_0, T))$  in view of the worst of all scenarios  $\delta \in \hat{\mathcal{D}}$  and  $y_0 \in \hat{\mathcal{Y}}_0$ . This can be achieved by adding the term  $\max_{\delta \in \hat{\mathcal{D}}} \max_{y_0 \in \hat{\mathcal{Y}}_0} \varphi(y(x^b, x^r, \delta, y_0, T))$  to the objective func-

## Reliable Frequency Regulation through Vehicle-to-Grid: Encoding Legislation with Robust Constraints

tion (2.3). In summary, the vehicle owner's decision problem can be cast as the following robust optimization problem with continuous (functional) uncertain parameters,

$$\begin{aligned}
\min_{x^b, x^r \in \mathcal{X}} \quad & c(x^b, x^r) + \max_{\delta \in \hat{\mathcal{D}}, y_0 \in \hat{\mathcal{Y}}_0} \varphi(y(x^b, x^r, \delta, y_0, T)) \\
\text{s.t.} \quad & y^+(x^b(t), x^r(t), \delta(t)) \leq \bar{y}^+(t) \quad \forall \delta \in \mathcal{D}, \forall t \in \mathcal{T} \\
& y^-(x^b(t), x^r(t), \delta(t)) \leq \bar{y}^-(t) \quad \forall \delta \in \mathcal{D}, \forall t \in \mathcal{T} \\
& y(x^b, x^r, \delta, y_0, t) \leq \bar{y} \quad \forall \delta \in \mathcal{D}, \forall t \in \mathcal{T}, \forall y_0 \in \mathcal{Y}_0 \\
& y(x^b, x^r, \delta, y_0, t) \geq \underline{y} \quad \forall \delta \in \mathcal{D}, \forall t \in \mathcal{T}, \forall y_0 \in \mathcal{Y}_0,
\end{aligned} \tag{R}$$

where  $\mathcal{X}$  denotes the set of all functions in  $\mathcal{L}(\mathcal{T}, \mathbb{R}_+)$  that are constant on the trading intervals. Using the conservative uncertainty sets  $\mathcal{D}$  and  $\mathcal{Y}_0$  in the constraints ensures that the delivery guarantee dictated by the European Commission can be fulfilled. Failing to fulfill this guarantee might lead to exclusion from the regulation market. In contrast, there are no drastic consequences of reaching an undesirable state-of-charge at time  $T$ . Hence, we use the less conservative uncertainty sets  $\hat{\mathcal{D}}$  and  $\hat{\mathcal{Y}}_0$  in the objective function, to steer the terminal state-of-charge toward a desirable value under all reasonably likely frequency deviation scenarios. The use of different uncertainty sets in the same model has previously been proposed in robust portfolio insurance problems (Zymler et al., 2011).

Recall from Proposition 2.1 that the function  $y(x^b, x^r, \delta, y_0, t)$  is concave in the decision variables  $x^b$  and  $x^r$ . Upper bounds on this function thus constitute non-convex constraints. This implies that (R) represents a non-convex robust optimization problem with functional uncertain parameters. In general, such problems are severely intractable.

**Remark 2.3** (Uncertain driving patterns). Although model (R) assumes deterministic driving patterns, it readily extends to uncertain driving times and distances. If it is only known that the vehicle will drive at some time within a prespecified interval, then the vehicle owner must not plan on exchanging any electricity with the grid during that interval. Similarly, if it is only known that the vehicle will drive some distance within a certain range, then the vehicle owner must plan with the low end of the range for the constraint on the maximum state-of-charge and with the high end of the range for the constraint on the minimum state-of-charge. The worst-case driving times and distances are thus independent of the vehicle owner's decisions and can be determined *ex-ante*.  $\square$

## 2.3 Time Discretization

In order to derive a lossless time discretization of the frequency deviation scenarios in problem (R), we assume from now on that the power demand for driving and the maximum charge and discharge power of the vehicle charger remain constant over the trading intervals. This assumption is justified because a vehicle that is both driving and parking in the same trading interval cannot offer constant market bids and is therefore unable to participate in the electricity market. Although the power demand for driving may fluctuate wildly, the bat-

tery state-of-charge cannot increase while the vehicle is driving, and therefore the power consumption for driving can be averaged over trading intervals without loss of generality. Note that we do *not* assume the frequency deviation scenarios  $\delta$  to remain constant over the trading intervals. In practice  $\delta$  may fluctuate on time scales of the order of milliseconds, and averaging out the frequency deviations across a trading interval could result in a dangerous oversimplification of reality. This phenomenon is illustrated in the following example.

**Example 2.1** (Risks of ignoring intra-period fluctuations). As the market decisions  $x^b$  and  $x^r$ , the power demand  $d$  and the charging limits  $\bar{y}^+$  and  $\bar{y}^-$  are piecewise constant, one might be tempted to replace the frequency deviation signal  $\delta$  with a piecewise constant signal obtained by averaging  $\delta$  over the trading intervals. As we will see, however, averaging  $\delta$  relaxes the battery state-of-charge constraints. Decisions  $x^b$  and  $x^r$  that are *infeasible* under the true signal may therefore appear to be feasible under the averaged signal. Hence, replacing the true signal with the averaged signal could make it impossible for the vehicle owner to honor her market commitments. As a simple example, assume that  $x^b(t) = 0$  and  $x^r(t) = x_1^r > 0$  are constant and that the true frequency deviation signal averages to 0 over the first trading interval  $[0, \Delta t]$ , that is,  $\frac{1}{\Delta t} \int_0^{\Delta t} \delta(t) dt = 0$ . The left chart of Figure 2.2 visualizes two such signals, which display a small and a high total variation and are denoted by  $\delta^{(1)}$  and  $\delta^{(2)}$ , respectively. The constant signal equal to their (vanishing) average over  $[0, \Delta t]$  is denoted by  $\delta^{(3)}$ . If  $\delta^{(1)}$  reflects reality but is incorrectly replaced with  $\delta^{(3)}$ , we are led to believe that the state-of-charge will remain constant at  $y_0$ . In reality, however, the battery dissipates the amount  $\Delta \eta x_1^r \Delta t / 2$  of energy over the first trading interval, where  $\Delta \eta = \frac{1}{\eta^-} - \eta^+ \geq 0$ , and the state-of-charge temporarily rises above  $y_0$  by  $\eta^+ x_1^r \Delta t / 2$ . If  $\delta^{(2)}$  reflects reality, on the other hand, then the repeated charging and discharging of the battery still dissipates energy. See the right chart of Figure 2.2 for a visualization. While scenario  $\delta^{(1)}$  is contrived for maximum impact, scenario  $\delta^{(2)}$  rapidly fluctuates around 0 and thus captures a stylized fact that one would expect to see in reality. This example suggests that finding the minimum or the maximum of the state-of-charge over the entire planning horizon and over all signals  $\delta \in \mathcal{D}$  should be non-trivial because intra-period fluctuations *do* matter. As a further complication, note that the constraints of the uncertainty set  $\mathcal{D}$  couple the frequency deviations across time.  $\square$

We will now argue that, in spite of Example 2.1,  $\mathcal{D}$  and  $\hat{\mathcal{D}}$  can be restricted to contain only piecewise constant frequency deviation signals *without* relaxing problem (R). To formalize the reasoning about piecewise constant functions, we introduce a lifting operator  $L : \mathbb{R}^K \rightarrow \mathcal{L}(\mathcal{T}, \mathbb{R})$  that maps any vector  $\mathbf{v} \in \mathbb{R}^K$  to a piecewise constant function  $L\mathbf{v}$  with  $K$  pieces defined through  $(L\mathbf{v})(t) = v_k$  if  $t \in \mathcal{T}_k$ ,  $k \in \mathcal{K} = \{1, \dots, K\}$ . We also introduce the adjoint operator  $L^\dagger : \mathcal{L}(\mathcal{T}, \mathbb{R}) \rightarrow \mathbb{R}^K$  that maps any function  $w \in \mathcal{L}(\mathcal{T}, \mathbb{R})$  to a  $K$ -dimensional vector  $L^\dagger w$  defined through  $(L^\dagger w)_k = \frac{1}{\Delta t} \int_{\mathcal{T}_k} w(t) dt$  for all  $k \in \mathcal{K}$ . Note that  $L$  and  $L^\dagger$  are indeed adjoint to each other because  $\int_{\mathcal{T}} (L\mathbf{v})(t) w(t) dt = \mathbf{v}^\top L^\dagger(w)$  for all  $\mathbf{v} \in \mathbb{R}^K$  and  $w \in \mathcal{L}(\mathcal{T}, \mathbb{R})$ . Mathematically, we impose from now on the following assumption.

**Assumption 2.1.** The functions  $d$ ,  $\bar{y}^+$  and  $\bar{y}^-$  are piecewise constant, that is, there exist  $\mathbf{d}, \bar{\mathbf{y}}^+, \bar{\mathbf{y}}^- \in \mathbb{R}^K$  such that  $d = L\mathbf{d}$ ,  $\bar{y}^+ = L\bar{\mathbf{y}}^+$  and  $\bar{y}^- = L\bar{\mathbf{y}}^-$ .

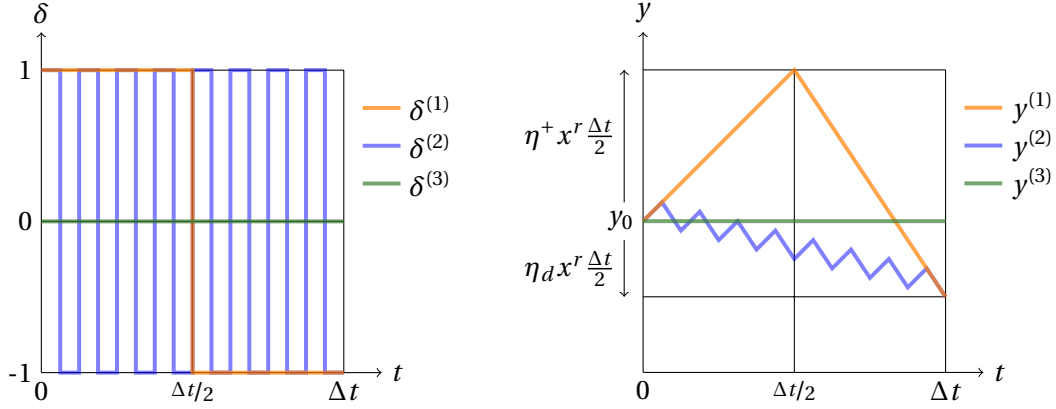


Figure 2.2: Frequency deviation signals (left) and their state-of-charge trajectories (right).

Next, we introduce a discretized uncertainty set

$$\mathcal{D}_{\mathcal{K}} = \left\{ \delta \in [-1, 1]^K : \sum_{l=1+[k-\Gamma/\Delta t]^+}^k |\delta_l| \leq \frac{\gamma}{\Delta t} \forall k \in \mathcal{K} \right\}$$

reminiscent of  $\mathcal{D}$ , where  $\Gamma/\Delta t$  and  $\gamma/\Delta t$  count the trading intervals within a regulation cycle and an activation period, respectively. Similarly, we define a smaller discretized uncertainty set  $\hat{\mathcal{D}}_{\mathcal{K}} \subseteq \mathbb{R}^K$  reminiscent of  $\hat{\mathcal{D}}$ , which is obtained from  $\mathcal{D}_{\mathcal{K}}$  by replacing  $\Gamma$  with  $\hat{\Gamma}$  and  $\gamma$  with  $\hat{\gamma}$ . In the remainder we impose the following divisibility assumption.

**Assumption 2.2.** The parameters  $\Gamma$ ,  $\gamma$ ,  $\hat{\Gamma}$  and  $\hat{\gamma}$  are (positive) multiplies of  $\Delta t$ .

The discretized uncertainty sets are of interest because of the following proposition.

**Proposition 2.3.** *The following statements hold.*

- (i)  $L\mathcal{D}_{\mathcal{K}} \subseteq \mathcal{D}$  and  $L^\dagger \mathcal{D} = \mathcal{D}_{\mathcal{K}}$ .
- (ii)  $L\mathcal{D}_{\mathcal{K}}^+ \subseteq \mathcal{D}^+$  and  $L^\dagger \mathcal{D}^+ = \mathcal{D}_{\mathcal{K}}^+$ .

Next, we define the finite-dimensional feasible set  $\mathcal{X}_{\mathcal{K}} = L^\dagger \mathcal{X}$ . As  $\mathcal{X}$  contains only piecewise constant functions, we have  $\mathcal{X} = L\mathcal{X}_{\mathcal{K}}$ . We further define the cost function  $c_{\mathcal{K}}(\mathbf{x}^b, \mathbf{x}^r) = c(L\mathbf{x}^b, L\mathbf{x}^r)$ , which is linear in  $\mathbf{x}^b \in \mathbb{R}^K$  and  $\mathbf{x}^r \in \mathbb{R}^K$ . In addition, for any  $k \in \mathcal{K}$  we define the function

$$\begin{aligned} y_k(\mathbf{x}^b, \mathbf{x}^r, \delta, y_0) &= y(L\mathbf{x}^b, L\mathbf{x}^r, L\delta, y_0, k\Delta t) \\ &= y_0 + \Delta t \sum_{l=1}^k \eta^+ y^+(x_l^b, x_l^r, \delta_l) - \frac{1}{\eta^-} y^-(x_l^b, x_l^r, \delta_l) - d_l, \end{aligned} \quad (2.4)$$

which represents the battery state-of-charge at the end of period  $k$  under the assumption that both the market bids and the frequency deviations are piecewise constant.

**Proposition 2.4.** *Holding all other factors fixed,  $y_k(\mathbf{x}^b, \mathbf{x}^r, \boldsymbol{\delta}, y_0)$  is concave nondecreasing in  $\mathbf{x}^b$ , concave in  $\mathbf{x}^r$ , concave nondecreasing in  $\boldsymbol{\delta}$ , and linear nondecreasing in  $y_0$  for any  $k \in \mathcal{K}$ .*

We are now ready to define the discrete-time counterpart of the robust optimization problem (R).

$$\begin{aligned}
 \min_{\mathbf{x}^b, \mathbf{x}^r \in \mathcal{X}_{\mathcal{K}}} \quad & c_{\mathcal{K}}(\mathbf{x}^b, \mathbf{x}^r) + \max_{\boldsymbol{\delta} \in \mathcal{D}_{\mathcal{K}}, y_0 \in \mathcal{Y}_0} \varphi(y_K(\mathbf{x}^b, \mathbf{x}^r, \boldsymbol{\delta}, y_0)) \\
 \text{s.t.} \quad & y^+(x_k^b, x_k^r, \delta_k) \leq \bar{y}_k^+ \quad \forall \boldsymbol{\delta} \in \mathcal{D}_{\mathcal{K}}, \forall k \in \mathcal{K} \\
 & y^-(x_k^b, x_k^r, \delta_k) \leq \bar{y}_k^- \quad \forall \boldsymbol{\delta} \in \mathcal{D}_{\mathcal{K}}, \forall k \in \mathcal{K} \\
 & y_k(\mathbf{x}^b, \mathbf{x}^r, \boldsymbol{\delta}, y_0) \leq \bar{y} \quad \forall \boldsymbol{\delta} \in \mathcal{D}_{\mathcal{K}}, \forall k \in \mathcal{K} \cup \{0\}, \forall y_0 \in \mathcal{Y}_0 \\
 & y_k(\mathbf{x}^b, \mathbf{x}^r, \boldsymbol{\delta}, y_0) \geq \underline{y} \quad \forall \boldsymbol{\delta} \in \mathcal{D}_{\mathcal{K}}, \forall k \in \mathcal{K} \cup \{0\}, \forall y_0 \in \mathcal{Y}_0
 \end{aligned} \tag{R_{\mathcal{K}}}$$

Unlike the original problem (R), the discrete-time counterpart (R<sub>ℳ</sub>) constitutes a standard robust optimization problem that involves only finite-dimensional uncertain parameters. For this reason, there is hope that (R<sub>ℳ</sub>) is easier to solve than (R).

**Theorem 2.1** (Lossless time discretization). *The problems (R) and (R<sub>ℳ</sub>) are equivalent.*

The equivalence of (R) and (R<sub>ℳ</sub>) is perhaps surprising in view of Example 2.1. It means that the worst-case frequency deviation scenarios are piecewise constant even though intra-period fluctuations matter. Theorem 2.1 is proved by showing that the four robust constraints in (R) with functional uncertainties are equivalent to the corresponding robust constraints in (R<sub>ℳ</sub>) with vectorial uncertainties and that the worst-case terminal cost functions in (R) and (R<sub>ℳ</sub>) coincide. For example, the equivalence of the first (second) robust constraints in (R) and (R<sub>ℳ</sub>) follows from the observation that, for any fixed  $t \in \mathcal{T}$ , the left hand side of the first (second) constraint in (R) is maximized by a scenario  $\boldsymbol{\delta} \in \mathcal{D}$  with  $\delta(t) = 1$  ( $\delta(t) = -1$ ), which exists by the definition of  $\mathcal{D}$ . The last two robust constraints in (R) are nonlocal as they depend on the entire frequency deviation scenario  $\boldsymbol{\delta}$  and not only on its value at a particular time. Thus, they are significantly more intricate. The robust upper bound on the state-of-charge can be reformulated as an upper bound on  $\max_{t \in \mathcal{T}} \max_{\boldsymbol{\delta} \in \mathcal{D}} y(\mathbf{x}^b, \mathbf{x}^r, \boldsymbol{\delta}, y_0, t)$ . By using Propositions 2.1 and 2.3, one can then show that the maximum over  $t \in \mathcal{T}$  must be attained at  $t = k\Delta t$  for some  $k \in \mathcal{K} \cup \{0\}$  and that for any such  $t$  the state-of-charge can be expressed as an integral of  $\delta$  against a piecewise constant function. Thus, averaging  $\delta$  across the trading intervals has no impact on the state-of-charge, which in turn allows us to focus on piecewise constant scenarios without restricting generality. The robust lower bound on the state-of-charge in (R) can be reformulated as a lower bound on  $\min_{t \in \mathcal{T}} \min_{\boldsymbol{\delta} \in \mathcal{D}} y(\mathbf{x}^b, \mathbf{x}^r, \boldsymbol{\delta}, y_0, t)$ , which appears to be intractable because the optimization problem over  $\boldsymbol{\delta}$  minimizes a concave function over a convex feasible set and is therefore non-convex. Classical robust optimization provides no general recipe for handling such constraints even if the uncertain parameters are finite-dimensional, and state-of-the-art research settles for deriving approximations (Roos et al., 2020). By exploiting a continuous total unimodularity property of the uncertainty set  $\mathcal{D}$  facilitated by Assumption 2.2, we first prove that the minimum of  $y(\mathbf{x}^b, \mathbf{x}^r, \boldsymbol{\delta}, y_0, t)$  over  $\mathcal{D}$  is attained by a frequency deviation trajec-



tory that takes only values in  $\{-1, 0\}$ . Next, we demonstrate that there exists an affine function of  $\delta$  that matches  $y(x^b, x^r, \delta, y_0, t)$  for all trajectories  $\delta \in \mathcal{D}$  valued in  $\{-1, 0\}$  and for all  $t \in \mathcal{T}$ . In the language of robust optimization, the state-of-charge  $y(x^b, x^r, \delta, y_0, t)$  can be viewed as an analysis variable that adapts to the uncertainty  $\delta$ , and the corresponding affine function constitutes a decision rule approximating  $y(x^b, x^r, \delta, y_0, t)$ . Decision rule approximations almost invariably introduce approximation errors (Ben-Tal et al., 2009, § 14). However, the affine decision rule proposed here is error-free because it coincides with  $y(x^b, x^r, \delta, y_0, t)$  for all scenarios  $\delta \in \mathcal{D}$  valued in  $\{-1, 0\}$  that may attain the worst case in  $\min_{t \in \mathcal{T}} \min_{\delta \in \mathcal{D}} y(x^b, x^r, \delta, y_0, t)$ . Using this decision rule in an elaborate sensitivity analysis, we can finally prove that the minimum over  $t \in \mathcal{T}$  must be attained at  $t = k\Delta t$  for some  $k \in \mathcal{K} \cup \{0\}$  and that for any such  $t$  the state-of-charge can be expressed as an integral of  $\delta$  against a piecewise constant function. Thus, we may focus again on piecewise constant scenarios without restricting generality. The full proof of Theorem 2.1 can be found in Appendix 2.C.

The new robust optimization techniques developed to prove Theorem 2.1 are of independent interest as they provide exact tractable reformulations for certain adjustable robust optimization problems with functional or vectorial uncertain parameters, where the embedded optimization problems over the uncertainty realizations are non-convex. We also note that the embedded optimization problems over  $\delta \in \mathcal{D}$  in problem (R) can be viewed as variants of the so-called *separated continuous linear programs* introduced by Anderson et al. (1983). The proof of Theorem 2.1 shows that these problems are solved by piecewise constant frequency deviation scenarios that can be computed efficiently, thereby extending the purely existential results by Pullan (1995). Our results are also orthogonal to those by Ghate (2020), who proves that *robust* separated continuous linear programs with budget uncertainty sets are equivalent to standard separated continuous linear programs.

Even though the non-convex robust optimization problem (R) with functional uncertainty admits a lossless time discretization, its discrete-time counterpart  $(R_{\mathcal{K}})$  still constitutes a non-convex robust optimization problem and thus appears to be hard. In the next section, however, we will show that (R) can be reformulated as a tractable linear program by exploiting its structural properties.

## 2.4 Linear Programming Reformulation

In order to establish the tractability of the non-convex robust optimization problem (R), it is useful to reformulate its time discretization  $(R_{\mathcal{K}})$  as the following *linear* robust optimization problem, where all constraint functions are bilinear in the decision variables and the uncertain

parameters.

$$\begin{aligned}
 \min \quad & c_{\mathcal{K}}(\mathbf{x}^b, \mathbf{x}^r) + z \\
 \text{s.t.} \quad & \mathbf{x}^b, \mathbf{x}^r \in \mathcal{X}_{\mathcal{K}}, \mathbf{m} \in \mathbb{R}^K \\
 & x_k^r + x_k^b \leq \bar{y}_k^+, \quad x_k^r - x_k^b \leq \bar{y}_k^- \quad \forall k \in \mathcal{K} \\
 & m_k - \eta^+ x_k^r \geq 0, \quad m_k - \frac{1}{\eta^-} x_k^r + \Delta\eta x_k^b \geq 0 \quad \forall k \in \mathcal{K} \\
 & \bar{y}_0 + \Delta t \sum_{l=1}^k \eta^+ (x_l^b + \delta_l x_l^r) - d_l \leq \bar{y} \quad \forall \delta \in \mathcal{D}_{\mathcal{K}}^+, \forall k \in \mathcal{K} \cup \{0\} \\
 & \underline{y}_0 + \Delta t \sum_{l=1}^k \eta^+ x_l^b - m_l \delta_l - d_l \geq \underline{y} \quad \forall \delta \in \mathcal{D}_{\mathcal{K}}^+, \forall k \in \mathcal{K} \cup \{0\} \\
 & \hat{y}_0 + \Delta t \sum_{k=1}^K \eta^+ (x_k^b + \delta_k x_k^r) - d_k \leq \frac{z - b_n}{a_n} \quad \forall \delta \in \hat{\mathcal{D}}_{\mathcal{K}}^+, \forall n \in \mathcal{N}_+ \\
 & \underline{\hat{y}}_0 + \Delta t \sum_{k=1}^K \eta^+ x_k^b - m_k \delta_k - d_k \geq \frac{z - b_n}{a_n} \quad \forall \delta \in \hat{\mathcal{D}}_{\mathcal{K}}^+, \forall n \in \mathcal{N}_- \\
 & z \geq b_n \quad \forall n \in \mathcal{N}_0
 \end{aligned} \tag{R'_{\mathcal{K}}}$$

Here,  $\Delta\eta = \frac{1}{\eta^-} - \eta^+ \geq 0$  is used as a shorthand for the reduction in the battery state-of-charge resulting from first charging and then discharging one unit of energy as seen from the grid. In addition, we set  $\mathcal{N}_+ = \{n \in \mathcal{N} : a_n > 0\}$ ,  $\mathcal{N}_- = \{n \in \mathcal{N} : a_n < 0\}$  and  $\mathcal{N}_0 = \mathcal{N} \setminus (\mathcal{N}_+ \cup \mathcal{N}_-)$ .

**Theorem 2.2** (Lossless linearization). *The problems  $(R_{\mathcal{K}})$  and  $(R'_{\mathcal{K}})$  are equivalent.*

The proof of Theorem 2.2 critically relies on the exact affine decision rule approximation discovered in the proof of Theorem 2.1. Note that the linear robust optimization problem  $(R'_{\mathcal{K}})$  still appears to be difficult because each robust constraint must hold for all frequency deviation scenarios in an uncountable uncertainty set  $\mathcal{D}_{\mathcal{K}}^+$  or  $\hat{\mathcal{D}}_{\mathcal{K}}^+$  and therefore corresponds to a continuum of ordinary linear constraints. Fortunately, standard robust optimization theory (Ben-Tal et al., 2004; Bertsimas and Sim, 2004) allows us to reformulate  $(R'_{\mathcal{K}})$  as the tractable linear program

$$\begin{aligned}
\min \quad & c_{\mathcal{K}}(\mathbf{x}^b, \mathbf{x}^r) + z \\
\text{s.t.} \quad & \mathbf{x}^b, \mathbf{x}^r \in \mathcal{X}_{\mathcal{K}}, z \in \mathbb{R}, \mathbf{m}, \boldsymbol{\lambda}^+, \boldsymbol{\lambda}^-, \boldsymbol{\theta}^+, \boldsymbol{\theta}^- \in \mathbb{R}_+^K, \boldsymbol{\Lambda}^+, \boldsymbol{\Lambda}^-, \boldsymbol{\Theta}^+, \boldsymbol{\Theta}^- \in \mathbb{R}_+^{K \times K} \\
& x_k^r + x_k^b \leq \bar{y}_k^+, \quad x_k^r - x_k^b \leq \bar{y}_k^- \quad \forall k \in \mathcal{K} \\
& m_k \geq \eta^+ x_k^r, \quad m_k \geq \frac{1}{\eta^-} x_k^r - \Delta \eta x_k^b \quad \forall k \in \mathcal{K} \\
& \sum_{l=1}^k \Delta t \left( \eta^+ x_l^b + \Lambda_{k,l}^+ - d_l \right) + \gamma \Theta_{k,l}^+ \leq \bar{y} - \bar{y}_0 \quad \forall k \in \mathcal{K} \cup \{0\} \\
& \sum_{l=1}^k \Delta t \left( \eta^+ x_l^b - \Lambda_{k,l}^- - d_l \right) - \gamma \Theta_{k,l}^- \geq \underline{y} - \underline{y}_0 \quad \forall k \in \mathcal{K} \cup \{0\} \\
& \sum_{k \in \mathcal{K}} \Delta t \left( \eta^+ x_k^b + \lambda_k^+ - d_k \right) + \hat{\gamma} \theta_k^+ \leq \frac{z - b_n}{a_n} - \hat{y}_0 \quad \forall n \in \mathcal{N}_+ \\
& \sum_{k \in \mathcal{K}} \Delta t \left( \eta^+ x_k^b - \lambda_k^- - d_k \right) - \hat{\gamma} \theta_k^- \geq \frac{z - b_n}{a_n} - \hat{y}_0 \quad \forall n \in \mathcal{N}_- \\
& b_n \leq z \quad \forall n \in \mathcal{N}_0 \\
& \Lambda_{k,l}^+ + \sum_{i=l}^{I(k,l)} \Theta_{k,i}^+ \geq \eta^+ x_l^r, \quad \Lambda_{k,l}^- + \sum_{i=l}^{I(k,l)} \Theta_{k,i}^- \geq m_l \quad \forall k, l \in \mathcal{K} : l \leq k \\
& \lambda_k^+ + \sum_{i=k}^{\hat{I}(K,k)} \theta_i^+ \geq \eta^+ x_k^r, \quad \lambda_k^- + \sum_{i=k}^{\hat{I}(K,k)} \theta_i^- \geq m_k \quad \forall k \in \mathcal{K},
\end{aligned} \tag{R''_{\mathcal{K}}}$$

where  $I(k, l) = \min\{k, l + \Gamma/\Delta t - 1\}$  and  $\hat{I}(k, l) = \min\{k, l + \hat{\Gamma}/\Delta t - 1\}$ .

**Theorem 2.3** (Linear programming reformulation). *The problems  $(R'_{\mathcal{K}})$  and  $(R''_{\mathcal{K}})$  are equivalent.*

The conversion of the robust optimization problem  $(R'_{\mathcal{K}})$  to the linear program  $(R''_{\mathcal{K}})$  comes at the expense of introducing  $4K^2 + 4K$  dual variables. For a daily planning horizon with half-hourly resolution, this amounts to introducing 9,408 additional continuous variables. Overall, the linear program  $(R''_{\mathcal{K}})$  involves  $4K^2 + 7K + 1$  variables and  $K^2 + 9K + N + 2$  constraints, that is, its size scales quadratically with  $K$ . In conjunction, Theorems 1–3 imply that the non-convex robust optimization problem (R) with continuous uncertain parameters can be reduced without any loss to the tractable linear program  $(R''_{\mathcal{K}})$ , which is amenable to efficient numerical solution with state-of-the-art linear programming solvers such as CPLEX or Gurobi.

**Remark 2.4** (Robustification reduces complexity). A striking property of the robust optimization model (R) is that it is much *easier* to solve than the underlying deterministic model, which would assume precise knowledge of the frequency deviation scenario  $\delta$ . Indeed, the textbook formulation of the deterministic model requires continuous decision variables to represent  $y^+(x^b(t), x^r(t), \delta(t))$  and  $y^-(x^b(t), x^r(t), \delta(t))$  and a binary decision variable to model their complementarity for every  $t \in \mathcal{T}$  (Taylor, 2015, p. 85). This results in a large-scale mixed-integer linear program even if  $\mathcal{T}$  is discretized. In contrast, the robust optimization model (R) is equivalent to the tractable linear program  $(R''_{\mathcal{K}})$ . To our best knowledge, we have thus discovered the first practically interesting class of optimization problems that become dramatically easier through robustification.  $\square$

## 2.5 Multi-Stage Extensions

Model (R) described in Section 2.2 looks only one day ahead and accounts for the future usage of the vehicle only through the cost-to-go function  $\varphi$ . We will now show that this static decision problem readily extends to a dynamic model that looks  $H$  days into the future. For ease of exposition, we assume that the market bids for day  $h \in \mathcal{H} = \{0, \dots, H-1\}$  are due at midnight of the previous day, which implies that the initial state-of-charge  $y_h$  on day  $h$  is precisely known. However, this assumption can be relaxed. A vehicle owner aiming to minimize worst-case expected costs (where the expectation is taken with respect to the prices, and the worst-case is taken with respect to the frequency deviation scenarios in  $\hat{\mathcal{D}}$ ) across  $H$  days solves the robust dynamic program

$$\varphi_h(y_h) = \min_{(x_h^b, x_h^r) \in \mathcal{X}_R(y_h)} c(x_h^b, x_h^r) + \max_{\delta_h \in \hat{\mathcal{D}}} \varphi_{h+1}(y(x_h^b, x_h^r, \delta_h, y_h, T)) \quad \forall h \in \mathcal{H}. \quad (2.5)$$

Here,  $\mathcal{X}_R(y_h)$  denotes the feasible set of the single-stage problem (R) with uncertainty sets  $\mathcal{D}$  and  $\mathcal{Y}_0 = \{y_h\}$ . In principle,  $\mathcal{X}_R(y_h)$  could be empty for some  $y_h$ . Under the reasonable assumption that each night the vehicle is plugged in long enough for the battery to be fully charged, however,  $\mathcal{X}_R(y_h)$  is guaranteed to be non-empty. In this case, problem (2.5) remains feasible on all days  $h \in \mathcal{H}$  irrespective of previous market decisions and even when facing a frequency deviation scenario  $\delta \notin \hat{\mathcal{D}}$ . The cost-to-go functions  $\varphi_h$ ,  $h \in \mathcal{H}$ , are defined recursively through (2.5). In practice, it proves useful to initialize the recursion by  $\varphi_H(y_H) = p^*|y_H - y^*|$  for some target state-of-charge  $y^*$  and penalty parameter  $p^* \geq 0$ , which can be calibrated to historical data via cross-validation (see Section 2.6.2).

**Proposition 2.5.** *The cost-to-go function  $\varphi_h$  is convex and piecewise affine for every  $h \in \mathcal{H}$ .*

By Proposition 2.5, problem (2.5) is structurally equivalent to problem (R) for any  $h \in \mathcal{H}$ . Theorems 2.1, 2.2 and 2.3 thus imply that (2.5) can be recast as a tractable linear program whose right hand side coefficients depend affinely on  $y_h$ . Computing the function value and an arbitrary subgradient of  $\varphi_h$  at a fixed  $y_h$  is therefore tantamount to solving a linear program. This insight suggests that convex piecewise affine bounds on the cost-to-go function  $\varphi_h$  can be constructed by solving a series of linear programs. If  $\varphi_{h+1}$  is precisely known for some  $h \in \mathcal{H}$ , for example, then a coarse upper bound is obtained by evaluating  $\varphi_h$  at  $\underline{y}$  and  $\bar{y}$  and by linearly interpolating the two function values. A coarse lower bound is given by the pointwise maximum of the two tangents of  $\varphi_h$  constructed from the function values and subgradients at  $\underline{y}$  and  $\bar{y}$ . The difference between these coarse bounds is maximal at the kink of the lower bound. To improve both bounds, we can then break the interval  $[\underline{y}, \bar{y}]$  apart at the kink and construct separate upper and lower bounds on the two resulting subintervals by repeating the above procedure. Iteratively partitioning the subinterval on which the gap between the bounds is maximal yields increasingly tight convex piecewise affine bounds that approximate  $\varphi_h$  uniformly on  $[\underline{y}, \bar{y}]$  to any precision. In each iteration one has to solve a linear program akin to  $(R''_{\mathcal{H}})$  in order to compute the value and a subgradient of  $\varphi_h$  at a new anchor point. Note that the outlined procedure remains applicable if  $\varphi_{h+1}$  in (2.5) is replaced with

a convex piecewise affine bound, in which case one has only access to an *inexact* oracle for the values and subgradients of  $\varphi_h$ . In this case the approximation errors accumulate over the dynamic programming recursions.

In reality, the market bids for day  $h$  are due around noon and not at midnight of day  $h - 1$ . As a consequence, the exact state-of-charge  $y_h$  at the beginning of day  $h$  is unknown at stage  $h$ , that is, at the time when  $(x_h^b, x_h^r)$  must be chosen. Instead, only the confidence intervals  $[\hat{y}_0, \hat{\bar{y}}_0]$  and  $[\underline{y}_0, \bar{y}_0]$  for  $y_h$  are available, which can be constructed from the current state-of-charge and from  $(x_{h-1}^b, x_{h-1}^r)$ ; see Section 2.2. In a more realistic multi-stage model, the information available at stage  $h$  is therefore encoded by the state vector  $(\hat{y}_0, \hat{\bar{y}}_0, \underline{y}_0, \bar{y}_0)$ , and thus the cost-to-go functions have four arguments, while the state transition functions have four components. By generalizing Theorems 2.1, 2.2 and 2.3 as well as Proposition 2.5, one can still show that all cost-to-go functions are convex and piecewise affine and that their values and subgradients can be computed by solving linear programs akin to  $(R''_{\mathcal{X}})$ . While tedious, the proofs of these generalized results require no fundamentally new ideas and are thus omitted for brevity. As the cost-to-go functions have four arguments, the construction of convex piecewise affine upper and lower bounds is more challenging but still possible via the robust dual dynamic programming algorithm by Georghiou et al. (2019).

Numerical experiments in Section 2.6.3 suggest that the benefits of solving a multi-stage instead of a single-stage problem are negligible in practice because electric vehicles can always be charged overnight. We emphasize, however, that the robust optimization models and techniques developed in this paper may also be useful to optimize the operation of other energy storage devices that are characterized by slower dynamics and therefore necessitate a proper multi-stage approach.

## 2.6 Numerical Experiments

In the following, we first describe how the vehicle owner’s decision problem is parametrized from data, and we explain the backtesting procedure that is used to assess the performance of a given bidding strategy. Next, we present numerical results and discuss policy implications. All experiments are run on an Intel i7-6700 CPU with 3.40GHz clock speed and 64GB of RAM. All linear programs are solved with GUROBI 9.1.2 using its PYTHON interface. In order to ensure the reproducibility of our experiments, we provide links to all data sources and make our code available at [www.github.com/lauinger/reliable-frequency-regulation-through-vehicle-to-grid](http://www.github.com/lauinger/reliable-frequency-regulation-through-vehicle-to-grid).

### 2.6.1 Model Parametrization

The French transmission system operator (RTE) publishes availability and delivery prices and frequency measurements.<sup>IV</sup> There have been two policy changes in frequency regulation

---

<sup>IV</sup><http://clients.rte-france.com/>

since 2015. While the availability prices were historically kept constant throughout the year, they change on a weekly basis since mid-January 2017 and on a daily basis since July 2019. At this point, the pricing mechanism also changed from a pay-as-bid auction to a clearing price auction. The average availability price over all years from 2015 to 2019 amounts to 0.8cts/kWh, but the yearly average *decreased* in 2017 and 2018, and *increased* again in 2019 to pre-2017 levels. For all practical purposes we may assume that the expected regulation price  $p^r(t) = p^a(t) + \mathbb{E}[\tilde{\delta}(t)\tilde{p}^d(t)]$  coincides with the availability price  $p^a(t)$  because the realized regulation price  $p^a(t) + \delta(t)p^d(t)$  oscillates rapidly around the availability price  $p^a(t)$  due to intra-day fluctuations of the frequency-adjusted delivery prices; see Figure 2.A.1 in Appendix 2.A. In fact,  $\delta(t)p^d(t)$  empirically averages to  $-2.36 \cdot 10^{-5} \text{€}$  over all 10s intervals from 2015 to 2019. We further identify the utility prices  $p^b(t)$  with the residential electricity prices charged by Electricité de France (EDF), the largest European electricity provider. These prices exhibit six different levels corresponding to peak- and off-peak hours on high, medium and low price days. High price days can occur exclusively on work days between November and March, whereas medium price days can occur on all days except Sundays. Low-price days can occur year-round. The peak hours are defined as the hours from 6 am to 10 pm on work days, and all the other hours are designated as off-peak hours. The prices corresponding to each type of day and hour are regulated and published in the official French government bulletin.<sup>V</sup> Over the past five years, these prices have not changed more than three times per year. On each day, RTE announces the next day's price levels by 10:30 am. The average utility price over the years from 2015 to 2019 amounts to 14cts/kWh and thus exceeds the average availability price by an order of magnitude.

When simulating the impact of the market decisions on the battery state-of-charge, it is important to track the frequency signal with a high time resolution. In fact, the European Commission (2017) requires regulation providers to adjust the power flow between the battery and the grid every ten seconds in order to ensure that it closely matches  $x^b(t) + \delta(t)x^r(t)$  for all  $t \in \mathcal{T}$ . This means that regulation providers need to measure the frequency deviation  $\delta(t)$  at least every ten seconds. Hence, we use a sampling rate of 100mHz when simulating the impact of the market decisions on the battery state-of-charge. This contrasts with previous studies, which used sampling rates below 20mHz (Han et al., 2010; Sortomme and El-Sharkawi, 2012; Donadee and Ilić, 2014; Wu and Sioshansi, 2019). Recall from Section 2.2 that the frequency deviation  $\delta(t)$  depends on the nominal grid frequency  $f_0 = 50\text{Hz}$  and on the normalization constant  $\Delta f = 200\text{mHz}$ . Moreover, recall that the uncertainty set  $\mathcal{D}$  is parametrized by  $\gamma = 0.5\text{h}$  and  $\Gamma = 2.5\text{h}$  in order to respect the delivery guarantee rules prescribed by the European Commission, while the less conservative uncertainty set  $\hat{\mathcal{D}}$  is parametrized by  $\hat{\gamma} = 0.5\text{h}$  and  $\hat{\Gamma} = 24\text{h}$  as described in the discussion of Figure 2.1.

The vehicle data is summarized in Table 2.A.1 in Appendix 2.A. The chosen parameter values are representative for commercially available midrange vehicle-to-grid-capable electric vehicles such as the 2018 Nissan Leaf, and they are in line with experimental measurements of

<sup>V</sup>Journal Officiel de la République Française: <https://www.legifrance.gouv.fr/>

charging and discharging efficiencies. For example, Apostolaki-Iosifidou et al. (2017) find that charging and discharging efficiencies  $\eta^+$  and  $\eta^-$ , respectively, vary between 64% and 88% for a LiPF<sub>6</sub> cobalt battery with a nominal voltage of 345V and a nominal capacity of 106Ah. We assume that the vehicle owner reserves the time windows from 7 am to 9 am and from 5 pm to 7 pm on workdays and from 8 am to 8 pm on weekends and public holidays for driving. At all other times, the car is connected to a bidirectional charging station. We also assume that the car's yearly mileage amounts to 10,000km, which approximately matches the French average of 13,000km (Commissariat général au développement durable, 2010). Hence, the car travels about 27km per day on average. Even though this distance is easily covered within one hour, it makes sense to reserve extended time slots for driving. Indeed, the vehicle owner may not be able to (nor wish to) pinpoint the exact driving times one day in advance. It may also be impossible to find bidirectional charging stations on weekend trips. With a standard vehicle efficiency of 0.2kWh/km, the car thus consumes 2,000kWh per year.

### 2.6.2 Backtesting Procedure and Baseline Strategy

In our experiments, we assess the performance of different bidding strategies over different test datasets covering one of the years between 2015 and 2019. A bidding strategy is any procedure that computes on each day at noon a pair of market decisions  $x^b$  and  $x^r$  for the following day. We call a strategy *non-anticipative* if it determines the market decisions using only information observed in the past. In addition, we call a strategy *feasible* if it allows the vehicle owner to honor all market commitments for all frequency deviation scenarios within the uncertainty set  $\mathcal{D}$ .

To measure the profit generated by a particular strategy over one year of test data, we use the following backtesting procedure. On each day at noon we compute the market decisions for the following day. We then use the actual frequency deviation data between noon and midnight and the market decisions for the current day to calculate the true battery state-of-charge at midnight. Next, we use the frequency deviation data of the following day to calculate the revenue from selling regulation power to the TSO, which is subtracted from the cost of buying electricity for charging the battery. If the strategy is infeasible and the vehicle owner is not able to deliver all promised regulation power even though the realized frequency deviation trajectory falls within the uncertainty set  $\mathcal{D}$ , then she pays a penalty. The penalty at time  $t$  is set to  $k_{\text{pen}} \cdot p^a(t) \cdot (x^r(t) - x_d^r(t))$ , where  $x_d^r(t)$  denotes the maximum amount of regulation power that could have been offered without risking an infeasibility, and the penalty factor  $k_{\text{pen}}$  ranges from 3 to 10.<sup>VI</sup> Repeated offenses may even lead to market exclusion. For simplicity, in each experiment we either assume that the vehicle owner pays a penalty corresponding to a fixed value of  $k_{\text{pen}}$  for every offense or is excluded from the regulation market directly upon the first offense. If the battery is depleted during a trip, any missing energy needed for driving is acquired at a high price  $p^y$  from a public fast charging station. We assume that  $p^y$  accounts for the price of energy as well as for the opportunity cost of the time lost in driving

---

<sup>VI</sup>For example, Réseau de transport d'électricité (2017a) sets  $k_{\text{pen}} = 5$ .

to the charging station and waiting to be serviced. In our experiments we set  $p^y$  either to 0.75 €/kWh (which corresponds to typical energy prices offered by the European fast charging network Ionity<sup>VII</sup>), to 7.5 €/kWh or to 75 €/kWh. The procedure described above is repeated on each day, and the resulting daily profits are accumulated over the entire test dataset.

Our baseline strategy is to determine the next day's market decisions by solving the robust optimization problem (R) with terminal cost function  $\varphi(y) = p^*|y - y^*|$ , where the calibration of  $y^*$  and  $p^*$  is described below. Thus, (R) is equivalent to an instance of the linear program (R''<sub>K</sub>). This problem is updated on each day because the driving pattern  $d$  as well as the market prices  $p^b$  and  $p^r$  change, and because the uncertainty sets  $\mathcal{U}_0$  and  $\mathcal{V}_0$  for the state-of-charge at midnight depend on the state-of-charge at noon and on the market commitments between noon and midnight that were chosen one day earlier. The baseline strategy is feasible thanks to the robust constraints in (R), which ensure that regulation power can be provided for all frequency deviation scenarios in  $\mathcal{D}$ .

The parameters  $p^*$  and  $y^*$  are kept constant throughout each backtest. Specifically, we set  $p^* = \frac{3+k}{40}$  €/kWh for some  $k = 1, \dots, 9$  and  $y^* = (\frac{\bar{y}+y}{2} + l)$  kWh for some  $l = 0, \dots, 5$ . Every tuple  $(p^*, y^*)$  encodes a different bidding strategy. Given a training dataset comprising one year of frequency measurements and market prices, we compute the cumulative profit of each strategy via the backtesting procedure outlined above, and we choose the tuple  $(p^*, y^*)$  that corresponds to the winning strategy. This strategy is non-anticipative if the year of the training dataset precedes the year of the test dataset. Table 2.1 shows that selecting  $p^*$  and  $y^*$  non-anticipatively on a historical training dataset has low regret relative to selecting these parameters anticipatively on the test dataset. Here, the regret is defined as the ratio of the absolute difference and the arithmetic mean of the cumulative profits generated by the anticipative and the non-anticipative strategies tuned on the test and training datasets, respectively. We always use the year immediately prior to the test dataset as training dataset. Table 2.1 shows that from 2017 onward, perhaps surprisingly, anticipative parameter tuning has no advantage over non-anticipative tuning. From now on, we assume that  $p^*$  and  $y^*$  are tuned non-anticipatively using the year of training data immediately prior to the test dataset. Additional robustness checks reveal that the cumulative profit (evaluated on 2019 data) is relatively insensitive to the choice of  $p^*$  and  $y^*$  within the suggested search grid, which indicates that its resolution is sufficiently high. Details are omitted for the sake of brevity.

### 2.6.3 Futility of Solving a Multi-Stage Model

The baseline strategy described in Section 2.6.2 looks only one day into the future. We now show numerically that the added value of solving a dynamic model that looks  $H > 1$  days into the future is negligible. Specifically, we compare the baseline strategy against a dynamic strategy, which computes the market commitments on each day in a receding horizon fashion by solving model (2.5) with  $H = 2$  and  $\varphi_2(y_2) = p^*|y_2 - y^*|$ , assuming that the electricity prices

<sup>VII</sup><https://ionity.eu/en/>



## Reliable Frequency Regulation through Vehicle-to-Grid: Encoding Legislation with Robust Constraints

Table 2.1: Calibration of  $p^*$  and  $y^*$ .

Test Dataset	Anticipative Calibration			Non-Anticipative Calibration			Regret (%)
	$p^*$ (€/kWh)	$\frac{y^*-y}{\bar{y}-\underline{y}}$ (%)	Profit (€)	$p^*$ (€/kWh)	$\frac{y^*-y}{\bar{y}-\underline{y}}$ (%)	Profit (€)	
2015	0.125	56.7	-74	n/a	n/a	n/a	n/a
2016	0.15		-101	0.15	56.7	-112	10
2017			-169			-169	0
2018			-190			-190	
2019	0.15	56.7	-153	0.15	56.7	-153	0

and the driving patterns for both subsequent days are known upfront. To compute the out-of-sample profits, we use the backtesting procedure outlined in Section 2.6.2 but assume that the market bids are due at midnight when the initial state-of-charge  $y_0$  is known. As explained in Section 2.5, this assumption greatly simplifies the computation of the dynamic strategy. We define the *value of vehicle-to-grid* under a particular bidding strategy as the cumulative excess profit of that strategy with respect to a simplified strategy that does not participate in the reserve market. This simplified strategy solves problem (R) under the additional constraint  $x^r = 0$ . When examining the value of vehicle-to-grid over the years from 2017 to 2019, we find that the dynamic strategy outperforms the baseline strategy only by 2.1%. Hence, the dynamic strategy does not generate significantly higher revenues even though it has the advantage of knowing the electricity prices and driving patterns *two* days in advance (which would not be the case in reality). We also emphasize that *both* strategies benefit from the assumption that  $y_0$  is known upfront. However, we conjecture that both strategies benefit equally from this information relaxation and that the dynamic strategy thus still fails to outperform the baseline strategy when the market bids are due at noon and  $y_0$  is uncertain. This reasoning justifies our use of a *static* baseline strategy that looks merely one day into the future.

### 2.6.4 Experiments: Set-up, Results and Discussion

In the remainder, we distinguish six different simulation scenarios. The nominal scenario uses the parameters of Table 2.A.1 in Appendix 2.A for both training and testing. All other scenarios are based on slightly modified parameters. Specifically, we consider a lossless energy conversion scenario, which trains and tests the baseline strategy under the assumption that  $\eta^+ = \eta^- = 1$ . A variant of this scenario assumes lossless energy conversion in training but tests the resulting strategy under the nominal values of  $\eta^+$  and  $\eta^-$ . We also consider two scenarios with weaker robustness guarantees that replace the uncertainty set  $\mathcal{D}$  in the training phase with its subset  $\hat{\mathcal{D}}$ . The resulting bidding strategy can be infeasible because it may fail to provide the legally required amount of reserve power. The two scenarios do not differ in training but impose different sanctions for infeasibilities in testing. In the first of the two scenarios the vehicle owner is immediately excluded from the reserve market upon the first infeasibility, thus loosing the opportunity to earn money by offering grid services for the rest of the year. In the second scenario, the vehicle owner is penalized by  $k_{\text{pen}} \cdot p^a(t)$  with  $k_{\text{pen}} = 5$  for energy

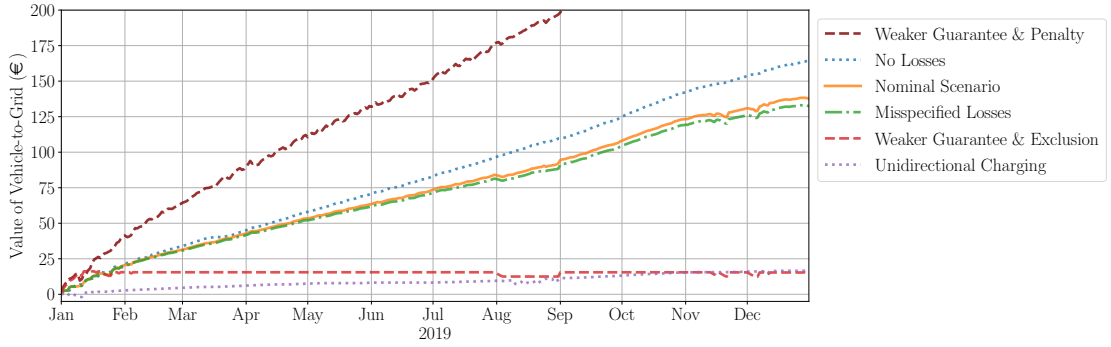


Figure 2.3: Value of vehicle-to-grid in 2019 in different simulation scenarios.

that is missing for frequency regulation (see also Section 2.6.2) and by  $p^y = 0.75 \text{ €/kWh}$  for energy that is missing for driving. Finally, we consider a scenario in which the vehicle is only equipped with a unidirectional charger, that is, we set  $\bar{y}^- = 0$ . Thus, the vehicle is unable to feed power back into the grid. Requests for up-regulation ( $\delta(t) < 0$ ) can therefore only be satisfied by consuming less energy, which is possible only if  $\delta(t)x^r(t) \leq x^b(t)$ .

Figure 2.3 visualizes the value of vehicle-to-grid in 2019 as a function of time for each of the six simulation scenarios. We first observe that the value of vehicle-to-grid in the lossless energy conversion scenario amounts to 165 € at the end of the year and thus significantly exceeds the respective value of 138 € in the nominal scenario. Using a perfectly efficient vehicle charger would thus have boosted the value of vehicle-to-grid by 20% in 2019. This is not surprising because a perfect charger prevents costly energy conversion losses. Note also that the scenario with misspecified efficiency parameters results in almost the same value of vehicle-to-grid as the nominal scenario, which suggests that misrepresenting  $\eta^+$  or  $\eta^-$  in training has a negligible effect on the test performance. However, the underlying bidding strategy is *not* guaranteed to be feasible because it neglects energy conversion losses. Even though this strategy happens to remain feasible throughout 2019, it bears the risk of financial penalties or market exclusion. The two bidding strategies with weakened robustness guarantees initially reap high profits by aggressively participating in the reserve market, but they already fail in the first half of January to fulfill all market commitments. If infeasibilities are sanctioned by market exclusion, the cumulative excess profit thus remains flat after this incident. If infeasibilities lead to financial penalties, on the other hand, the cumulative excess profit drops sharply below zero near the incident but recovers quickly and then continues to grow steadily. As only a few other mild infeasibilities occur in 2019, the end-of-year excess profit of this aggressive bidding strategy still piles up to 296 €, which is more than twice the excess profit in the nominal scenario. We conclude that the current level of financial penalties is too low to deter vehicle owners from making promises they cannot honor. Finally, with a unidirectional charger, the 2019 value of vehicle-to-grid falls to 15 €, which is only 11% of the respective value with a bidirectional charger.

As the bidding strategy with a weakened robustness guarantee can earn high profits when

## Reliable Frequency Regulation through Vehicle-to-Grid: Encoding Legislation with Robust Constraints

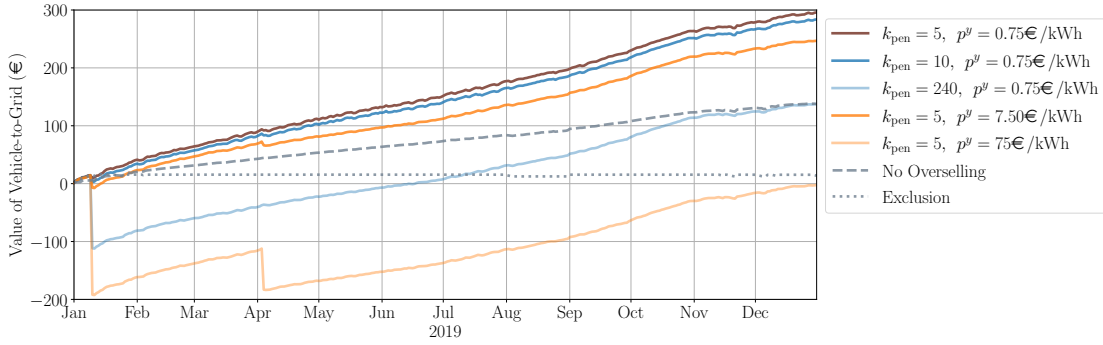


Figure 2.4: Value of vehicle-to-grid in 2019 for different penalty parameters.

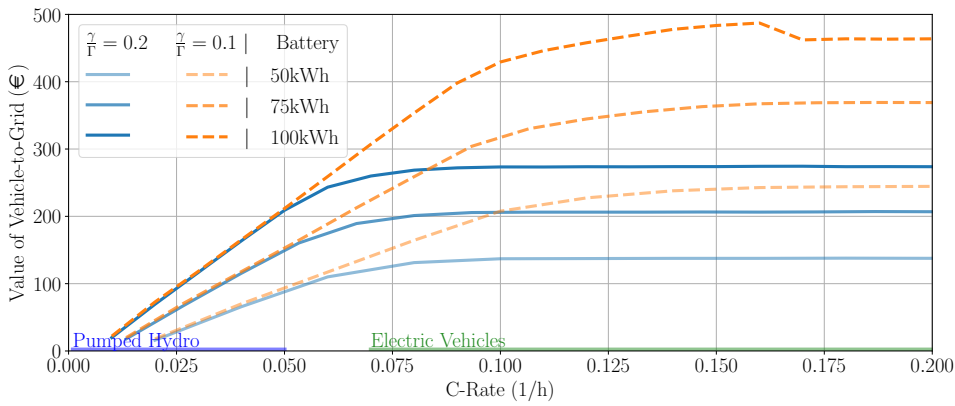


Figure 2.5: Value of vehicle-to-grid in 2019 as a function of the C-rate.

infringements of the EU delivery guarantee incur only financial penalties, we carry out an additional experiment to analyze the impact of the penalty parameters  $k_{\text{pen}}$  and  $p^y$  on the value of vehicle-to-grid; see Figure 2.4. We observe that for  $p^y = 0.75 \text{ €/kWh}$ , doubling the penalty factor to  $k_{\text{pen}} = 10$  decreases the value of vehicle-to-grid by only 4.1% to 284 €. An additional calculation reveals that the TSO would have to set  $k_{\text{pen}} \approx 240$  in order to push the value of vehicle-to-grid below that attained in the baseline scenario, which fulfills the EU delivery guarantee. On the other hand, for  $k_{\text{pen}} = 5$ , a tenfold increase of  $p^y$  to 7.50 €/kWh decreases the value of vehicle-to-grid by 16.6% to 247 €, and an additional tenfold increase of  $p^y$  to 75 €/kWh pushes the value of vehicle-to-grid below zero. Increasing  $p^y$  from 0.75 €/kWh to 7.50 €/kWh also reduces the number of days on which the vehicle owner does not have enough energy to drive from 7 to 2.

Since the market prices display distinct regime shifts as European energy policies evolve, the value of vehicle-to-grid fluctuates over the years. Indeed, Figure 2.B.1 in Appendix 2.B shows that the value of vehicle-to-grid averages to 108 € per year from 2016 to 2019 with a minimum of 76 € in 2018.

In the next experiment we investigate how the value of vehicle-to-grid depends on the acti-

vation ratio  $\gamma/\Gamma$  and the battery's size and charge rate (C-rate). The C-rate is defined as the ratio of the charger power and the battery size, and thus it expresses the percentage of the battery's total capacity that can be charged within one hour. Figure 2.5 shows that the value of vehicle-to-grid increases with the C-rate up to a saturation point that is insensitive to the battery size but decreases with the activation ratio. In the saturation regime, the value of vehicle-to-grid increases with the battery size. Typical electric vehicles can be fully charged overnight, within about 8 hours. The corresponding C-rate of  $0.125\text{h}^{-1}$  falls within the saturation regime for both investigated activation ratios of 0.1 and 0.2. This observation has two implications. First, for typical electric vehicles the value of vehicle-to-grid cannot be increased by increasing the charger power (and thereby increasing the C-rate). This insight contradicts previous studies by Kempton and Tomić (2005a), Codani et al. (2015) and Borne (2019), which advocate for electric vehicles with higher C-rates of 1, 0.45, and 0.37, respectively. The reason for this discrepancy is that none of the previous studies faithfully account for the EU delivery guarantee. In particular, Borne (2019) allows the vehicle owner to anticipate future frequency deviations, and Codani et al. (2015) assume that the bidding strategy can be updated on an hourly basis, thereby exploiting information that is not available at the time when the market bids are collected by the TSO (*i.e.*, one day in advance). By underestimating the amount of energy that the vehicle owner must be able to exchange with the TSO to satisfy all future obligations on the reserve market, these studies overestimate the amount of regulation power that can be sold, which makes potent battery chargers appear more useful than they actually are. The second implication is that the activation ratio has a critical impact on the value of vehicle-to-grid. The incumbent storage providers of the European electricity grid, namely pumped-hydro storage power plants, have C-rates of about  $0.0125\text{h}^{-1}$  (Andrey et al., 2020), which are significantly smaller than the C-rates of electric vehicles. At such C-rates, the value of providing frequency regulation is the same for activation ratios of 0.1 and 0.2. To minimize competition from vehicle-to-grid, pumped-hydro storage operators may thus have an incentive to lobby for high activation ratios. From the perspective of a TSO, the higher the activation ratio, the larger the uncertainty set  $\mathcal{D}$  and the lower the probability of blackouts. However, Figure 2.1 suggests that an activation period of 30 minutes is already conservative. On the other hand, the larger  $\mathcal{D}$ , the harder it is for storage operators to provide regulation power, which may lead to less competition, higher market prices, and a higher total cost of frequency regulation. As the system operator is a public entity, this cost is ultimately borne by the public, and the choice of the activation ratio is a political decision.

The last two experiments study the influence of the driving time and distance on the value of vehicle-to-grid. Figure 2.B.2 in Appendix 2.B shows that the value of vehicle-to-grid in 2019 approximately displays a concave dependence on the yearly driving distance and plateaus at 138 € for driving distances between 5,000km and 10,000km. It is perhaps surprising that the value of vehicle-to-grid is *not* globally decreasing in the driving distance. An explanation for this phenomenon is provided in Appendix 2.B.

Figure 2.6 shows the value of vehicle-to-grid in 2019 against the daily plug time, that is, the total amount of time during which the vehicle is connected to a bidirectional charger. In this

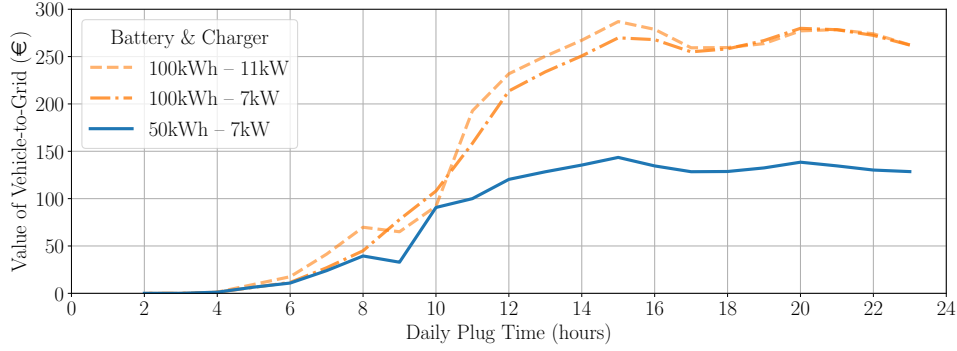


Figure 2.6: Value of vehicle-to-grid in 2019 versus daily plug time.

experiment, we assume that a daily plug time of  $t_p \in [0h, 24h]$  means that cars are plugged from midnight to  $\frac{t_p}{2}$  am and from  $12h - \frac{t_p}{2}$  pm to midnight the next day. Whenever the car is not plugged, it consumes a constant amount of power such that the total consumption over the year corresponds to a mileage of 10,000 km as in the baseline experiment. We observe that the value of vehicle-to-grid increases with the daily plug time and saturates after 15 hours at a level that scales with the battery size. Thus, a daily plug time of 15 hours suffices for offering the maximal possible amount of regulation power. Additional experiments show that for an activation ratio of 0.1 instead of 0.2, the saturation point increases to 20 hours.

## 2.7 Conclusions

We develop an optimization model for the decision problem of an electricity storage operator offering frequency regulation. To our best knowledge, this is the first model that faithfully accounts for the delivery guarantees required by the European Commission (2017). In contrast, all existing models relax the true delivery guarantee constraints and therefore risk that the electricity storage is empty (full) when a request for up- (down-)regulation arrives. In its original formulation, our model represents a non-convex robust optimization problem with functional uncertain parameters and thus appears to be severely intractable. Indeed, the state-of-the-art methods for solving the deterministic version of this problem for a single frequency deviation scenario in discrete time rely on techniques from mixed-integer linear programming. Maybe surprisingly, however, our robust optimization problem is equivalent to a tractable linear program. This is an exact result and does not rely on any approximations. To our best knowledge, we have thus discovered the first practically interesting class of optimization problems that become significantly easier through robustification.

In the numerical experiments centered around electric vehicles we restrict the planning horizon of our model to 24 hours. This is justified because the batteries of electric vehicles can be fully charged overnight and because vehicle owners may not know their driving needs several days in advance. Numerical experiments provide strong evidence that the added value of looking two or more days into the future is marginal even if future market prices and driving

patterns were known.

As our optimization model faithfully captures effective legislation, it enables us to quantify the true value of vehicle-to-grid. This capability is relevant for understanding the economic incentives of different stakeholders such as vehicle owners, aggregators, equipment manufacturers, and regulators.

As for the vehicle owners, we find that their profits from frequency regulation range from 100 € to 500 € per year under typical driving patterns. It seems unlikely that such profits are sufficient for vehicle owners to forego the freedom of using their car whenever they please to. Nevertheless, some vehicle owners may choose to participate in vehicle-to-grid for idealistic reasons such as advancing the energy transition away from fossil fuels. Our numerical results also reveal that the value of vehicle-to-grid saturates at daily plug times above 15 hours. Thus, maximal profits from frequency regulation can be reaped even if the vehicle is disconnected from the grid up to 9 hours per day. This means that vehicle owners participating in vehicle-to-grid still enjoy considerable flexibility as to when to drive, which could help to promote the adoption of vehicle-to-grid.

Our results also have ramifications for aggregators, which pool multiple vehicles to offer regulation power. Indeed, aggregators may allow vehicle owners to reserve their vehicles for up to 9 hours of driving per day without sacrificing profit. This leaves vehicle owners ample freedom and reduces the probability that they exceed their driving slots. Thus, the actual number of vehicles available for frequency regulation at any point in time closely matches its prediction. This allows aggregators to place reserve market bids with small safety margins, which ultimately lowers transaction costs. In practice, aggregators can use our results as follows. On each day, they either ask drivers to schedule their driving needs for the next day, or they infer these needs from past travel patterns. Next, they solve our linear program for each car individually, which can be done efficiently by parallel computing even for large fleets with thousands of vehicles. Last, they add up the maximum regulation power each car can provide and sell it to the grid operator. This approach is easy to implement and requires few computational resources at the expense of sacrificing some optimality.

As opposed to individual vehicle owners, aggregators can decide which cars (or other flexible electric devices) to use to provide a given amount of regulation power. This has two advantages. First, battery degradation can be reduced by managing the state-of-charge of vehicles more precisely. Second, charging and discharging losses can be reduced by running vehicle chargers at their nominal operating points. In addition, aggregators may be able to trade on intraday markets, which would allow them to offer more regulation power for a given aggregate battery size. For example, if they encounter an extreme deviation trajectory, they can buy or sell electricity on the intraday market to maintain the state-of-charge within its bounds. This is risky, however, because intraday markets may not be liquid enough for aggregators to find trading partners. Especially not when the grid is already in distress, which is the case when extreme frequency deviations occur.

## **Reliable Frequency Regulation through Vehicle-to-Grid: Encoding Legislation with Robust Constraints**

---

Equipment manufacturers design and sell bidirectional vehicle chargers. Contrary to previous studies that relax the exact delivery guarantee constraints, we find that the battery size and not the charger power is limiting the profits from frequency regulation. Manufacturers thus have no incentive to produce overly powerful bidirectional chargers.

The electricity system and the society as a whole could benefit significantly from vehicle-to-grid, which harnesses the idle storage capacities of electric vehicles and thereby reduces the need for other sources of flexible electricity supply, such as gas power plants or stationary batteries. This in turn reduces the need for imports of natural gas and critical raw materials, increases the long-term security of electricity supply, and decreases greenhouse gas emissions. Regulators may therefore want to make vehicle-to-grid more attractive by prescribing the availability and delivery prices, defining appropriate delivery guarantee requirements and setting the penalties charged for non-compliance. Our results show that the vehicle owners' profits from frequency regulation decrease with the activation ratio and that current penalties are too low to incentivize vehicle owners to respect the law. Regulators could thus make vehicle-to-grid more attractive by decreasing the activation ratio and thereby relaxing the delivery guarantee requirements. Given that the delivery guarantee in our nominal scenario is very restrictive, this would only slightly decrease the reliability of frequency regulation. If, at the same time, regulators were to increase the penalties for non-compliance, then the reliability of frequency regulation might even increase because more vehicle owners would honor their contractual obligations. Our new model can be used for finding the appropriate level of the penalty. Our results also show that incumbent storage operators with low charge rates may lobby against weaker delivery guarantees because these would increase their competition from vehicle-to-grid but not increase their profits.

# Appendices

## 2.A Problem Data and Model Parameters

Table 2.A.1: Parameters of the Nominal Simulation Scenario.

Parameter	Symbol	Value	Unit
Vehicle Data			
Minimum State-of-Charge	$\underline{y}$	10	kWh
Maximum State-of-Charge	$\bar{y}$	40	kWh
Target State-of-Charge	$y^*$	27	kWh
Deviation Penalty	$p^*$	0.15	€/kWh
Charging Efficiency	$\eta^+$	85	%
Discharging Efficiency	$\eta^-$	85	%
Maximum Charging Power	$\bar{y}^+$	7	kW
Maximum Discharging Power	$\bar{y}^-$	7	kW
Yearly Energy for Driving		2,000	kWh
Fraction of Time Driving		27	%
Grid Data			
Nominal frequency	$f_0$	50	Hz
Normalization constant	$\Delta f$	200	mHz
Average Utility Price from 2015 to 2019		14.31	cts/kWh
Average Availability Price from 2015 to 2019		0.825	cts/kW/h
General Parameters			
Trading Interval	$\Delta t$	30	min
Activation Period in $\mathcal{D}$	$\gamma$	30	min
Regulation Cycle in $\mathcal{D}$	$\Gamma$	2.5	h
Activation Period in $\hat{\mathcal{D}}$	$\hat{\gamma}$	30	min
Regulation Cycle in $\hat{\mathcal{D}}$	$\hat{\Gamma}$	1	day
Sampling Rate for Frequency Measurements		0.1	Hz
Planning Horizon	$T$	1	day



## Reliable Frequency Regulation through Vehicle-to-Grid: Encoding Legislation with Robust Constraints

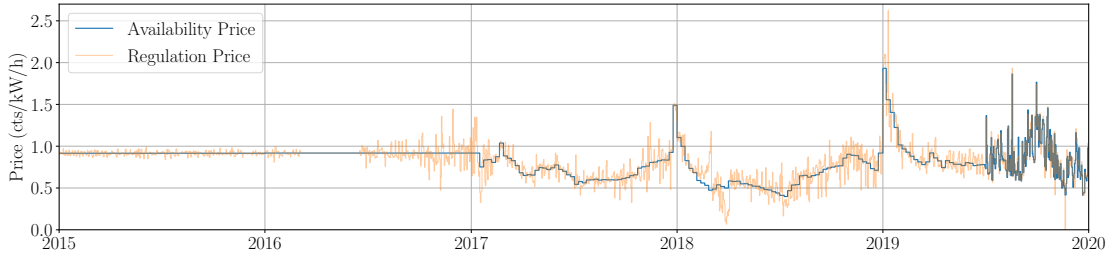


Figure 2.A.1: Evolution of the availability and regulation prices from 2015 to 2019. The regulation price changes every 10s. For better visibility, we show its daily averages.

## 2.B Additional Experiments and Results

In the first additional experiment we assess the heterogeneity of the value of vehicle-to-grid across the years 2016 to 2019. Figure 2.B.1 visualizes the temporal evolution of the value of vehicle-to-grid and shows that it may vary between 75 € and 140 € at the end of the year. The second additional experiment compares two vehicles with uni- and bidirectional chargers. Figure 2.B.2 indicates that the value of vehicle-to-grid is approximately concave in the yearly mileage for both vehicles and for mileages up to 30,000km. Since a vehicle with a bidirectional charger can be used for unidirectional charging, the value of vehicle-to-grid with a bidirectional charger exceeds that of the same vehicle with a unidirectional charger. Furthermore, a higher mileage necessitates higher utility purchases  $x^b$ , which has two opposing effects on regulation profits. On the one hand, power discharges become less likely because they only occur when  $\delta(t)x^r(t) < -x^b(t)$ , which reduces energy conversion losses and makes the provision of frequency regulation more cost-effective. On the other hand, the effective upper bound  $\bar{y}^+(t) - x^b(t)$  on  $x^r(t)$  tightens, which reduces the amount of regulation power that can be offered on the market. The value of vehicle-to-grid peaks at 138 € for a vehicle with a bidirectional charger traveling between 5,000km and 10,000km per year and at 42 € for a vehicle with a unidirectional charger traveling 30,000km per year. For yearly mileages greater than 5,000km, the higher the yearly mileage, the lower the added value of a bidirectional charger. This result may be of particular interest for operators of shared electric vehicles. However, even for a yearly mileage of 30,000km, using a bidirectional instead of a unidirectional charger more than doubles the value of vehicle-to-grid. Furthermore, many drivers may prefer vehicles with internal combustion engines or fuel cells over electric vehicles to cover high yearly mileages because of their greater ranges and shorter refueling times. Therefore, owners of electric vehicle are more likely to cover yearly mileages close to the French average of 13,000km. Providing frequency regulation with a unidirectional charger would thus earn them about 20 € per year. In practice, these earnings would have to be shared with vehicle aggregators and equipment manufacturers.

To complement the analysis of the nominal scenario described in Section 2.6.4, Figure 2.B.3 shows the relationships between market bids, prices, driving needs, frequency deviations, and the battery state-of-charge on 9 August 2019 in a 10 second resolution. As expected, the

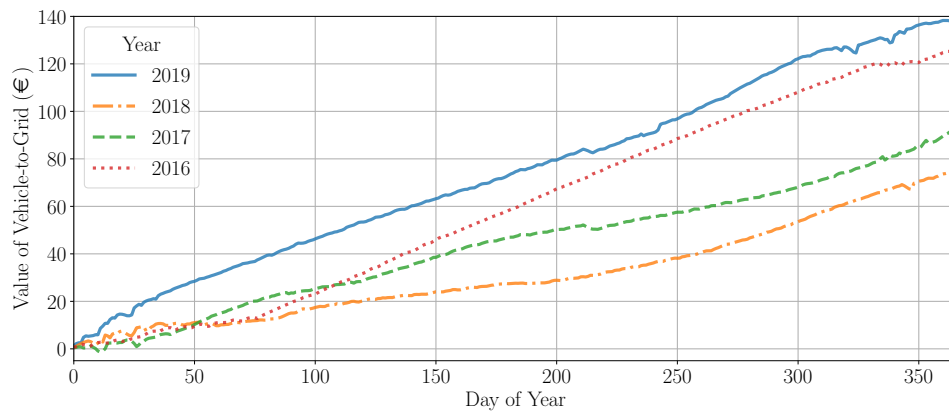


Figure 2.B.1: Value of vehicle-to-grid from 2016 to 2019.

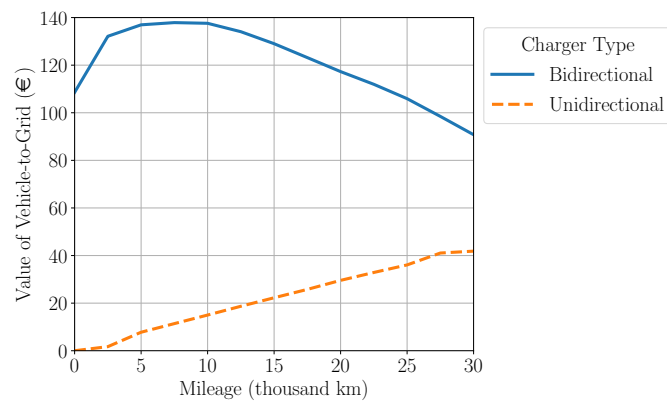


Figure 2.B.2: Value of vehicle-to-grid in 2019 vs mileage.

vehicle owner charges the battery at night when utility prices are low. We also observe that the vehicle participates in the regulation market at a more or less constant level whenever it is not driving. This reduces the exposure to extreme frequency deviations at any one time. The battery state-of-charge naturally decreases when the vehicle is driving, increases when the vehicle is being charged and remains essentially constant when the vehicle provides only frequency regulation because the frequency deviations fluctuate rapidly around zero.

## 2.C Proofs

This appendix contains the proofs of all theorems and propositions in the main text.

## Reliable Frequency Regulation through Vehicle-to-Grid: Encoding Legislation with Robust Constraints

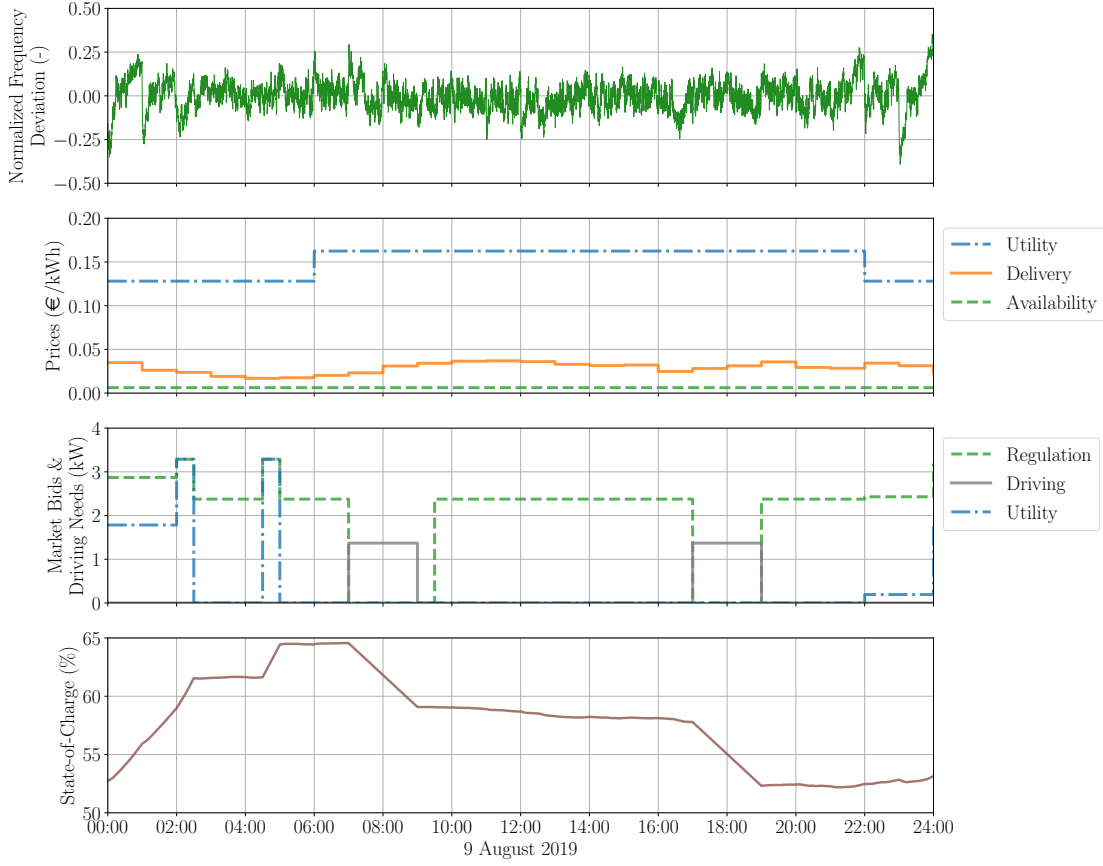


Figure 2.B.3: Frequency deviations, prices, market bids, driving needs, and state-of-charge on 9 August 2019.

*Proof of Proposition 2.1.* By definition we have

$$\begin{aligned} y(x^b, x^r, \delta, y_0, t) &= y_0 + \int_0^t \eta^+ \left[ x^b(t') + \delta(t')x^r(t') \right]^+ - \frac{[x^b(t') + \delta(t')x^r(t')]^-}{\eta^-} - d(t') dt' \\ &= y_0 + \int_0^t \min \left\{ \eta^+ \left( x^b(t') + \delta(t')x^r(t') \right), \frac{x^b(t') + \delta(t')x^r(t')}{\eta^-} \right\} - d(t') dt', \end{aligned}$$

where the second equality holds because  $\eta^+ < \frac{1}{\eta^-}$ . The postulated properties of  $y(x^b, x^r, \delta, y_0, t)$  follow from the observation that the minimum of two (nondecreasing) affine functions is a concave (nondecreasing) function (Boyd and Vandenberghe, 2004, p. 73).  $\square$

*Proof of Proposition 2.2.* We will show that  $\max_{\delta \in \mathcal{D}} \text{Var}(\delta) \leq \beta/T$ , where  $\beta = \lceil T/\Gamma \rceil \gamma$ . To this end, we note that

$$\max_{\delta \in \mathcal{D}} \text{Var}(\delta) = \max_{\delta \in \mathcal{D}^+} \text{Var}(\delta) \leq \max_{\delta \in \mathcal{D}_\beta} \text{Var}(\delta), \quad (2.6)$$

where  $\mathcal{D}_\beta = \{\delta \in \mathcal{L}(\mathcal{T}, [0, 1]) : \int_0^T \delta(t) dt \leq \beta\}$ . The equality in (2.6) holds because  $\text{Var}(\delta)$  remains unchanged when  $\delta(t)$  is replaced with  $|\delta(t)|$  for every  $t \in \mathcal{T}$ . Moreover, the inequality holds because  $\mathcal{D}^+ \subseteq \mathcal{D}_\beta$ . To see this, observe that for any  $\delta \in \mathcal{D}^+$  we have

$$\int_0^T \delta(t) dt = \sum_{n=1}^{\lceil T/\Gamma \rceil} \int_{(n-1)\Gamma}^{\min\{n\Gamma, T\}} \delta(t) dt \leq \left\lceil \frac{T}{\Gamma} \right\rceil \gamma = \beta.$$

Note that  $\mathcal{D}_\beta$  constitutes a budget uncertainty set of the type introduced by Bertsimas and Sim (2004), where the uncertainty budget  $\beta$  corresponds to the maximum number of regulation cycles within the planning horizon multiplied by the duration of an activation period. Thus,  $\beta$  can be viewed as the maximum amount of time within the planning horizon during which all reserve commitments must be honored. By weak duality, the highest variance of any scenario in  $\mathcal{D}_\beta$  satisfies

$$\begin{aligned} \max_{\delta \in \mathcal{D}_\beta} \text{Var}(\delta) &\leq \min_{\lambda \geq 0} \max_{\delta \in \mathcal{L}(\mathcal{T}, [0, 1])} \frac{1}{T} \int_0^T \delta^2(t) dt + \lambda \left( \beta - \int_0^T \delta(t) dt \right) \\ &= \min_{\lambda \geq 0} \lambda \beta + \max_{\delta \in \mathcal{L}(\mathcal{T}, [0, 1])} \int_0^T \delta(t) (\delta(t)/T - \lambda) dt \\ &= \min_{\lambda \geq 0} \lambda \beta + T \max_{\delta \in [0, 1]} \delta (\delta/T - \lambda) \\ &= \min_{\lambda \geq 0} \lambda \beta + \max\{0, 1 - \lambda T\} \\ &= \min_{\lambda \geq 0} \max\{\lambda \beta, 1 - \lambda(T - \beta)\} = \frac{\beta}{T}. \end{aligned}$$

The claim now follows by substituting the above result into (2.6) and recalling the definition of  $\beta$ .  $\square$

*Proof of Proposition 2.3.* As for assertion (i) we first prove that  $L\mathcal{D}_{\mathcal{K}} \subseteq \mathcal{D}$ . To this end, select any  $\delta \in \mathcal{D}_{\mathcal{K}}$ , and define  $\delta = L\delta$ . It is easy to see that  $\delta \in \mathcal{L}(\mathcal{T}, [-1, 1])$ . Next, select any  $t \in \mathcal{T}$ . If  $t \leq \Gamma$ , note that

$$\int_{[t-\Gamma]^+}^t |\delta(t')| dt' = \int_0^t |\delta(t')| dt' \leq \int_0^\Gamma |\delta(t')| dt' = \Delta t \sum_{l=1}^{\Delta k} |\delta_l| \leq \gamma,$$

where the auxiliary parameter  $\Delta k = \Gamma/\Delta t$  is integral thanks to Assumption 2.2. The second inequality in the above expression holds because  $\delta \in \mathcal{D}_{\mathcal{K}}$ . If  $t \geq \Gamma$ , on the other hand, we

define  $k = \lceil \frac{t}{\Delta t} \rceil$  and  $\alpha = \lceil \frac{t}{\Delta t} \rceil - \frac{t}{\Delta t} \in [0, 1)$ . Then, we find

$$\begin{aligned} \int_{[t-\Gamma]^+}^t |\delta(t')| dt' &= \int_{t-\Gamma}^{(k-\Delta k)\Delta t} |\delta(t')| dt' + \int_{(k-\Delta k)\Delta t}^{(k-1)\Delta t} |\delta(t')| dt' + \int_{(k-1)\Delta t}^t |\delta(t')| dt' \\ &= (k\Delta t - t) |\delta_{k-\Delta k}| + \Delta t \sum_{l=k-\Delta k+1}^{k-1} |\delta_l| + (t - (k-1)\Delta t) |\delta_k| \\ &= \Delta t \left( \alpha \sum_{l=k-\Delta k}^{k-1} |\delta_l| + (1-\alpha) \sum_{l=k-\Delta k+1}^k |\delta_l| \right) \leq \gamma, \end{aligned}$$

where the inequality holds because  $\delta \in \mathcal{D}_{\mathcal{K}}$ , which ensures that both  $\sum_{l=k-\Delta k}^{k-1} |\delta_l|$  and  $\sum_{l=k-\Delta k+1}^k |\delta_l|$  are smaller or equal to  $\gamma/\Delta t$ . As  $t \in \mathcal{T}$  was chosen arbitrarily, this implies that  $\delta \in L\mathcal{D}_{\mathcal{K}}$ . In summary, we have shown that  $L\mathcal{D}_{\mathcal{K}} \subseteq \mathcal{D}$ .

Next, we show that  $L^\dagger \mathcal{D} \subseteq \mathcal{D}_{\mathcal{K}}$ . To this end, select any  $\delta \in \mathcal{D}$  and define  $\delta = L^\dagger \delta$ . It is easy to see that  $\delta \in [-1, 1]^K$ . Moreover, for any  $k \in \mathcal{K}$  we have

$$\sum_{l=1+[k-\Gamma/\Delta t]^+}^k \delta_l = \sum_{l=1+[k-\Gamma/\Delta t]^+}^k \frac{1}{\Delta t} \int_{\mathcal{T}_l} \delta(t') dt' = \frac{1}{\Delta t} \int_{[k\Delta t-\Gamma]^+}^{k\Delta t} \delta(t') dt' \leq \frac{\gamma}{\Delta t},$$

where the inequality holds because  $\delta \in \mathcal{D}$ . As  $k \in \mathcal{K}$  was chosen arbitrarily, this implies that  $\delta \in L^\dagger \mathcal{D}$ . In summary, we have shown that  $L^\dagger \mathcal{D} \subseteq \mathcal{D}_{\mathcal{K}}$ .

Finally, we prove that  $\mathcal{D}_{\mathcal{K}} \subseteq L^\dagger \mathcal{D}$ . To this end, we observe that  $L^\dagger L$  coincides with the identity mapping on  $\mathbb{R}^K$ . As  $L\mathcal{D}_{\mathcal{K}} \subseteq \mathcal{D}$ , this implies that

$$\mathcal{D}_{\mathcal{K}} = L^\dagger L\mathcal{D}_{\mathcal{K}} \subseteq L^\dagger \mathcal{D}.$$

Since both  $L^\dagger \mathcal{D} \subseteq \mathcal{D}_{\mathcal{K}}$  and  $\mathcal{D}_{\mathcal{K}} \subseteq L^\dagger \mathcal{D}$ , we have in fact shown that  $L^\dagger \mathcal{D} = \mathcal{D}_{\mathcal{K}}$ . Thus assertion (i) follows. Assertion (ii) can be proved in a similar manner. Details are omitted for brevity.  $\square$

*Proof of Proposition 2.4.* The proof widely parallels that of Proposition 2.1 and is therefore omitted.  $\square$

The proof of Theorem 2.1 relies on Propositions 2.6–2.9 below.

**Proposition 2.6.** *The following equivalences hold.*

- (i)  $y^+ \left( x^b(t), x^r(t), \delta(t) \right) \leq \bar{y}^+(t) \forall \delta \in \mathcal{D}, \forall t \in \mathcal{T} \iff y_k^+ \left( x_k^b, x_k^r, \delta_k \right) \leq \bar{y}_k^+ \forall \delta \in \mathcal{D}_{\mathcal{K}}, \forall k \in \mathcal{K}$
- (ii)  $y^- \left( x^b(t), x^r(t), \delta(t) \right) \leq \bar{y}^-(t) \forall \delta \in \mathcal{D}, \forall t \in \mathcal{T} \iff y_k^- \left( x_k^b, x_k^r, \delta_k \right) \leq \bar{y}_k^- \forall \delta \in \mathcal{D}_{\mathcal{K}}, \forall k \in \mathcal{K}$

*Proof.* Assertion (i) can be reexpressed as

$$\max_{t \in \mathcal{T}} \max_{\delta \in \mathcal{D}} y^+ \left( x^b(t), x^r(t), \delta(t) \right) - \bar{y}^+(t) \leq 0 \iff \max_{k \in \mathcal{K}} \max_{\delta \in \mathcal{D}_{\mathcal{K}}} y_k^+ \left( x_k^b, x_k^r, \delta_k \right) - \bar{y}_k^+ \leq 0.$$

We will prove this equivalence by showing that the left hand sides of the two inequalities are equal. Indeed, a direct calculation reveals that

$$\begin{aligned}
 \max_{t \in \mathcal{T}} \max_{\delta \in \mathcal{D}} y^+ \left( x^b(t), x^r(t), \delta(t) \right) - \bar{y}^+(t) &= \max_{t \in \mathcal{T}} \max_{-1 \leq \delta(t) \leq 1} \left[ x^b(t) + \delta(t) x^r(t) \right]^+ - \bar{y}^+(t) \\
 &= \max_{t \in \mathcal{T}} x^b(t) + x^r(t) - \bar{y}^+(t) \\
 &= \max_{k \in \mathcal{K}} x_k^b + x_k^r - \bar{y}_k^+ \\
 &= \max_{k \in \mathcal{K}} \max_{-1 \leq \delta_k \leq 1} \left[ x_k^b + \delta_k x_k^r \right]^+ - \bar{y}_k^+ \\
 &= \max_{k \in \mathcal{K}} \max_{\delta \in \mathcal{D}_{\mathcal{K}}} y^+ \left( x_k^b, x_k^r, \delta \right) - \bar{y}_k^+,
 \end{aligned} \tag{2.8}$$

where the first equality follows from the definition of  $y^+$  in (2.1a) and the observation that  $\{\delta(t) : \delta \in \mathcal{D}\} = [-1, 1]$ , while the second equality holds because  $x^b(t) \geq 0$  and  $x^r(t) \geq 0$  which implies that  $\delta(t) = 1$  maximizes the instantaneous charging rate. The third equality exploits our assumption that  $x^b, x^r$ , and  $\bar{y}^+$  are piecewise constant functions. The fourth equality holds because  $x_k^b \geq 0$  and  $x_k^r \geq 0$ , which implies that  $\delta_k = 1$  maximizes the per-period charging rate. The fifth equality follows again from the definition of  $y^+$  in (2.1a) and the observation that  $\{\delta_k : \delta \in \mathcal{D}_{\mathcal{K}}\} = [-1, 1]$ .

The proof of assertion (ii) is similar and therefore omitted.  $\square$

**Proposition 2.7.** *The following equivalence holds.*

$$y \left( x^b, x^r, \delta, y_0, t \right) \leq \bar{y} \quad \forall \delta \in \mathcal{D}, \forall t \in \mathcal{T} \iff y_k \left( \mathbf{x}^b, \mathbf{x}^r, \boldsymbol{\delta}, y_0 \right) \leq \bar{y} \quad \forall \boldsymbol{\delta} \in \mathcal{D}_{\mathcal{K}}, \forall k \in \mathcal{K} \cup \{0\}$$

*Proof.* The claim follows if we can show that

$$\max_{t \in \mathcal{T}} \max_{\delta \in \mathcal{D}} y \left( x^b, x^r, \delta, y_0, t \right) = \max_{k \in \mathcal{K} \cup \{0\}} \max_{\boldsymbol{\delta} \in \mathcal{D}_{\mathcal{K}}} y_k \left( \mathbf{x}^b, \mathbf{x}^r, \boldsymbol{\delta}, y_0 \right). \tag{2.9}$$

To this end, assume first that  $t = k\Delta t$  for some  $k \in \mathcal{K} \cup \{0\}$ . In this case, we have

$$\begin{aligned}
 \max_{\delta \in \mathcal{D}} y \left( x^b, x^r, \delta, y_0, t \right) &= \max_{\delta \in \mathcal{D}^+} y \left( x^b, x^r, \delta, y_0, t \right) \\
 &= y_0 + \max_{\delta \in \mathcal{D}^+} \int_0^t \eta^+ \left( x^b(t') + \delta(t') x^r(t') \right) - d(t') dt' \\
 &= y_0 + \max_{\delta \in \mathcal{D}^+} \sum_{l=1}^k \int_{\mathcal{T}_l} \eta^+ \left( x_l^b + \delta(t') x_l^r \right) - d_l dt' \\
 &= y_0 + \max_{\delta \in \mathcal{D}^+} \Delta t \sum_{l=1}^k \eta^+ \left( x_l^b + (L^\dagger \delta)_l x_l^r \right) - d_l \\
 &= y_0 + \max_{\boldsymbol{\delta} \in \mathcal{D}_{\mathcal{K}}^+} \Delta t \sum_{l=1}^k \eta^+ \left( x_l^b + \delta_l x_l^r \right) - d_l \\
 &= \max_{\boldsymbol{\delta} \in \mathcal{D}_{\mathcal{K}}^+} y_k \left( \mathbf{x}^b, \mathbf{x}^r, \boldsymbol{\delta}, y_0 \right) = \max_{\boldsymbol{\delta} \in \mathcal{D}_{\mathcal{K}}} y_k \left( \mathbf{x}^b, \mathbf{x}^r, \boldsymbol{\delta}, y_0 \right),
 \end{aligned} \tag{2.10}$$

## Reliable Frequency Regulation through Vehicle-to-Grid: Encoding Legislation with Robust Constraints

where the first equality holds because  $\delta \in \mathcal{D}$  if and only if  $|\delta| \in \mathcal{D}^+$  and because  $y$  is nondecreasing in  $\delta$  thanks to Proposition 2.1. The second equality follows from the definitions of  $y$ ,  $y^+$ , and  $y^-$  and from the non-negativity of  $x^b$ ,  $x^r$  and  $\delta$ . The third equality exploits our assumption that  $d$ ,  $x^b$  and  $x^r$  are piecewise constant. As  $\delta$  is integrated against a piecewise constant function, it may be averaged over the trading intervals without changing its objective function value. The fifth equality then follows from Proposition 2.3, while the sixth equality follows from the definitions of  $y_k$ ,  $y^+$  and  $y^-$  and from the non-negativity of  $x^b$ ,  $x^r$  and  $\delta$ . The seventh equality, finally, holds because  $\delta \in \mathcal{D}_{\mathcal{K}}$  if and only if  $|\delta| \in \mathcal{D}_{\mathcal{K}}^+$  and because  $y_k$  is nondecreasing in  $\delta$  thanks to Proposition 2.6.

Assume now more generally that  $t \in \mathcal{T}_k$  for some  $k \in \mathcal{K}$ . If the vehicle is driving in trading interval  $\mathcal{T}_k$ , then  $\bar{y}^+(t) = \bar{y}^-(t) = 0$  for all  $t \in \mathcal{T}_k$ . Thus, we have

$$\begin{aligned} \max_{\delta \in \mathcal{D}} y(x^b, x^r, \delta, y_0, t) &= \max_{\delta \in \mathcal{D}} y(x^b, x^r, \delta, y_0, (k-1)\Delta t) - \int_{(k-1)\Delta t}^t d(t') dt' \\ &\leq \max_{\delta \in \mathcal{D}} y(x^b, x^r, \delta, y_0, (k-1)\Delta t) = \max_{\delta \in \mathcal{D}_{\mathcal{K}}} y_{k-1}(x^b, x^r, \delta, y_0) \quad \forall t \in \mathcal{T}_k, \end{aligned}$$

where the inequality holds because  $d(t) \geq 0$  for all  $t \in \mathcal{T}_k$ , and the second equality follows from the first part of the proof. Alternatively, if the vehicle is parked in trading interval  $\mathcal{T}_k$ , then  $d(t) = 0$  for all  $t \in \mathcal{T}_k$ . Thus, we have

$$\begin{aligned} \max_{\delta \in \mathcal{D}} y(x^b, x^r, \delta, y_0, t) &= \max_{\delta \in \mathcal{D}^+} y(x^b, x^r, \delta, y_0, t) \\ &= \max_{\delta \in \mathcal{D}^+} y(x^b, x^r, \delta, y_0, (k-1)\Delta t) + \int_{(k-1)\Delta t}^t \eta^+ y^+(x^b(t'), x^r(t'), \delta(t')) dt' \\ &\leq \max_{\delta \in \mathcal{D}^+} y(x^b, x^r, \delta, y_0, k\Delta t) = \max_{\delta \in \mathcal{D}_{\mathcal{K}}^+} y_k(x^b, x^r, \delta, y_0) = \max_{\delta \in \mathcal{D}_{\mathcal{K}}} y_k(x^b, x^r, \delta, y_0) \end{aligned}$$

for all  $t \in \mathcal{T}_k$ , where the inequality holds because the integral is nondecreasing in  $t$ , and the equalities follow from the first part of the proof. In summary, we have shown that

$$\max_{\delta \in \mathcal{D}} y(x^b, x^r, \delta, y_0, t) \leq \max \left\{ \max_{\delta \in \mathcal{D}_{\mathcal{K}}} y_{k-1}(x^b, x^r, \delta, y_0), \max_{\delta \in \mathcal{D}_{\mathcal{K}}} y_k(x^b, x^r, \delta, y_0) \right\}$$

for all  $t \in \mathcal{T}_k$  and  $k \in \mathcal{K}$ . This implies that

$$\max_{t \in \mathcal{T}} \max_{\delta \in \mathcal{D}} y(x^b, x^r, \delta, y_0, t) \leq \max_{k \in \mathcal{K} \cup \{0\}} \max_{\delta \in \mathcal{D}_{\mathcal{K}}} y_k(x^b, x^r, \delta, y_0).$$

On the other hand, we have

$$\max_{t \in \mathcal{T}} \max_{\delta \in \mathcal{D}} y(x^b, x^r, \delta, y_0, t) \geq \max_{k \in \mathcal{K} \cup \{0\}} \max_{\delta \in \mathcal{D}} y(x^b, x^r, \delta, y_0, k\Delta t) = \max_{k \in \mathcal{K} \cup \{0\}} \max_{\delta \in \mathcal{D}_{\mathcal{K}}} y_k(x^b, x^r, \delta, y_0),$$

where the equality follows from the first part of the proof. Combining the above inequalities implies (2.9), and thus the claim follows.  $\square$

**Proposition 2.8.** *The following equivalence holds.*

$$y(x^b, x^r, \delta, y_0, t) \geq \underline{y} \quad \forall \delta \in \mathcal{D}, \forall t \in \mathcal{T} \iff y_k(x^b, x^r, \delta, y_0) \geq \underline{y} \quad \forall \delta \in \mathcal{D}_{\mathcal{K}}, \forall k \in \mathcal{K} \cup \{0\}$$

The proof of Proposition 2.8 is significantly more challenging than that of Proposition 2.7 because  $y(x^b, x^r, \delta, y_0, t)$  is concave in  $\delta$ . We make it more digestible by first proving two lemmas.

**Lemma 2.1.** *If  $f: \mathbb{R} \times \mathcal{T} \rightarrow \mathbb{R}$  is concave, continuous and nonincreasing in its first argument and piecewise constant on the trading intervals  $\mathcal{T}_k$ ,  $k \in \mathcal{K}$ , in its second argument, then*

$$\min_{\delta \in \mathcal{D}^+} \int_0^t f(\delta(t'), t') dt' = \min_{\delta \in \mathcal{D}^+ \cap \mathcal{L}(\mathcal{T}, \{0,1\})} \int_0^t f(\delta(t'), t') dt' \quad \forall t \in \mathcal{T}.$$

*Proof.* For ease of exposition, assume first that  $t = T$  and define  $t_k = \Delta t(k-1)$  for every  $k \in \mathcal{K}$ . For every approximation parameter  $N \in \mathbb{N}$  we define  $\mathcal{N} = \{1, \dots, N\}$  and set

$$\mathcal{T}_{k,n}^N = \left[ \Delta t \left( k-1 + \frac{n-1}{N} \right), \Delta t \left( k-1 + \frac{n}{N} \right) \right) \quad \forall k \in \mathcal{K}, \forall n \in \mathcal{N}.$$

Note that the  $\mathcal{T}_{k,n}^N$ ,  $n \in \mathcal{N}$ , are mutually disjoint and that their union coincides with the  $k$ -th trading interval  $\mathcal{T}_k$ . Next, introduce a lifting operator  $L_N: \mathbb{R}^{K \times N} \rightarrow \mathcal{L}(\mathcal{T}, \mathbb{R})$  defined through  $(L_N \delta)(t) = \delta_{k,n}$  if  $t \in \mathcal{T}_{k,n}^N$  for  $k \in \mathcal{K}$  and  $n \in \mathcal{N}$ . In addition, let  $L_N^\dagger: \mathcal{L}(\mathcal{T}, \mathbb{R}) \rightarrow \mathbb{R}^{K \times N}$  be the corresponding adjoint operator defined through  $(L_N^\dagger \delta)_{k,n} = \frac{N}{\Delta t} \int_{\mathcal{T}_{k,n}^N} \delta(t) dt$  for  $k \in \mathcal{K}$  and  $n \in \mathcal{N}$ . Using this notation, we first prove that

$$\lim_{N \rightarrow \infty} \sum_{k \in \mathcal{K}} \sum_{n \in \mathcal{N}} f\left((L_N^\dagger \delta)_{k,n}, t_k\right) \frac{\Delta t}{N} = \int_0^T f(\delta(t), t) dt \quad (2.11)$$

for any fixed  $\delta \in \mathcal{D}^+$ . As  $f$  is continuous and nonincreasing in its first argument and piecewise constant in its second argument, we have

$$\inf_{t \in \mathcal{T}_{k,n}^N} f(\delta(t), t) = f\left(\sup_{t \in \mathcal{T}_{k,n}^N} \delta(t), t_k\right) \leq f\left((L_N^\dagger \delta)_{k,n}, t_k\right) \leq f\left(\inf_{t \in \mathcal{T}_{k,n}^N} \delta(t), t_k\right) = \sup_{t \in \mathcal{T}_{k,n}^N} f(\delta(t), t)$$

for every  $k \in \mathcal{K}$ ,  $n \in \mathcal{N}$  and  $N \in \mathbb{N}$ . Summing over  $k$  and  $n$  thus yields

$$\sum_{k \in \mathcal{K}} \sum_{n \in \mathcal{N}} \inf_{t \in \mathcal{T}_{k,n}^N} f(\delta(t), t) \frac{\Delta t}{N} \leq \sum_{k \in \mathcal{K}} \sum_{n \in \mathcal{N}} f\left((L_N^\dagger \delta)_{k,n}, t_k\right) \frac{\Delta t}{N} \leq \sum_{k \in \mathcal{K}} \sum_{n \in \mathcal{N}} \sup_{t \in \mathcal{T}_{k,n}^N} f(\delta(t), t) \frac{\Delta t}{N}$$

for every  $N \in \mathbb{N}$ . As  $f(\delta(t), t)$  constitutes a composition of a continuous function with a Riemann integrable function, it is also Riemann integrable. Thus, the lower and upper Riemann sums in the above inequality both converge to  $\int_0^T f(\delta(t), t) dt$  as  $N$  tends to infinity. This



## Reliable Frequency Regulation through Vehicle-to-Grid: Encoding Legislation with Robust Constraints

---

observation establishes (2.11). As  $\delta \in \mathcal{D}^+$  was chosen arbitrarily, we may thus conclude that

$$\inf_{\delta \in \mathcal{D}^+} \int_0^T f(\delta(t), t) dt = \inf_{\delta \in \mathcal{D}^+} \lim_{N \rightarrow \infty} \sum_{k \in \mathcal{K}} \sum_{n \in \mathcal{N}} f\left(\left(L_N^\dagger \delta\right)_{k,n}, t_k\right) \frac{\Delta t}{N}.$$

For the following derivations we introduce the auxiliary uncertainty set

$$\mathcal{D}_{KN}^+ = \left\{ \delta \in [-1, 1]^{KN} : \sum_{l=1+[m-NT/\Delta t]^+}^m \delta_l \leq N \frac{\gamma}{\Delta t} \quad \forall m = 1, \dots, KN \right\}$$

for  $N \in \mathbb{N}$ . By slight abuse of notation, we henceforth naturally identify any matrix  $\delta \in \mathbb{R}^{K \times N}$  with the vector obtained by concatenating the rows of  $\delta$ . This convention allows us, for example, to write  $\delta \in \mathcal{D}_{KN}^+$  even if  $\delta$  was initially defined as a  $K \times N$ -matrix. By repeating the arguments of Proposition 2.3, it is easy to show that  $L_N \mathcal{D}_{KN}^+ \subseteq \mathcal{D}^+$  and  $L_N^\dagger \mathcal{D}^+ = \mathcal{D}_{KN}^+$  for all  $N \in \mathbb{N}$ . Using these relations, we will now prove that

$$\inf_{\delta \in \mathcal{D}^+} \int_0^T f(\delta(t), t) dt = \lim_{N \rightarrow \infty} \inf_{\delta \in \mathcal{D}_{KN}^+} \sum_{k \in \mathcal{K}} \sum_{n \in \mathcal{N}} f(\delta_{k,n}, t_k) \frac{\Delta t}{N}. \quad (2.12)$$

To this end, select any  $\epsilon > 0$  and  $\delta^* \in \mathcal{D}^+$  with  $\int_0^T f(\delta^*(t), t) dt \leq \inf_{\delta \in \mathcal{D}^+} \int_0^T f(\delta(t), t) dt + \epsilon$ , and choose  $N_\epsilon$  large enough such that

$$\left| \sum_{k \in \mathcal{K}} \sum_{n \in \mathcal{N}} f\left(\left(L_N^\dagger \delta^*\right)_{k,n}, t_k\right) \frac{\Delta t}{N} - \int_0^T f(\delta^*(t), t) dt \right| \leq \epsilon \quad \forall N \geq N_\epsilon.$$

Note that such an  $N_\epsilon$  exists thanks to (2.11). For any  $N \geq N_\epsilon$ , we thus find

$$\begin{aligned} 0 &\leq \inf_{\delta \in \mathcal{D}_{KN}^+} \sum_{k \in \mathcal{K}} \sum_{n \in \mathcal{N}} f(\delta_{k,n}, t_k) \frac{\Delta t}{N} - \inf_{\delta \in \mathcal{D}^+} \int_0^T f(\delta(t), t) dt \\ &\leq \inf_{\delta \in \mathcal{D}_{KN}^+} \sum_{k \in \mathcal{K}} \sum_{n \in \mathcal{N}} f(\delta_{k,n}, t_k) \frac{\Delta t}{N} - \int_0^T f(\delta^*(t), t) dt + \epsilon \\ &\leq \sum_{k \in \mathcal{K}} \sum_{n \in \mathcal{N}} f\left(\left(L_N^\dagger \delta^*\right)_{k,n}, t_k\right) \frac{\Delta t}{N} - \int_0^T f(\delta^*(t), t) dt + \epsilon \leq 2\epsilon, \end{aligned}$$

where the first inequality holds because  $L_N \mathcal{D}_{KN}^+ \subseteq \mathcal{D}^+$ , the second inequality follows from the choice of  $\delta^*$ , the third inequality exploits the identity  $L_N^\dagger \mathcal{D}^+ = \mathcal{D}_{KN}^+$ , and the fourth inequality holds because  $N \geq N_\epsilon$ . As  $\epsilon > 0$  was chosen arbitrarily, Equation (2.12) follows.

In order to prove that

$$\inf_{\delta \in \mathcal{D}^+} \int_0^T f(\delta(t), t) dt = \inf_{\delta \in \mathcal{D}^+ \cap \mathcal{L}(\mathcal{T}, \{0,1\})} \int_0^T f(\delta(t), t) dt, \quad (2.13)$$

we first observe that

$$\begin{aligned} \inf_{\delta \in \mathcal{D}^+} \int_0^T f(\delta(t), t) dt &= \lim_{N \rightarrow \infty} \inf_{\delta \in \mathcal{D}_{KN}^+} \sum_{k \in \mathcal{K}} \sum_{n \in \mathcal{N}} f(\delta_{k,n}, t_k) \frac{\Delta t}{N} \\ &= \lim_{N \rightarrow \infty} \inf_{\delta \in \mathcal{D}_{KN}^+ \cap \{0,1\}^{KN}} \sum_{k \in \mathcal{K}} \sum_{n \in \mathcal{N}} f(\delta_{k,n}, t_k) \frac{\Delta t}{N}. \end{aligned} \quad (2.14)$$

Here, the first equality follows from (2.12), and the second equality holds because  $f$  is concave in its first argument, which implies that the minimum over  $\delta$  is attained at a vertex of the polyhedron  $\mathcal{D}_{KN}^+$ . As all vertices of  $\mathcal{D}_{KN}^+$  are binary by virtue of Lemma 2.2 below, we can restrict  $\delta$  to  $\{0,1\}^{KN}$  without loss of optimality. To prove (2.13), select any  $\epsilon > 0$  and  $N \in \mathbb{N}$  large enough such that

$$\left| \min_{\delta \in \mathcal{D}_{KN}^+ \cap \{0,1\}^{KN}} \sum_{k \in \mathcal{K}} \sum_{n \in \mathcal{N}} f(\delta_{k,n}, t_k) \frac{\Delta t}{N} - \inf_{\delta \in \mathcal{D}^+} \int_0^T f(\delta(t), t) dt \right| \leq \epsilon. \quad (2.15)$$

Note that such an  $N$  exists because of (2.14). Next, let  $\delta^*$  be a minimizer of the discrete optimization problem on the left hand side of the above expression, and set  $\delta^* = L_N \delta^*$ . By (2.15) and because  $\delta^*$  is constant on the intervals  $\mathcal{T}_{k,n}^N$ , we thus have

$$\left| \int_0^T f(\delta^*(t), t) dt - \inf_{\delta \in \mathcal{D}^+} \int_0^T f(\delta(t), t) dt \right| \leq \epsilon.$$

As  $L_N \mathcal{D}_{KN}^+ \subseteq \mathcal{D}^+$  and  $\delta^* \in \{0,1\}^{KN}$ , we further have  $\delta^* \in \mathcal{D}^+ \cap \mathcal{L}(\mathcal{T}, \{0,1\})$ . As  $\epsilon$  was chosen arbitrarily, Equation (2.13) follows.

If  $t \in \mathcal{T}$  is a multiple of  $1/(KN)$  for some  $N \in \mathbb{N}$ , then  $f(\delta(t'), t')$  can be set to 0 for all  $t' \geq t$ , and the above proof remains valid with obvious minor modifications. For any other  $t \in \mathcal{T}$ , the claim follows from a continuity argument. Details are omitted for brevity.  $\square$

**Lemma 2.2.** For any  $N \in \mathbb{N}$ , all vertices of the polyhedron

$$\mathcal{D}_{KN}^+ = \left\{ \delta \in [0,1]^{KN} : \sum_{l=1+[m-NT/\Delta t]^+}^m \delta_l \leq N \frac{\gamma}{\Delta t} \quad \forall m = 1, \dots, KN \right\}$$

are binary vectors.

*Proof.* The polyhedron  $\mathcal{D}_{KN}^+$  can be represented more concisely as  $\{\delta \in \mathbb{R}_+^{KN} : A\delta \leq b\}$ , where

$$A = \begin{pmatrix} C \\ I \end{pmatrix} \in \mathbb{R}^{2KN \times KN}, \quad b = \begin{bmatrix} N \frac{\gamma}{\Delta t} \mathbf{1} \\ \mathbf{1} \end{bmatrix} \in \mathbb{R}^{2KN}$$

and  $C \in \mathbb{R}^{KN \times KN}$  is defined through  $C_{ij} = 1$  if  $i - NT/\Delta t < j \leq i$  and  $C_{ij} = 0$  otherwise. Here,  $I$  denotes the identity matrix and  $\mathbf{1}$  the column vector of 1s in  $\mathbb{R}^{KN}$ . By construction,  $A$  is a binary matrix where the 1s appear consecutively in each row. Proposition 2.1 and Corollary 2.10 by

## Reliable Frequency Regulation through Vehicle-to-Grid: Encoding Legislation with Robust Constraints

Nemhauser and Wolsey (1999) thus imply that  $\mathbf{A}$  is totally unimodular. As  $\mathbf{b} \in \mathbb{Z}^{KN}$  because of Assumption 2.2, all vertices of  $\mathcal{D}_{KN}^+$  are integral thanks to Proposition 2.2 again by Nemhauser and Wolsey (1999). In addition, as  $D_{KN}^+ \subseteq [0, 1]^{KN}$ , the vertices of  $\mathcal{D}_{KN}^+$  are in fact binary vectors.  $\square$

We are now ready to prove Proposition 2.8.

*Proof of Proposition 2.8.* The claim follows if we can show that

$$\min_{t \in \mathcal{T}} \min_{\delta \in \mathcal{D}} y(x^b, x^r, \delta, y_0, t) = \min_{k \in \mathcal{K} \cup \{0\}} \min_{\delta \in \mathcal{D}_{\mathcal{K}}} y_k(x^b, x^r, \delta, y_0). \quad (2.16)$$

In the first part of the proof, we reformulate the continuous non-convex minimization problem  $\min_{\delta \in \mathcal{D}} y(x^b, x^r, \delta, y_0, t)$  as a continuous linear program. To ease notation, we set  $\Delta\eta = \frac{1}{\eta^-} - \eta^+ \geq 0$  and define the auxiliary functions

$$\chi(\delta(t), t) = \max \left\{ \eta^+ x^r(t) \delta(t), \frac{1}{\eta^-} x^r(t) \delta(t) - \Delta\eta x^b(t) \right\}$$

and

$$m(t) = \max \left\{ \eta^+ x^r(t), \frac{1}{\eta^-} x^r(t) - \Delta\eta x^b(t) \right\}$$

for all  $t \in \mathcal{T}$ . The function  $\chi(\delta(t), t)$  can be viewed as a *nonlinear decision rule* of the uncertain frequency deviation  $\delta(t)$ . Using these conventions, we find

$$\begin{aligned} \min_{\delta \in \mathcal{D}} y(x^b, x^r, \delta, y_0, t) &= \min_{\delta \in \mathcal{D}^+} y(x^b, x^r, -\delta, y_0, t) \\ &= y_0 + \min_{\delta \in \mathcal{D}^+} \int_0^t \eta^+ x^b(t') - \chi(\delta(t'), t') - d(t') dt' \\ &= y_0 + \min_{\delta \in \mathcal{D}^+ \cap \mathcal{L}(\mathcal{T}, \{0,1\})} \int_0^t \eta^+ x^b(t') - \chi(\delta(t'), t') - d(t') dt' \quad (2.17) \\ &= y_0 + \min_{\delta \in \mathcal{D}^+ \cap \mathcal{L}(\mathcal{T}, \{0,1\})} \int_0^t \eta^+ x^b(t') - m(t') \delta(t') - d(t') dt' \\ &= y_0 + \min_{\delta \in \mathcal{D}^+} \int_0^t \eta^+ x^b(t') - m(t') \delta(t') - d(t') dt', \end{aligned}$$

where the first equality holds because the statements  $\delta \in \mathcal{D}$ ,  $-\delta \in \mathcal{D}$  and  $|\delta| \in \mathcal{D}^+$  are all equivalent and because  $y$  is nondecreasing in  $\delta$  thanks to Proposition 2.1. The second equality follows from the definitions of  $y$ ,  $y^+$ ,  $y^-$  and  $\chi$ , and the third equality is a direct consequence of Lemma 2.1, which applies because  $-\chi$  is concave and nonincreasing in its first argument and, by virtue of Assumption 2.1, piecewise constant in its second argument. The fourth equality holds because  $\chi(\delta(t'), t') = m(t') \delta(t')$  whenever  $\delta(t') \in \{0, 1\}$ , and the last equality follows again from Lemma 2.1. Note that  $m(t') \delta(t')$  constitutes a *linear decision rule* of  $\delta(t)$ .

In the second part of the proof we assume that  $t = k\Delta t$  for some  $k \in \mathcal{K} \cup \{0\}$  and show that

$$\min_{\delta \in \mathcal{D}} y(x^b, x^r, \delta, y_0, t) = \min_{\delta \in \mathcal{D}_{\mathcal{K}}} y_k(\mathbf{x}^b, \mathbf{x}^r, \boldsymbol{\delta}, y_0).$$

To this end, we define  $\chi_l(\delta_l) = \max\{\eta^+ x_l^r \delta_l, \frac{1}{\eta^-} x_l^r \delta_l - \Delta \eta x_l^b\}$  and  $m_l = \max\{\eta^+ x_l^r, \frac{x_l^r}{\eta^-} - \Delta \eta x_l^b\}$  for all  $l \in \mathcal{K}$ . By (2.17), we thus have

$$\begin{aligned} \min_{\delta \in \mathcal{D}} y(x^b, x^r, \delta, y_0, k\Delta t) &= y_0 + \min_{\delta \in \mathcal{D}^+} \int_0^{k\Delta t} \eta^+ x^b(t') - m(t')\delta(t') - d(t') dt' \\ &= y_0 + \min_{\delta \in \mathcal{D}^+} \sum_{l=1}^k \int_{\mathcal{T}_l} \eta^+ x_l^b - m_l \delta(t') - d_l dt' \\ &= y_0 + \min_{\delta \in \mathcal{D}_{\mathcal{K}}^+} \Delta t \sum_{l=1}^k \eta^+ x_l^b - m_l \delta_l - d_l \\ &= \min_{\delta \in \mathcal{D}_{\mathcal{K}}} y_k(\mathbf{x}^b, \mathbf{x}^r, \boldsymbol{\delta}, y_0), \end{aligned} \tag{2.18}$$

where the second equality holds because  $d, x^b$  and  $x^r$  are piecewise constant by virtue of Assumption 2.1, which implies that  $m(t') = m_l$  for every  $t' \in \mathcal{T}_l$ . The third equality then follows from Proposition 2.3. The fourth equality can be proved by reversing the arguments from (2.17) with obvious minor modifications. In fact, as the frequency deviation scenarios are now piecewise constant and can be encoded by finite-dimensional vectors, the proof requires no cumbersome limiting arguments as the ones developed in the proof of Lemma 2.1. We omit the details for brevity.

In the third part of the proof we assume that  $t \in \mathcal{T}_k$  for some  $k \in \mathcal{K}$  and show that

$$\min_{t \in \mathcal{T}_k} \min_{\delta \in \mathcal{D}} y(x^b, x^r, \delta, y_0, t) = \min_{l \in \{k-1, k\}} \min_{\delta \in \mathcal{D}_{\mathcal{K}}} y_l(\mathbf{x}^b, \mathbf{x}^r, \boldsymbol{\delta}, y_0).$$

As in the proof of Proposition 2.7, we distinguish whether or not the vehicle is driving in period  $\mathcal{T}_k$ . Specifically, if the vehicle is driving in period  $\mathcal{T}_k$ , then  $\bar{y}^+(t) = \bar{y}^-(t) = 0$ , which implies that

$$\begin{aligned} \min_{\delta \in \mathcal{D}} y(x^b, x^r, \delta, y_0, t) &= \min_{\delta \in \mathcal{D}} y(x^b, x^r, \delta, y_0, (k-1)\Delta t) - \int_{(k-1)\Delta t}^t d(t') dt \\ &= \min_{\delta \in \mathcal{D}} y(x^b, x^r, \delta, y_0, k\Delta t) + \int_t^{k\Delta t} d(t') dt \\ &\geq \min_{\delta \in \mathcal{D}} y(x^b, x^r, \delta, y_0, k\Delta t) = \min_{\delta \in \mathcal{D}_{\mathcal{K}}} y_k(\mathbf{x}^b, \mathbf{x}^r, \boldsymbol{\delta}, y_0). \end{aligned}$$

Here, the inequality holds because  $d(t) \geq 0$  for all  $t \in \mathcal{T}_k$ , and the last equality follows from (2.18). Otherwise, if the vehicle is parked in period  $\mathcal{T}_k$ , then  $d(t) = 0$  for all  $t \in \mathcal{T}_k$ ,

and hence

$$\begin{aligned}
& \min_{\delta \in \mathcal{D}} y(x^b, x^r, \delta, y_0, t) \\
&= y_0 + \min_{\delta \in \mathcal{D}^+(t)} \sum_{l=1}^{k-1} \int_{\mathcal{T}_l} \eta^+ x_l^b - m_l \delta(t') - d_l dt' + \int_{(k-1)\Delta t}^t \eta^+ x_k^b - m_k \delta(t') dt' \\
&= y_0 + \min_{\delta \in \mathcal{D}^+(t)} \Delta t \sum_{l=1}^{k-1} \eta^+ x_l^b - d_l + (t - (k-1)\Delta t) \eta^+ x_k^b - \sum_{l=1}^k \int_{\mathcal{T}_l} m_l \delta(t') dt' \\
&= y_0 + \Delta t \sum_{l=1}^{k-1} \eta^+ x_l^b - d_l + (t - (k-1)\Delta t) \eta^+ x_k^b - \max_{\delta \in \mathcal{D}_{\mathcal{K}}^+(t)} \Delta t \sum_{l=1}^k m_l \delta_l,
\end{aligned} \tag{2.19}$$

where we use the time-dependent uncertainty sets

$$\mathcal{D}^+(t) = \left\{ \delta \in \mathcal{D}^+ : \delta(t') = 0 \ \forall t' \in [t, k\Delta t] \right\} \quad \text{and} \quad \mathcal{D}_{\mathcal{K}}^+(t) = \left\{ \delta \in \mathcal{D}_{\mathcal{K}}^+ : \delta_k \leq \frac{t - (k-1)\Delta t}{\Delta t} \right\}$$

to simplify the notation. The first equality in (2.19) follows from (2.17) and Assumption 2.1. Note that  $\delta(t')$  does not impact the objective function of the resulting minimization problem over  $\mathcal{D}^+$  for any  $t' > t$ . It is therefore optimal to set  $\delta(t') = 0$  for all  $t' \geq t$  and, in particular, for all  $t' \in [t, k\Delta t]$ . This restriction has no impact on the objective function but maximizes nature's flexibility in selecting harmful frequency deviations  $\delta(t')$  for  $t' \leq t$ . Hence, the second equality in (2.19) follows. As  $\delta$  is now integrated against a piecewise constant function, it may be averaged over the trading intervals without changing its objective function value. The third equality in (2.19) thus holds because  $L^\dagger \mathcal{D}^+(t) = \mathcal{D}_{\mathcal{K}}^+(t)$ , which can be proved similarly to Proposition 2.3 by noting that

$$(\mathcal{L}^\dagger \delta)_k = \frac{1}{\Delta t} \int_{(k-1)\Delta t}^t \delta(t') dt' \leq \frac{t - (k-1)\Delta t}{\Delta t} \quad \forall \delta \in \mathcal{D}^+(t).$$

In the following we show that (2.19) is piecewise affine in  $t$ . To this end, note that the optimization problem in the last line of (2.19) can be expressed more concisely as the standard form linear program

$$\begin{aligned}
& \min_{\mathbf{z} \geq \mathbf{0}} \quad \mathbf{c}^\top \mathbf{z} \\
& \text{s.t.} \quad \mathbf{A}\mathbf{z} = \mathbf{b}(t),
\end{aligned} \tag{2.20}$$

where  $\mathbf{z}^\top = (\boldsymbol{\delta}^\top, \mathbf{s}^\top) \in \mathbb{R}^K \times \mathbb{R}^{2K}$  combines the (averaged) frequency deviations in the trading intervals with a vector of slack variables. Here, the vector  $\mathbf{c} \in \mathbb{R}^{3K}$  of objective function coefficients is defined through  $c_l = -m_l \Delta t$  if  $l \leq k$  and  $c_l = 0$  otherwise. The constraints involve the matrix

$$\mathbf{A} = \begin{pmatrix} \mathbf{C} & \mathbf{I} & \mathbf{0} \\ \mathbf{I} & \mathbf{0} & \mathbf{I} \end{pmatrix} \in \mathbb{R}^{2K \times 3K},$$

where  $\mathbf{C} \in \mathbb{R}^{K \times K}$  is defined through  $C_{ij} = 1$  if  $i - \Gamma/\Delta t < j \leq i$  and  $C_{ij} = 0$  otherwise, and the

vector  $\mathbf{b}(t) \in \mathbb{R}^{2K}$  is defined through  $b_l(t) = \frac{t-(k-1)\Delta t}{\Delta t}$  if  $l = k + K$  and  $b_l = 1$  otherwise. By Lemma 2.2 and Proposition 2.1 of Nemhauser and Wolsey (1999),  $\mathbf{A}$  is totally unimodular.

Note that (2.20) is solvable for every  $t \in \mathcal{T}_k$  because its feasible set is non-empty and compact. Next, choose any  $t_0$  in the interior of  $\mathcal{T}_k$ , denote by  $\mathbf{B}$  an optimal basis matrix for problem (2.20) at  $t = t_0$ , and define  $\mathbf{z}^*(t) = \mathbf{B}^{-1}\mathbf{b}(t)$  for all  $t \in \mathcal{T}_k$ . In the following, we will use local sensitivity analysis of linear programming to show that  $\mathbf{z}^*(t)$  is optimal in (2.20) for all  $t \in \mathcal{T}_k$ . As the basis  $\mathbf{B}$  remains dual feasible when  $t$  deviates from  $t_0$ , it suffices to show that

$$\mathbf{z}^*(t) = \mathbf{z}^*(t_0) + \frac{t-t_0}{\Delta t} \mathbf{B}^{-1} \mathbf{e}_{K+k} \geq \mathbf{0} \quad \forall t \in \mathcal{T}_k, \quad (2.21)$$

where  $\mathbf{e}_{K+k}$  denotes the  $(K+k)$ -th standard basis vector in  $\mathbb{R}^{2K}$  (Bertsimas and Tsitsiklis, 1997, p. 207). To this end, note that  $\mathbf{B}$  is a non-singular square matrix constructed from  $2K$  columns of  $\mathbf{A}$  and is therefore also totally unimodular. Moreover,  $\mathbf{B}^{-1}$  is totally unimodular because pivot operations preserve total unimodularity (Nemhauser and Wolsey, 1999, Proposition 2.1). Hence, we have  $\mathbf{B}^{-1} \mathbf{e}_{K+k} \in \{-1, 0, 1\}^{2K}$ . By construction, we further have  $\mathbf{b}(t) \in \{0, 1\}^{2K}$  for  $t = k\Delta t$ , which implies that  $\mathbf{z}^*(k\Delta t) \in \mathbb{Z}^{2K}$ . Evaluating (2.21) at  $t = k\Delta t$  then yields

$$\mathbf{z}^*(t_0) = \mathbf{z}^*(k\Delta t) - \frac{k\Delta t - t_0}{\Delta t} \mathbf{B}^{-1} \mathbf{e}_{K+k},$$

which ensures that  $\mathbf{z}^*(k\Delta t) \geq \mathbf{0}$ . Indeed, if any component of the integral vector  $\mathbf{z}^*(k\Delta t)$  was strictly negative, it would have to be smaller or equal to  $-1$ . As  $t_0$  resides in the interior of  $\mathcal{T}_k$  and thus  $|(k\Delta t - t_0)/\Delta t| < 1$ , the corresponding component of  $\mathbf{z}^*(t_0)$  would then also have to be strictly negative. This, however, contradicts the optimality of  $\mathbf{z}^*(t_0)$ , which implies that  $\mathbf{z}^*(t_0) \geq \mathbf{0}$ . Hence, we have  $\mathbf{z}^*(k\Delta t) \geq \mathbf{0}$ . One can use similar arguments to prove that  $\mathbf{z}^*((k-1)\Delta t) \geq \mathbf{0}$ . As  $\mathbf{z}^*(t)$  is affine in  $t$ , it is indeed non-negative for all  $t \in \mathcal{T}_k$ .

The above reasoning shows that  $\mathbf{z}^*(t)$  is optimal in (2.20) and that the minimum of (2.20) is affine in  $t$  on  $\mathcal{T}_k$ . Equation (2.19) further implies that  $\min_{\delta \in \mathcal{D}} y(x^b, x^r, \delta, y_0, t)$  is affine in  $t$  on  $\mathcal{T}_k$ , and thus

$$\min_{t \in \mathcal{T}_k} \min_{\delta \in \mathcal{D}} y(x^b, x^r, \delta, y_0, t) = \min_{l \in \{k-1, k\}} \min_{\delta \in \mathcal{D}} y(x^b, x^r, \delta, y_0, l\Delta t) = \min_{l \in \{k-1, k\}} \min_{\delta \in \mathcal{D}_k} y_l(\mathbf{x}^b, \mathbf{x}^r, \boldsymbol{\delta}, y_0),$$

where the second equality follows from (2.18). As  $k \in \mathcal{K}$  was chosen arbitrarily, (2.16) follows.  $\square$

**Proposition 2.9.** *The following equality holds.*

$$\max_{\delta \in \hat{\mathcal{D}}, y_0 \in \mathcal{Y}_0} \varphi(y(x^b, x^r, \delta, y_0, T)) = \max_{\delta \in \hat{\mathcal{D}}_{\mathcal{K}}, y_0 \in \mathcal{Y}_0} \varphi(y_K(\mathbf{x}^b, \mathbf{x}^r, \boldsymbol{\delta}, y_0))$$

## Reliable Frequency Regulation through Vehicle-to-Grid: Encoding Legislation with Robust Constraints

---

*Proof.* By introducing an auxiliary epigraphical variable  $z$ , we find

$$\begin{aligned}
 \max_{\delta \in \hat{\mathcal{D}}, y_0 \in \hat{\mathcal{Y}}_0} \varphi(y(x^b, x^r, \delta, y_0, T)) &= \begin{cases} \min_z & z \\ \text{s.t.} & z \geq \max_{\delta \in \hat{\mathcal{D}}, y_0 \in \hat{\mathcal{Y}}_0} \varphi(y(x^b, x^r, \delta, y_0, T)) \end{cases} \\
 &= \begin{cases} \min_z & z \\ \text{s.t.} & z \geq \max_{\delta \in \hat{\mathcal{D}}, y_0 \in \hat{\mathcal{Y}}_0} a_n y(x^b, x^r, \delta, y_0, T) + b_n \quad \forall n \in \mathcal{N} \end{cases} \\
 &= \begin{cases} \min_z & z \\ \text{s.t.} & z \geq \max_{\delta \in \hat{\mathcal{D}}, y_0 \in \hat{\mathcal{Y}}_0} a_n y_K(\mathbf{x}^b, \mathbf{x}^r, \delta, y_0) + b_n \quad \forall n \in \mathcal{N} \end{cases} \\
 &= \max_{\delta \in \hat{\mathcal{D}}, y_0 \in \hat{\mathcal{Y}}_0} \varphi(y_K(\mathbf{x}^b, \mathbf{x}^r, \delta, y_0)).
 \end{aligned} \tag{2.22}$$

The second equality follows from the definition of  $\varphi$  and the third equality follows from Propositions 2.7 and 2.8, which apply since  $\hat{\mathcal{D}}$  and  $\hat{\mathcal{D}}_{\mathcal{K}}$  have the same structures as  $\mathcal{D}$  and  $\mathcal{D}_{\mathcal{K}}$ , respectively.  $\square$

*Proof of Theorem 2.1.* The claim follows immediately from Propositions 2.6–2.9.  $\square$

*Proof of Theorem 2.2.* By introducing embedded optimization problems that evaluate the (decision-dependent) worst-case frequency deviation scenarios and by replacing the uncertain initial state-of-charge in each robust constraint with its (decision-*independent*) worst-case value,  $(\mathbf{R}_{\mathcal{K}})$  becomes

$$\begin{aligned}
 \min_{\mathbf{x}^b, \mathbf{x}^r \in \mathcal{X}_{\mathcal{K}}, z \in \mathbb{R}} \quad & c_{\mathcal{K}}(\mathbf{x}^b, \mathbf{x}^r) + z \\
 \text{s.t.} \quad & \max_{\delta \in \mathcal{D}_{\mathcal{K}}} y^+(x_k^b, x_k^r, \delta_k) \leq \bar{y}_k^+ \quad \forall k \in \mathcal{K} \tag{a} \\
 & \max_{\delta \in \mathcal{D}_{\mathcal{K}}} y^-(x_k^b, x_k^r, \delta_k) \leq \bar{y}_k^- \quad \forall k \in \mathcal{K} \tag{b} \\
 & \max_{\delta \in \mathcal{D}_{\mathcal{K}}} y_k(\mathbf{x}^b, \mathbf{x}^r, \delta, \bar{y}_0) \leq \bar{y} \quad \forall k \in \mathcal{K} \cup \{0\} \tag{c} \\
 & \min_{\delta \in \mathcal{D}_{\mathcal{K}}} y_k(\mathbf{x}^b, \mathbf{x}^r, \delta, \underline{y}_0) \geq \underline{y} \quad \forall k \in \mathcal{K} \cup \{0\} \tag{d} \\
 & \max_{y_0 \in \hat{\mathcal{Y}}_0} \max_{\delta \in \hat{\mathcal{D}}_{\mathcal{K}}} \varphi(y_K(\mathbf{x}^b, \mathbf{x}^r, \delta, y_0)) \leq z \tag{e}
 \end{aligned} \tag{2.23}$$

Here, the worst-case cost-to-go has been moved from the objective function to the constraints by introducing the auxiliary epigraphical variable  $z$ . To show that (2.23) is equivalent to  $(\mathbf{R}'_{\mathcal{K}})$ , we reuse several results derived for the proof of Theorem 2.1. First, by Equation (2.8) in the proof of Proposition 2.6 the maximum charging power in (2.23a) equals

$$\max_{\delta \in \mathcal{D}_{\mathcal{K}}} y^+(x_k^b, x_k^r, \delta_k) = x_k^r + x_k^b.$$

Using similar arguments, it can be shown that the maximum discharging power in (2.23b)

reduces to

$$\max_{\boldsymbol{\delta} \in \mathcal{D}_{\mathcal{K}}} y^-(x_k^b, x_k^r, \delta_k) = x_k^r - x_k^b.$$

Next, Equation (2.10) in the proof of Proposition 2.7 reveals that, for any  $k \in \mathcal{K} \cup \{0\}$ , the maximum state-of-charge in (2.23c) is given by

$$\max_{\boldsymbol{\delta} \in \mathcal{D}_{\mathcal{K}}} y_k(\mathbf{x}^b, \mathbf{x}^r, \boldsymbol{\delta}, \bar{y}_0) = \bar{y}_0 + \max_{\boldsymbol{\delta} \in \mathcal{D}_{\mathcal{K}}^+} \Delta t \sum_{l=1}^k \eta^+(x_l^b + \delta_l x_l^r) - d_l.$$

Similarly, Equation (2.18) in the proof of Proposition 2.8 implies that, for every  $k \in \mathcal{K} \cup \{0\}$ , the minimum state-of-charge in (2.23d) amounts to

$$\min_{\boldsymbol{\delta} \in \mathcal{D}_{\mathcal{K}}} y_k(\mathbf{x}^b, \mathbf{x}^r, \boldsymbol{\delta}, y_0) = y_0 + \min_{\boldsymbol{\delta} \in \mathcal{D}_{\mathcal{K}}^+} \Delta t \sum_{l=1}^k \eta^+ x_l^b - m_l \delta_l - d_l,$$

where  $m_l = \max\{\eta^+ x_l^r, \frac{1}{\eta^-} x_l^r - \Delta \eta x_l^b\}$  constitutes an implicit function of the market decisions  $x_l^b$  and  $x_l^r$ . As (2.23d) imposes a *lower* bound on the minimum state-of-charge,  $m_l$  may be reinterpreted as an auxiliary epigraphical variable that satisfies  $m_l \geq \eta^+ x_l^r$  and  $m_l \geq \frac{1}{\eta^-} x_l^r - \Delta \eta x_l^b$ .

Finally, the maximum cost-to-go in (2.23e) can be reformulated as

$$\begin{aligned} \max_{y_0 \in \hat{\mathcal{Y}}_0} \max_{\boldsymbol{\delta} \in \hat{\mathcal{D}}_{\mathcal{K}}} \varphi(y_K(\mathbf{x}^b, \mathbf{x}^r, \boldsymbol{\delta}, y_0)) &= \max_{y_0 \in \hat{\mathcal{Y}}_0} \max_{\boldsymbol{\delta} \in \hat{\mathcal{D}}_{\mathcal{K}}} \max_{n \in \mathcal{N}} a_n y_K(\mathbf{x}^b, \mathbf{x}^r, \boldsymbol{\delta}, y_0) + b_n \\ &= \max_{\boldsymbol{\delta} \in \hat{\mathcal{D}}_{\mathcal{K}}} \max \left\{ \max_{n \in \mathcal{N}_+} b_n + a_n y_K(\mathbf{x}^b, \mathbf{x}^r, \boldsymbol{\delta}, \hat{y}_0), \max_{n \in \mathcal{N}_-} b_n + a_n y_K(\mathbf{x}^b, \mathbf{x}^r, \boldsymbol{\delta}, \hat{y}_0), \max_{n \in \mathcal{N}_0} b_n \right\}, \end{aligned}$$

where the first equality follows from the definition of the convex piecewise affine function  $\varphi$ . The second equality holds because the order of maximization is immaterial, because  $a_n > 0$  for all  $n \in \mathcal{N}_+$ ,  $a_n < 0$  for all  $n \in \mathcal{N}_-$  and  $a_n = 0$  for all  $n \in \mathcal{N}_0$  and because the state-of-charge  $y_K(\mathbf{x}^b, \mathbf{x}^r, \boldsymbol{\delta}, y_0)$  increases with  $y_0$ . Requiring the last expression to be smaller than or equal to  $z$  is equivalent to

$$\max_{y_0 \in \hat{\mathcal{Y}}_0} \max_{\boldsymbol{\delta} \in \hat{\mathcal{D}}_{\mathcal{K}}} \varphi(y_K(\mathbf{x}^b, \mathbf{x}^r, \boldsymbol{\delta}, y_0)) \leq z \iff \begin{cases} \max_{\boldsymbol{\delta} \in \hat{\mathcal{D}}_{\mathcal{K}}} y_K(\mathbf{x}^b, \mathbf{x}^r, \boldsymbol{\delta}, \hat{y}_0) \leq (z - b_n)/a_n & \forall n \in \mathcal{N}_+ \\ \min_{\boldsymbol{\delta} \in \hat{\mathcal{D}}_{\mathcal{K}}} y_K(\mathbf{x}^b, \mathbf{x}^r, \boldsymbol{\delta}, \hat{y}_0) \geq (z - b_n)/a_n & \forall n \in \mathcal{N}_- \\ b_n \leq z & \forall n \in \mathcal{N}_0. \end{cases}$$

As  $\mathcal{D}_{\mathcal{K}}$  and  $\hat{\mathcal{D}}_{\mathcal{K}}$  have the same structure, the embedded optimization problems over  $\boldsymbol{\delta} \in \hat{\mathcal{D}}_{\mathcal{K}}$  admit similar linear reformulations as the embedded optimization problems over  $\boldsymbol{\delta} \in \mathcal{D}_{\mathcal{K}}$  in (2.23c) and (2.23d). Substituting all obtained reformulations into (2.23) yields (R' <sub>$\mathcal{K}$</sub> ).  $\square$

*Proof of Theorem 2.3.* Problem (R' <sub>$\mathcal{K}$</sub> ) can be reformulated as a linear program by using the



## Reliable Frequency Regulation through Vehicle-to-Grid: Encoding Legislation with Robust Constraints

---

standard machinery of robust optimization (Bertsimas and Sim, 2004; Ben-Tal et al., 2009). For example, the robust upper bound on the state-of-charge for a fixed  $k \in \mathcal{K} \cup \{0\}$  is equivalent to

$$\bar{y}_0 + \Delta t \sum_{l=1}^k \eta^+ (x_l^b + \delta_l x_l^r) - d_l \leq \bar{y} \quad \forall \delta \in \mathcal{D}_{\mathcal{K}}^+ \iff \max_{\delta \in \mathcal{D}_{\mathcal{K}}^+} \Delta t \sum_{l=1}^k \eta^+ (x_l^b + \delta_l x_l^r) - d_l \leq \bar{y} - \bar{y}_0. \quad (2.24)$$

By strong linear programming duality, the maximization problem in (2.24) is equivalent to

$$\begin{aligned} \min_{\Lambda^+, \Theta^+ \in \mathbb{R}_+^{K \times K}} \quad & \sum_{l=1}^k \Delta t \left( \eta^+ x_l^b + \Lambda_{k,l}^+ - d_l \right) + \gamma \Theta_{k,l}^+ \\ \text{s.t.} \quad & \Lambda_{k,l}^+ + \sum_{i=l}^{j(k,l)} \Theta_{k,i}^+ \geq \eta^+ x_l^r \quad \forall l \in \mathcal{K} : l \leq k, \end{aligned} \quad (2.25)$$

and the minimum of (2.25) is smaller or equal to  $\bar{y} - \bar{y}_0$  if and only if problem (2.25) has a feasible solution whose objective value is smaller or equal to  $\bar{y} - \bar{y}_0$ . Therefore, the robust constraint (2.24) is equivalent to the following system of ordinary linear constraints.

$$\begin{aligned} \sum_{l=1}^k \Delta t \left( \eta^+ x_l^b + \Lambda_{k,l}^+ - d_l \right) + \gamma \Theta_{k,l}^+ & \leq \bar{y} - \bar{y}_0 \\ \Lambda_{k,l}^+ + \sum_{i=l}^{I(k,l)} \Theta_{k,i}^+ & \geq \eta^+ x_l^r \quad \forall l \in \mathcal{K} : l \leq k \end{aligned}$$

The remaining robust constraints in  $(R'_{\mathcal{K}})$  can be simplified in a similar manner.  $\square$

*Proof of Proposition 2.5.* We prove the claim by backward induction. Note first that  $\varphi_H$  is convex and piecewise affine by definition. Next, fix any  $h \in \mathcal{H}$ , and assume that  $\varphi_{h+1}$  is convex and piecewise affine, which implies that problem (2.5) is structurally equivalent to problem (R). By Theorems 2.1, 2.2 and 2.3, problem (2.5) can therefore be reformulated as a linear program whose right hand side coefficients depend affinely on  $y_h$ . Global sensitivity analysis of linear programming (Bertsimas and Tsitsiklis, 1997, p. 214) then ensures that  $\varphi_h(y_h)$  is convex and piecewise affine in  $y_h$ .  $\square$

# 3 The Economics of Frequency Regulation through Electricity Storage: An Analytical Solution

Every time a cloud goes by and diminishes solar output for a second or two, we burn some fossil fuels to generate enough little jolts of electricity to even out the electron flow. If we use a traditional power plant for this job, it will operate at only 2 percent of its productive capacity.

— Gretchen A. Bakke, *The Grid*, 2016.

We derive an analytical solution for a simplified version of the decision-making problem in Chapter 2, which only considers stationary storage devices. The decision-making problem applies to storage operators that can sell regulation power and buy or sell electricity on retail or wholesale markets. Mathematically, we formulate again a nonconvex robust optimization problem and treat future frequency deviation trajectories as functional uncertainties. This time, we constrain the expected terminal state-of-charge to be equal to some target, which should allow storage operators to not only make good decisions for the present but also for the future. We show that, thanks to the expected state-of-charge constraint, the amount of electricity bought on the market is an implicit function of the regulation power sold to the grid operator. The decision-making problem thus reduces to a one-dimensional problem, which we show to be convex for all storage devices with realistic roundtrip efficiencies. The implicit function quantifies the amount of power that needs to be purchased to cover the expected energy loss that results from providing frequency regulation. For energy-constrained storage devices, we find that the profits from frequency regulation over the lifetime of the storage devices are roughly inversely proportional to both the percentage and the duration of time for which promised regulation power must be committed and delivered, respectively.

## 3.1 Introduction

In Chapter 2, we have considered a rather general decision-making problem of an electric vehicle aggregator providing primary frequency regulation. Although we showed that the

## The Economics of Frequency Regulation through Electricity Storage: An Analytical Solution

---

decision-making problem is equivalent to a linear program that can be solved efficiently, the solution as such provides only limited intuition on how the profits from frequency regulation depend on the problem parameters, namely the roundtrip efficiency of the vehicle battery, the dispersion of the frequency deviations, and the regulatory parameters, that is, the percentage and duration of time for which promised regulation power must be delivered and committed, respectively.

In this chapter, we consider a simplified version of the decision-making problem for generic stationary electricity storage devices and describe the structure of its solution analytically, which allows us to characterize the impact of these problem parameters.

Our simplifying assumptions consist of

1. constant market bids,
2. a budget uncertainty in function space that captures EU market regulations with a single budget constraint that limits the mean absolute deviation of admissible frequency deviation trajectories,
3. a bidding system for frequency regulation in which bids are submitted just before they become effective.

Other than these assumptions, the main difference to Chapter 2 is that we use a constraint on the expected terminal state-of-charge, rather than a value function, to steer the decision-maker toward decisions that work well for both the present and the future. In Section 3.3 we show that the amount of power bought on electricity markets is an implicit function of the amount of regulation power sold to the grid operator under this constraint. This leads to a one-dimensional decision problem, which we can be solved highly efficiently by bisection for general frequency deviation distributions (see Section 3.4) and analytically for two- and three-point distributions (see Section 3.5)

To ease readability, we refer to generic electricity storage devices as batteries and relegate all proofs to Appendix 3.B.

**Notation.** We denote all random variables by tilde signs. Their realizations are designated by the same symbols without tilde signs. For any  $z \in \mathbb{R}$ , we define  $[z]^+ = \max\{z, 0\}$  and  $[z]^- = \max\{-z, 0\}$ . For any closed intervals  $\mathcal{T}, \mathcal{U} \subseteq \mathbb{R}$ , we define  $\mathcal{L}(\mathcal{T}, \mathcal{U})$  as the space of all Riemann integrable functions  $f : \mathcal{T} \rightarrow \mathcal{U}$ , and we denote the intersection of a set  $\mathcal{B} \subseteq \mathcal{L}(\mathcal{T}, \mathbb{R})$  with  $\mathcal{L}(\mathcal{T}, \mathbb{R}_+)$  as  $\mathcal{B}^+$ . For any signed function  $\delta \in \mathcal{L}(\mathcal{T}, \mathbb{R})$ , we denote by  $|\delta|$  the absolute value function with  $|\delta|(t) = |\delta(t)|$  for every  $t \in \mathcal{T}$ . We denote the subdifferential of a convex function  $f : \mathcal{X} \rightarrow \mathbb{R}$  with nonempty domain  $\mathcal{X} \subseteq \mathbb{R}^n$  at a point  $\mathbf{x}_0 \in \mathcal{X}$  by  $\partial f(\mathbf{x}_0)$ .

### 3.2 Problem Description

We study the decision problem of a battery operator who can sell frequency regulation power  $x^r \in \mathbb{R}_+$  to a grid operator and buy electric power  $x^b \in \mathbb{R}$  on a wholesale or retail market. We allow  $x^b$  to be negative, in which case the amount  $|x^b|$  of power is sold. Both  $x^r$  and  $x^b$  are chosen ex ante and kept constant over a prescribed planning horizon  $\mathcal{T} = [0, T]$  (e.g., the next day). At any time  $t \in \mathcal{T}$ , the battery operator must measure the normalized deviation  $\tilde{\delta}(t) \in [-1, 1]$  of the uncertain instantaneous grid frequency  $\tilde{v}(t)$  from the nominal frequency  $v_0$  and must consume the amount  $x^b + \tilde{\delta}(t)x^r$  of power from the grid. Mathematically, the normalized frequency deviation at time  $t$  is given by

$$\tilde{\delta}(t) = \begin{cases} +1 & \text{if } \tilde{v}(t) > v_0 + \Delta v, \\ \frac{\tilde{v}(t) - v_0}{\Delta v} & \text{if } v_0 - \Delta v \leq \tilde{v}(t) \leq v_0 + \Delta v, \\ -1 & \text{if } \tilde{v}(t) < v_0 - \Delta v, \end{cases}$$

where  $\Delta v$  is the maximum frequency deviation against which the grid operator seeks protection.

The remuneration for offering frequency regulation is twofold. On the one hand, the power  $x^r$  set aside for frequency regulation is compensated at the availability price  $\tilde{p}^a(t)$ . On the other hand, the regulation power  $\tilde{\delta}(t)x^r$  actually delivered at time  $t$  is compensated at the delivery price  $\tilde{p}^d(t)$ . The power  $x^b$  acquired on the market is bought at the price  $\tilde{p}^b(t)$ . In summary, the expected cost over the planning horizon  $\mathcal{T}$  amounts to

$$\mathbb{E} \int_{\mathcal{T}} \tilde{p}^b(t)x^b - \left( \tilde{p}^a(t) - \tilde{\delta}(t)\tilde{p}^d(t) \right) x^r dt.$$

The net power flow leaving the grid at time  $t \in \mathcal{T}$  is given by  $x^b + \delta(t)x^r$ . To reason about the constraints on this power flow imposed by the battery and the charging infrastructure, we henceforth distinguish the charging power  $y^+(x^b, x^r, \delta(t)) = [x^b + \delta(t)x^r]^+$  from the discharging power  $y^-(x^b, x^r, \delta(t)) = [x^b + \delta(t)x^r]^-$ . Specifically, we assume that the charging power is bounded above by the charging capacity  $\bar{y}^+ \in \mathbb{R}_+$ , and the discharging power is bounded above by the discharging capacity  $\bar{y}^- \in \mathbb{R}_+$ . When the battery is charging ( $y^+ > 0$ ), then only a fraction  $\eta^+$  of the charging power enters the battery, where  $\eta^+ \in (0, 1]$  represents the charging efficiency. The rest is dissipated during the charging process. Conversely, when the battery is discharging ( $y^- > 0$ ), then a multiple  $\frac{1}{\eta^-}$  of the discharging power leaves the battery, where  $\eta^- \in (0, 1]$  represents the discharging efficiency. The battery state-of-charge at any time  $t \in \mathcal{T}$  can thus be expressed as

$$y(x^b, x^r, \delta, y_0, t) = y_0 + \int_0^t \eta^+ y^+(x^b, x^r, \delta(t')) - \frac{1}{\eta^-} y^-(x^b, x^r, \delta(t')) dt', \quad (3.1)$$

where  $y_0$  denotes the initial state-of-charge and  $\delta \in \mathcal{L}(\mathcal{T}, [-1, 1])$  is a given frequency deviation trajectory. Throughout the planning horizon, the battery state-of-charge must remain

## The Economics of Frequency Regulation through Electricity Storage: An Analytical Solution

---

between 0 and the battery capacity  $\bar{y} > 0$ . For consistency, we assume from now on that  $0 \leq y_0 \leq \bar{y}$ . The following proposition establishes fundamental qualitative properties of the state-of-charge function  $y$ .

**Proposition 3.1.** *All else being equal, the battery state-of-charge  $y(x^b, x^r, \delta, y_0, t)$  is concave and strictly increasing in  $x^b$ , concave in  $x^r$ , concave nondecreasing in  $\delta$ , and affine nondecreasing in  $y_0$ .*

Proposition 3.1 strengthens Proposition 1 by Lauinger et al. (2022), which characterizes the state-of-charge of an electric vehicle battery providing frequency regulation. The difference is that Proposition 3.1 reveals that the state-of-charge is *strictly* increasing and not just nondecreasing in  $x^b$ . The strict monotonicity will be important for the dimensionality reduction in Section 3.3.

The battery may be used beyond the immediate planning horizon  $\mathcal{T}$  for selling more regulation power, for exchanging power on other electricity markets, or for supplying power to electric devices. The extent to which this is possible depends on the state-of-charge at the end of the immediate planning horizon. The value of any particular terminal state-of-charge  $y(x^b, x^r, \delta, y_0, T)$  could be captured by a reward-to-go function as in dynamic programming. This would allow the battery operator to trade off present and future costs when selecting  $x^b$  and  $x^r$ . Another approach is to constrain the terminal state-of-charge to be close to some target  $y^\star$  that will guarantee satisfactory future performance. Both terminal costs and terminal constraints are widely studied in model predictive control (Mayne et al., 2000).

The terminal state-of-charge is uncertain at time 0 when the battery operator selects  $x^b$  and  $x^r$  because it depends on the frequency deviation trajectory  $\delta$  during the planning horizon  $\mathcal{T}$ . In fact, the battery operator can only be sure to meet a fixed target  $y^\star$  if she sells no regulation power ( $x^r = 0$ ), which shields her from the uncertainty of the frequency deviations. If the battery operator sells regulation power ( $x^r > 0$ ), however, then all she can hope for is to reach a terminal state-of-charge that is close to the target  $y^\star$  on average. In the following, we will thus require that the terminal state-of-charge be equal to  $y^\star$  in expectation. We emphasize that this constraint is *not* dictated by physics but is simply a means to contain future operating costs, which are not modeled explicitly.

Throughout the planning horizon, the battery operator must be able to honor all market commitments for all reasonably likely frequency deviation trajectories  $\delta$ . Anvari et al. (2020) show that extreme frequency deviation trajectories are very uncommon. It would thus appear overly conservative to impose the charging, discharging, and battery state-of-charge constraints robustly for all possible frequency deviation trajectories. Inspired by applicable European regulations, we assume instead that the battery operator must satisfy the constraints only for the frequency deviation trajectories in the uncertainty set

$$\mathcal{D} = \left\{ \delta \in \mathcal{L}(\mathcal{T}, [-1, 1]) : \int_{\mathcal{T}} |\delta(t)| dt \leq \gamma \right\}$$

parametrized by the uncertainty budget  $\gamma \in (0, T]$ . Note that  $\gamma$  represents the maximum amount of time for which a scenario  $\delta \in \mathcal{D}$  may adopt an extreme value  $\delta(t) \in \{-1, 1\}$ . Note also that  $\mathcal{D}$  can be seen as an extension of the budget uncertainty sets introduced by Bertsimas and Sim (2004) to functional uncertainties. The symmetry properties of  $\mathcal{D}$  will allow us to reduce the decision problem of the battery operator to an equivalent deterministic optimization problem, which is convex for typical problem parameters. The following property of  $\mathcal{D}$  will be crucial for the subsequent results.

**Lemma 3.1.** We have  $\delta \in \mathcal{D}$  if and only if  $|\delta| \in \mathcal{D}^+$ .

In summary, the battery operator's decision problem is to select  $x^b$  and  $x^r$  so as to minimize expected costs while meeting the battery state-of-charge target  $y^\star$  in expectation and ensuring that the charger, discharger, and battery capacities are respected at all times and under all frequency deviation trajectories  $\delta \in \mathcal{D}$ . This gives rise to the following robust optimization problem with functional uncertain parameters.

$$\begin{aligned}
 \min_{x^b \in \mathbb{R}, x^r \in \mathbb{R}_+} \quad & \mathbb{E} \int_{\mathcal{T}} \bar{p}^b(t) x^b - \left( \bar{p}^a(t) - \tilde{\delta}(t) \bar{p}^d(t) \right) x^r dt \\
 \text{s.t.} \quad & y^+(x^b, x^r, \delta(t)) \leq \bar{y}^+ \quad \forall \delta \in \mathcal{D}, \forall t \in \mathcal{T} \\
 & y^-(x^b, x^r, \delta(t)) \leq \bar{y}^- \quad \forall \delta \in \mathcal{D}, \forall t \in \mathcal{T} \\
 & y(x^b, x^r, \delta, y_0, t) \leq \bar{y} \quad \forall \delta \in \mathcal{D}, \forall t \in \mathcal{T} \\
 & y(x^b, x^r, \delta, y_0, t) \geq 0 \quad \forall \delta \in \mathcal{D}, \forall t \in \mathcal{T} \\
 & \mathbb{E} \left[ y(x^b, x^r, \tilde{\delta}, y_0, T) \right] = y^\star
 \end{aligned} \tag{R}$$

The battery operator only needs to insure frequency deviation trajectories in  $\mathcal{D}$ . For trajectories outside of  $\mathcal{D}$ , the battery operator has to deliver regulation power up to the smallest time instant  $t_\gamma$  such that  $\int_0^{t_\gamma} |\delta(t)| dt = \gamma$ . At all time instants  $t > t_\gamma$ , the battery operator does not need to deliver any regulation power and may consider that  $\delta(t) = 0$ . When evaluating the expectations in the objective function and the terminal state-of-charge constraint, we thus consider that  $\mathbb{P}[\delta \in \mathcal{D}] = 1$ . For later use, we note that any  $\delta \in \mathcal{D}$  has a mean absolute deviation  $\frac{1}{T} \int_{\mathcal{T}} |\delta(t)| dt$  no greater than  $\frac{\gamma}{T}$ .

For a fixed frequency deviation trajectory  $\delta$ , the textbook approach to solving the deterministic counterpart of problem (R) is to first discretize the planning horizon into  $N$  periods and then introduce  $N$  binary variables expressing whether the battery is charging or discharging during the respective periods (Taylor, 2015, p. 85). This results in a large-scale mixed-integer linear program. In the remainder, we will show that the robust optimization problem (R) is much easier to solve than its deterministic counterpart. In fact, we will see that the search space can be reduced to merely three candidate solutions for realistic values of the roundtrip efficiency  $\eta^+ \eta^-$ . All candidate solutions can be computed highly efficiently by bisection. For specific distributions of the frequency deviations, problem (R) can even be solved in closed form. This implies that robustification reduces complexity. In the next section, we first show

that the robust optimization problem (R) is equivalent to a one-dimensional deterministic optimization problem.

### 3.3 Reduction to a Deterministic Optimization Problem

In order to simplify problem (R), we first rewrite its objective function more compactly as an explicit linear function of the decision variables. Next, we show that the robust constraints are equivalent to deterministic linear constraints. Finally, we exploit the terminal state-of-charge constraint to express  $x^b$  as an implicit function of  $x^r$ , which allows us to reformulate problem (R) only in terms of  $x^r$ .

Note first that the objective function of problem (R) can be expressed as  $T(c^b x^b - c^r x^r)$ , where  $c^b = \mathbb{E} \frac{1}{T} \int_{\mathcal{T}} \tilde{p}^b(t) dt$  denotes the expected average market price of electricity, and  $c^r = \mathbb{E} \frac{1}{T} \int_{\mathcal{T}} \tilde{p}^a(t) - \tilde{\delta}(t) \tilde{p}^d(t) dt$  denotes the expected average price of regulation power. In the following, we will assume without much loss of generality that  $c^b > 0$  and  $c^r > 0$ .

We now show that the robust constraints are equivalent to deterministic linear constraints. This may be surprising because the state-of-charge is concave in the decision variables, implying that the upper bounds on the state-of-charge represent nonconvex constraints. Similarly, as the state-of-charge is concave in  $\delta$ , finding the worst-case frequency deviation trajectories for the lower bounds on the state-of-charge amounts to solving a nonconvex optimization problem. In addition to these complications, the bounds on the state-of-charge also need to hold for all time instants in the planning horizon. In general, constraints with such properties are severely intractable. Given that  $x^b$  and  $x^r$  must be held constant over the planning horizon, it may be tempting to think that  $\delta$  can be restricted to a constant function of time without loss of generality. This restriction of the uncertainty set, however, relaxes the feasible set, and one can show that the relaxed feasible set contains decisions that are infeasible in practice. Indeed, averaging the real frequency deviation signals *underestimates* the maximum state-of-charge and *overestimates* the minimum state-of-charge (Lauinger et al., 2022, Example 1).

Although the robust constraints of problem (R) seem intractable, we can reformulate them as deterministic linear constraints. This is possible because the worst-case frequency deviation trajectories and the worst-case time instants can be evaluated *a priori*. The following proposition summarizes our results.

**Proposition 3.2** (Constraint reduction). *If  $0 \leq y_0 \leq \bar{y}$ , then the following equivalences hold.*

$$\begin{aligned}
 (i) \quad & y^+(x^b, x^r, \delta(t)) \leq \bar{y}^+ \quad \forall \delta \in \mathcal{D}, \forall t \in \mathcal{T} \iff x^r + x^b \leq \bar{y}^+ \\
 (ii) \quad & y^-(x^b, x^r, \delta(t)) \leq \bar{y}^- \quad \forall \delta \in \mathcal{D}, \forall t \in \mathcal{T} \iff x^r - x^b \leq \bar{y}^- \\
 (iii) \quad & y(x^b, x^r, \delta, y_0, t) \leq \bar{y} \quad \forall \delta \in \mathcal{D}, \forall t \in \mathcal{T} \iff x^r + \max \left\{ \frac{T}{\gamma} x^b, x^b \right\} \leq \frac{\bar{y} - y_0}{\eta^+ \gamma} \\
 (iv) \quad & y(x^b, x^r, \delta, y_0, t) \geq 0 \quad \forall \delta \in \mathcal{D}, \forall t \in \mathcal{T} \iff x^r - \min \left\{ \frac{T}{\gamma} x^b, x^b \right\} \leq \frac{\eta^- y_0}{\gamma}
 \end{aligned}$$

Proposition 3.2 is inspired by Theorems 1 and 2 by Lauinger et al. (2022). The proof critically exploits the monotonicity properties of  $y$  established in Proposition 3.1 and the symmetry of the uncertainty set  $\mathcal{D}$  established in Lemma 3.1. The proof reveals that the upper bound on the charging power and the upper bound on the state-of-charge are valid for all frequency deviations signals  $\delta \in \mathcal{D}$  and all time instants  $t \in \mathcal{T}$  if and only if they are valid for the time instants  $\gamma$  and  $T$  and for the particular frequency deviation signal  $\delta^{(+)}$ , defined as  $\delta^{(+)}(t) = 1$  if  $t \leq \gamma$  and  $\delta^{(+)}(t) = 0$  otherwise. Similarly, the upper bound on the discharging power and the lower bound on the state-of-charge are valid for all frequency deviations signals  $\delta \in \mathcal{D}$  and all time instants  $t \in \mathcal{T}$  if and only if they are valid for the time instants  $\gamma$  and  $T$  and for the particular frequency deviation signal  $\delta^{(-)} = -\delta^{(+)}$ .

Intuitively, if  $x^b \geq 0$ , then the maximum state-of-charge is achieved at time  $T$  by any non-negative frequency deviation trajectory that exhausts the uncertainty budget, *i.e.*, that has a cumulative deviation of  $\gamma$ , such as  $\delta^{(+)}$ . If  $x^b < 0$ , then the maximum state-of-charge is achieved at time  $\gamma$  by the frequency deviation trajectory that exhausts the uncertainty budget as quickly as possible, *i.e.*, that achieves a cumulative deviation of  $\gamma$  as soon as possible. Since  $\delta \in \mathcal{L}(\mathcal{T}, [-1, 1])$ , the nonnegative signal that exhausts the uncertainty budget as quickly as possible is  $\delta^{(+)}$ . As  $\delta^{(+)}(\gamma) = 1$  and  $\delta(t) \leq 1$  for all  $\delta \in \mathcal{D}$  and all  $t \in \mathcal{T}$ , the maximum charging power is achieved at time  $\gamma$  by the frequency deviation trajectory  $\delta^{(+)}$ . The intuition for the lower bound on the state-of-charge and the upper bound on the discharging power is similar.

In the following, we will exploit the constraint on the expected terminal state-of-charge to express  $x^b$  as an implicit function of  $x^r$ . To this end, we first compress the stochastic process  $\{\tilde{\delta}(t)\}_{t \in \mathcal{T}}$  to a single random variable  $\tilde{\xi} = \tilde{\delta}(\tilde{t})$ , where  $\tilde{t}$  is a random time independent of all frequency deviation scenarios that follows the uniform distribution on the planning horizon  $\mathcal{T}$ . The marginal probability distribution  $\mathbb{P}_{\tilde{\xi}}$  of  $\tilde{\xi}$  is defined through  $\mathbb{P}_{\tilde{\xi}}[\mathcal{B}] = \mathbb{P}[\tilde{\xi} \in \mathcal{B}]$  for every Borel set  $\mathcal{B} \subseteq \mathbb{R}$ . One readily verifies that

$$\mathbb{P}_{\tilde{\xi}}[\mathcal{B}] = \mathbb{P}[\tilde{\xi} \in \mathcal{B}] = \mathbb{E}[\mathbb{P}[\tilde{\delta}(\tilde{t}) \in \mathcal{B} \mid \tilde{t}]] = \frac{1}{T} \int_{\mathcal{T}} \mathbb{P}[\tilde{\delta}(\tilde{t}) \in \mathcal{B} \mid \tilde{t} = t] dt = \frac{1}{T} \int_{\mathcal{T}} \mathbb{P}[\tilde{\delta}(t) \in \mathcal{B}] dt$$

for every Borel set  $\mathcal{B} \subseteq \mathcal{T}$ , where the third and the fourth equalities hold because  $\tilde{t}$  is uniformly distributed on  $\mathcal{T}$ , and because  $\tilde{t}$  is independent of  $\tilde{\delta}(t)$  for every  $t \in \mathcal{T}$ , respectively. Historical frequency deviation data suggest that the marginal distribution of  $\tilde{\xi}$  is symmetric around zero (see Figure 3.A.1 in Section 3.A). From now on, we will thus make the following assumption.

**Assumption 3.1** (Symmetry). We have  $\mathbb{P}_{\tilde{\xi}}[\mathcal{B}] = \mathbb{P}_{\tilde{\xi}}[-\mathcal{B}]$  for every Borel set  $\mathcal{B} \subseteq \mathcal{T}$ .

If the stochastic process  $\{\tilde{\delta}(t)\}_{t \in \mathcal{T}}$  is stationary, then the marginal distribution of  $\tilde{\delta}(t)$  coincides with  $\mathbb{P}_{\tilde{\xi}}$  for every  $t \in \mathcal{T}$ . Based on data from the UK and the Central European electricity grid, Anvari et al. (2020) show, however, that frequency deviations may not be stationary on timescales of up to 24 hours but become stationary on longer timescales. The 24 hour threshold coincides with the typical length of planning horizons for frequency regulation. This suggests that  $\mathbb{P}_{\tilde{\xi}}$  does not change from one planning horizon to the next and can thus be estimated from historical data.



## The Economics of Frequency Regulation through Electricity Storage: An Analytical Solution

---

In the following, we define  $F : \mathbb{R} \rightarrow [0, 1]$  as the cumulative distribution function corresponding to  $\mathbb{P}_\xi$ , and we define  $\varphi : \mathbb{R} \rightarrow \mathbb{R}_+$  as the antiderivative of  $F$  with  $\varphi(-1) = 0$ . For short, we will refer to  $\varphi$  as the super-cumulative distribution function. We are now ready to investigate the expected terminal state-of-charge as a function of  $x^b$  and  $x^r$ . To this end, we define  $\eta_d = \frac{1}{\eta^-} - \eta^+$ .

**Proposition 3.3** (Properties of the expected terminal state-of-charge). *The expected terminal state-of-charge is continuous, differentiable almost everywhere and jointly concave in  $x^b$  and  $x^r$ , strictly increasing and unbounded above in  $x^b$ , and nonincreasing in  $x^r$ . It is given by*

$$\mathbb{E} \left[ y(x^b, x^r, \tilde{\delta}, y_0, T) \right] = y_0 + T \left( \eta^+ x^b - \eta_d x^r \varphi \left( -\frac{x^b}{x^r} \right) \right) \quad \forall (x^b, x^r) \in \mathbb{R} \times \mathbb{R}_+. \quad (3.2)$$

Note that  $x^r \varphi(-\frac{x^b}{x^r})$  represents the perspective function of  $\varphi(-x^b)$ , which is jointly convex in  $x^b$  and  $x^r$  because  $\varphi$  is convex (Boyd and Vandenberghe, 2004, p. 89). For  $x^r = 0$ , the perspective function is defined as  $\lim_{x^r \rightarrow 0^+} x^r \varphi(-\frac{x^b}{x^r})$  and coincides thus with  $[x^b]^-$ .

We know from Proposition 3.1 that the battery state-of-charge is strictly increasing in  $x^b$ , and thus it is unsurprising that its expected value is also strictly increasing in  $x^b$ . We emphasize, however, that the state-of-charge may display a complicated nonmonotonic dependence on  $x^r$ . Nevertheless, Proposition 3.3 reveals that the *expected* state-of-charge is nonincreasing in  $x^r$ , which means that, on average, providing frequency regulation causes energy losses and thereby discharges the battery. Even though the average frequency deviations vanish by virtue of Assumption 3.1, frequency regulation fails to be energy-neutral unless  $\eta^+ = 1$  and  $\eta^- = 1$ . We will explain this phenomenon by reasoning about the power flow entering the battery as opposed to the power flow exiting the electricity grid. If there are no losses, then the power flow entering the battery and the power flow exiting the electricity grid coincide with  $x^b + \delta(t)x^r$ . They thus follow the same probability distribution as the frequency deviations with the mean value shifted from 0 to  $x^b$  and the standard deviation scaled by  $x^r$ . Providing frequency regulation hence only increases the dispersion of the power flow entering the battery but does not affect its mean. In the general case, when  $\eta^+, \eta^- < 1$ , the power flow exiting the electricity grid follows the same probability distribution as before, but the power flow entering the battery follows a different probability distribution. In fact, charging losses *compress* the positive part of the original distribution, while discharging losses *stretch* the negative part of the original distribution. The losses thereby *decrease* the average power flow entering the battery. The higher the dispersion of the power flow, the more pronounced the decrease. Since the dispersion increases in  $x^r$ , the average power flow entering the battery and, by extension, the expected terminal state-of-charge of the battery decrease in  $x^r$ . Figure 1 visualizes the distribution of the power flow entering the battery for  $x^b = 0$  with and without losses.

The monotonicity properties of the expected terminal state-of-charge established in Proposition 3.3 imply that the last constraint of problem (R) determines  $x^b$  as an implicit function of  $x^r$ . Instead of reasoning about the state-of-charge of the battery directly, we will reason about the

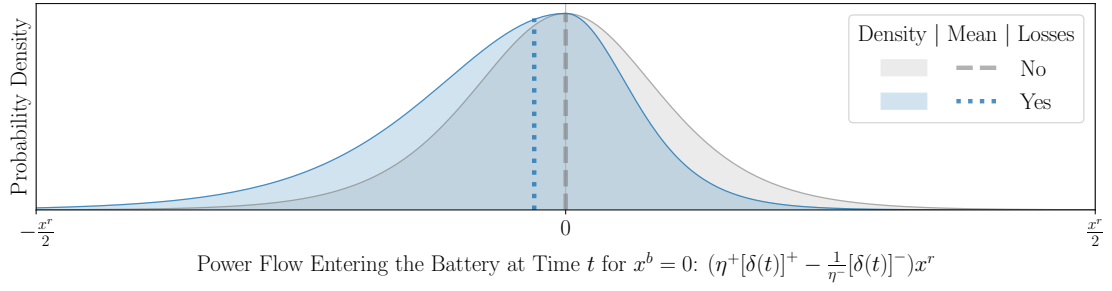


Figure 1: Distribution of the power flow entering the battery.

power flow entering the battery, which is independent of the initial state-of-charge  $y_0$  and of the length of the planning horizon  $T$ . By defining the average expected charging rate and the desired charging rate as

$$\dot{y}(x^b, x^r) = \frac{\mathbb{E}[y(x^b, x^r, \tilde{\delta}, y_0, T)] - y_0}{T} = \eta^+ x^b - \eta_d x^r \varphi\left(-\frac{x^b}{x^r}\right) \quad \text{and} \quad \dot{y}^* = \frac{y^* - y_0}{T},$$

respectively, the constraint  $\mathbb{E}[y(x^b, x^r, \tilde{\delta}, y_0, T)] = y^*$  can be reformulated equivalently as  $\dot{y}(x^b, x^r) = \dot{y}^*$ . Since  $T > 0$ , the expected charging rate  $\dot{y}$  inherits the concavity and monotonicity properties of the state-of-charge established in Proposition 3.3. In particular, if  $x^r = 0$ , then  $\dot{y}(x^b, 0) = \eta^+ [x^b]^+ - \frac{1}{\eta^-} [x^b]^-$ . Hence,  $\dot{y}(x^b, 0) = \dot{y}^*$  is valid if and only if  $x^b = \frac{1}{\eta^+} [\dot{y}^*]^+ - \eta^- [\dot{y}^*]^-$ , which is fully determined by the desired charging rate  $\dot{y}^*$  and by the charging and discharging efficiencies  $\eta^+$  and  $\eta^-$ . As  $x^r$  increases, the expected charging rate  $\dot{y}(x^b, x^r)$  may decrease due to increased charging and discharging losses. The battery operator, however, can compensate this decrease by increasing  $x^b$ . Since  $\dot{y}$  is strictly increasing, continuous, and surjective onto  $\mathbb{R}$  for any fixed  $x^r$ , there is a unique  $x^b$  that satisfies the equation  $\dot{y}(x^b, x^r) = \dot{y}^*$ . This means that  $x^b$  can be expressed as an implicit function of  $x^r$ . This implicit function depends on the expected charging rate  $\dot{y}^*$ , the charging and discharging efficiencies, and the mean absolute deviation of the frequency deviations. The latter is defined as  $\Delta = \mathbb{E}[|\tilde{\xi}|] = 2\varphi(0)$ , where the second equality can be proved via integration by parts.

**Remark 3.1** (Mean absolute deviation). We have  $\Delta \leq \frac{\gamma}{T}$  because all relevant frequency deviation trajectories reside in  $\mathcal{D}$  and have thus a mean absolute deviation no greater than  $\frac{\gamma}{T}$ . Formally,

$$\mathbb{P}[\delta \in \mathcal{D}] = 1 \quad \implies \quad \Delta \leq \frac{\gamma}{T}. \quad \square$$

**Proposition 3.4** (Implicit function). *The constraint  $\dot{y}(x^b, x^r) = \dot{y}^*$  defines a unique implicit function  $g: \mathbb{R}_+ \rightarrow \mathbb{R}$  such that  $\dot{y}(g(x^r), x^r) = \dot{y}^*$  for all  $x^r \in \mathbb{R}_+$ . The function  $g$  is convex, continuous, nondecreasing and almost everywhere differentiable with derivative*

$$g'(x^r) = \eta_d \frac{\varphi(-\frac{x^b}{x^r}) + \frac{x^b}{x^r} F(-\frac{x^b}{x^r})}{\eta^+ + \eta_d F(-\frac{x^b}{x^r})} \quad (3.3)$$

## The Economics of Frequency Regulation through Electricity Storage: An Analytical Solution

(if it exists), where  $x^b = g(x^r)$ . We have  $g'(x^r) = 0$  for all  $x^r \in (0, |g(0)|)$ , and  $m = \lim_{x^r \rightarrow \infty} g'(x^r) \in [0, 1]$ . In addition, the asymptotic slope  $m$  is the unique solution of the equation

$$m = (1 - \eta^+ \eta^-) \varphi(m). \quad (3.4)$$

Proposition 3.4 implies that for any fixed  $x^r$ , the battery operator must buy the amount  $x^b = g(x^r)$  of power in order to meet the expected state-of-charge target. One can interpret  $g(0)$  as the amount of power needed to meet the target in the absence of frequency regulation. Accordingly,  $g(x^r) - g(0)$  reflects the amount of power needed to compensate the charging and discharging losses due to frequency regulation. These losses vanish for  $x^r = 0$  and increase in  $x^r$  at a rate that is smaller than or equal to  $m$  if  $y_0 \neq y^*$ . Otherwise, they increase at rate  $m$ . Maybe surprisingly, the losses due to frequency regulation are thus smaller when the initial state-of-charge differs from the target.

The asymptotic slope is of particular interest because it is an upper bound on the percentage of regulation power that the battery operator needs to purchase in order to cover the losses from providing frequency regulation.

**Lemma 3.2** (Asymptotic slope). The asymptotic slope  $m$  is convex and nonincreasing in the roundtrip efficiency  $\eta^+ \eta^-$  and nondecreasing in the mean absolute deviation  $\Delta$  of the frequency deviations.

Proposition 3.4 further reveals that  $g'(0) = 0$  whenever  $\dot{y}^* \neq 0$ , which is the case whenever  $g(0) \neq 0$  since  $g(0) = \frac{1}{\eta^+} [\dot{y}^+] - \eta^- [\dot{y}^*]^-$ . Otherwise, we have  $g'(0) = m$ .

**Lemma 3.3** (Linearity). If  $\dot{y}^* = 0$ , then the function  $g$  is linear with slope  $m$ .

**Remark 3.2** (Computability). The asymptotic slope  $m$  can be found by bisection on the interval  $[0, 1]$ . For  $x^r = 0$ , we have  $g(0) = \frac{1}{\eta^+} [\dot{y}^+] - \eta^- [\dot{y}^*]^-$ . For  $x^r > 0$ ,  $g(x^r)$  can be computed by finding the root of the function  $\dot{y}(g(x^r), x^r) - \dot{y}^*$  by bisection on the interval  $[g(0), g(0) + mx^r]$ . Once  $x^b = g(x^r)$  is known,  $g'(x^r)$  can be obtained from equation (3.3).  $\square$

Using Propositions 3.2 and 3.4, we can now reformulate problem (R) as the one-dimensional deterministic optimization problem

$$\begin{aligned} \min_{x^r \in \mathbb{R}_+} \quad & T \left( c^b g(x^r) - c^r x^r \right) \\ \text{s.t.} \quad & x^r + g(x^r) \leq \bar{y}^+ \\ & x^r - g(x^r) \leq \bar{y}^- \\ & x^r + \max \left\{ \frac{T}{\gamma} g(x^r), g(x^r) \right\} \leq \frac{\bar{y} - y_0}{\eta^+ \gamma} \\ & x^r - \min \left\{ \frac{T}{\gamma} g(x^r), g(x^r) \right\} \leq \frac{\eta^- y_0}{\gamma}. \end{aligned} \quad (\text{P})$$

**Theorem 3.1** (Constraint and dimensionality reduction). The problems (R) and (P) are equivalent.

Note that the objective function of problem (P) is convex as the implicit function  $g$  is convex. The feasible set of (P) can be represented concisely as  $\mathcal{X} = \{x^r \in \mathbb{R}_+ : \ell(x^r) \leq g(x^r) \leq u(x^r)\}$ , where

$$\ell(x^r) = \max \left\{ x^r - \min \left\{ \bar{y}^-, \frac{\eta^- y_0}{\gamma} \right\}, \frac{\gamma}{T} x^r - \frac{\eta^- y_0}{T} \right\}$$

and

$$u(x^r) = \min \left\{ \min \left\{ \bar{y}^+, \frac{\bar{y} - y_0}{\eta^+ \gamma} \right\} - x^r, \frac{\bar{y} - y_0}{\eta^+ T} - \frac{\gamma}{T} x^r \right\}.$$

Due to the lower bounds on the convex function  $g(x^r)$ , the set  $\mathcal{X}$  is generally nonconvex. If  $g(x^r) - \ell(x^r)$  is monotonic, then the constraint  $\ell(x^r) \leq g(x^r)$  defines nevertheless a convex feasible set. This is the case under the following assumption.

**Assumption 3.2** (Roundtrip efficiency). We have  $\eta^+ \eta^- > \frac{1}{3}$ .

Assumption 3.2 is non-restrictive. Indeed, all relevant electricity storage technologies, as identified by the World Energy Council (2020), have a roundtrip efficiency higher than  $\frac{1}{3}$ .

**Lemma 3.4** (Convex feasible set). If Assumption 3.2 holds, then the set  $\mathcal{X}$  is convex.

Lemma 3.4 asserts that under realistic parameter settings the feasible set  $\mathcal{X}$  is a line segment. As the objective function of problem (P) is convex, an optimal solution  $x_*^r$  coincides either with a boundary point of the line segment  $\mathcal{X}$  or with a stationary point of the objective function in the interior of this line segment. All three candidate solutions can be computed conveniently via bisection. We point out that if Assumption 3.2 fails to hold, then  $\mathcal{X}$  consists of two disjoint line segments, and it becomes necessary to check five different candidate solutions. We emphasize that all of these candidate solutions can again be computed by bisection. A detailed discussion of this generalized setting is omitted, however, because it has little practical relevance.

### 3.4 Candidate Solutions

In the following, we examine first the boundary points of the line segment  $\mathcal{X}$  and then the stationary points of the objective function of problem (P).

One can show that  $u(x^r) - g(x^r)$  is strictly decreasing and that  $g(x^r) - \ell(x^r)$  is strictly decreasing under Assumption 3.2. This means that there is a unique  $x_u^r$  such that  $u(x_u^r) = g(x_u^r)$  and a unique  $x_\ell^r$  such that  $g(x_\ell^r) = \ell(x_\ell^r)$ . The feasible set  $\mathcal{X}$  can thus be expressed as the line segment  $\{x^r \in \mathbb{R}_+ : x^r \leq x_\ell^r, x^r \leq x_u^r\} = [0, \bar{x}^r]$ , where  $\bar{x}^r = \min\{x_\ell^r, x_u^r\}$ .

**Remark 3.3.** Since  $\ell$  is strictly increasing and  $u$  is strictly decreasing, there exists a unique  $\bar{x}^r$  such that  $\ell(\bar{x}^r) = u(\bar{x}^r)$ . As neither  $x_\ell^r$  nor  $x_u^r$  are greater than  $\bar{x}^r$ , they can be computed by

## The Economics of Frequency Regulation through Electricity Storage: An Analytical Solution

bisection on  $[0, \bar{x}^r]$ . The point  $\bar{x}^r$  itself can be expressed in closed form as

$$\bar{x}^r = \min \left\{ \frac{\bar{y}^+ + \bar{y}^-}{2}, \frac{\bar{y}^+ + \frac{\eta^-}{\gamma} y_0}{2}, \frac{T\bar{y}^+ + \eta^- y_0}{\gamma + T}, \frac{\bar{y}^- + \frac{\bar{y}^- y_0}{\eta^+ \gamma}}{2}, \frac{T\bar{y}^- + \frac{\bar{y}^- y_0}{\eta^+}}{\gamma + T}, \right. \\ \left. \frac{\bar{y} + (\eta^+ \eta^- \frac{T}{\gamma} - 1) y_0}{\eta^+ (\gamma + T)}, \frac{\frac{T}{\gamma} \bar{y} - (\frac{T}{\gamma} - \eta^+ \eta^-) y_0}{\eta^+ (\gamma + T)} \right\}. \quad \square$$

The stationary points of the objective function of problem (P) are such that the expected marginal cost,  $Tc^b g'(x^r)$ , of providing frequency regulation equals the expected marginal revenue,  $Tc^r$ , from providing frequency regulation. The set of all stationary points in  $\mathcal{X}$  is thus  $\mathcal{X}_\star = \{x^r \in [0, \bar{x}^r] : \frac{c^r}{c^b} \in \partial g(x^r)\}$ . Note that  $\frac{c^r}{c^b} > 0$  because  $c^b > 0$  and  $c^r > 0$ . If  $\bar{x}^r = 0$ , then 0 is the unique feasible solution to problem (P). If  $\min \partial g(\bar{x}^r) < \frac{c^r}{c^b}$ , then  $\mathcal{X}_\star$  is empty, and  $\bar{x}^r$  is the optimal solution to problem (P) because the marginal revenue of providing frequency regulation is strictly higher than the marginal cost for all feasible  $x^r$ . Similarly, if  $g'(0) > \frac{c^r}{c^b}$ , then  $\mathcal{X}_\star$  is again empty, and 0 is the optimal solution because the marginal cost of providing frequency regulation is strictly higher than the marginal revenue for all  $x^r \in (0, \infty]$ . Otherwise,  $\mathcal{X}_\star$  may be non-empty and contain several stationary points, all of which would be optimal solutions to problem (P). In this case, it makes sense to assume that the battery operator selects the smallest stationary point to avoid unnecessary battery usage. Theorem 3.2 formalizes these results.

**Theorem 3.2.** *The smallest optimal solution to problem (P) is*

$$x_\star^r = \begin{cases} 0 & \text{if } \bar{x}^r = 0 \text{ or } \bar{x}^r > 0 \text{ and } g'(0) \geq \frac{c^r}{c^b}, \\ \bar{x}^r & \text{if } \bar{x}^r > 0 \text{ and } \min \partial g(\bar{x}^r) < \frac{c^r}{c^b}, \\ \min \mathcal{X}_\star & \text{otherwise.} \end{cases}$$

**Remark 3.4.** If  $\dot{y}^\star = 0$ , then  $g(x^r) = mx^r$ . Therefore,  $x_\star^r = \bar{x}^r$  if  $m < \frac{c^r}{c^b}$  and  $x_\star^r = 0$  otherwise.  $\square$

**Remark 3.5.** If  $\mathcal{X}_\star$  is non-empty,  $\min \mathcal{X}_\star$  can be found by bisection on  $\mathcal{X}$  as  $g'$  is nondecreasing.  $\square$

To compute the optimal solution, we first need to compute  $\bar{x}^r$ . If  $\bar{x}^r > 0$ , we then need to evaluate  $g'(0)$  and  $\min \partial g(\bar{x}^r)$ . By Proposition 3.4 and Lemma 3.3, we find  $g'(0) = 0$  if  $\dot{y}^\star \neq 0$ ;  $= m$  otherwise. Finally, if  $\mathcal{X}_\star$  is non-empty, we need to compute its minimum. By Remarks 3.2, 3.3, and 3.5,  $\bar{x}^r$ ,  $\min \partial g(\bar{x}^r)$ , and  $\min \mathcal{X}_\star$  can all be computed by bisection. The optimal solution  $x_\star^r$  can thus also be computed highly efficiently by bisection.

The expected marginal cost of providing frequency regulation depends on the desired charging rate  $\dot{y}^\star$ , which is only known to the battery operator but unknown to the grid operator. Nevertheless, the grid operator knows that the expected marginal cost amounts to at most  $c^b m$  and can therefore infer that it is profitable for the battery operator to offer all available regulation power if  $\frac{c^r}{c^b} > m$ . Thanks to Lemma 3.2, we know that  $m$  is convex and nonincreasing in

the roundtrip efficiency  $\eta^+ \eta^-$  and nondecreasing in the mean absolute deviation  $\Delta$  of the frequency deviations, but we do not know the explicit dependence of  $m$  on  $\eta^+ \eta^-$  and  $\Delta$ . In the next section, we will derive explicit lower and upper bounds on  $m$  that are tight for certain degenerate frequency deviation distributions. For these particular distributions, we will then explain how to derive analytical solutions to problem (P).

### 3.5 Analytical Solution

We now construct two discrete distributions  $\mathbb{P}_\xi$  and  $\bar{\mathbb{P}}_\xi$  with the same mean absolute deviation as  $\mathbb{P}_\xi$ , which is given by  $\Delta = 2\varphi(0)$ . Recall that  $\Delta \leq 1$  because  $\xi$  is supported on  $[-1, 1]$ . Specifically, we define  $\mathbb{P}_\xi$  as a two-point distribution with mass  $\frac{1}{2}$  at  $-\Delta$  and  $\Delta$ , and  $\bar{\mathbb{P}}_\xi$  as a three-point distribution with mass  $\frac{\Delta}{2}$  at  $-1$  and  $1$ , and mass  $1 - \Delta$  at  $0$ . The super-cumulative distribution function  $\varphi$  of  $\mathbb{P}_\xi$  with  $\varphi(-1) = 0$  is  $\varphi(\xi) = \max\{0, \frac{1}{2}(\xi + \Delta), \xi\}$ . Similarly, the super-cumulative distribution function of  $\bar{\mathbb{P}}_\xi$  with  $\bar{\varphi}(-1) = 0$  is  $\bar{\varphi}(\xi) = \max\{0, \frac{\Delta}{2}(\xi + 1), (1 - \frac{\Delta}{2})\xi + \frac{\Delta}{2}, \xi\}$ . As  $\xi$  is supported on  $[-1, 1]$  under all three distributions, we have  $\varphi(\xi) = \varphi(\xi) = \bar{\varphi}(\xi)$  for all  $|\xi| \geq 1$ . For any  $|\xi| < 1$ ,  $\varphi(\xi)$  is a lower bound on  $\varphi(\xi)$  as  $\varphi$  is the piecewise maximum of three affine functions that are tangent to the convex function  $\varphi$  at  $\xi = -1$ ,  $\xi = 0$ , and  $\xi = 1$ . Conversely,  $\bar{\varphi}(\xi)$  is an upper bound on  $\varphi(\xi)$  as  $\bar{\varphi}$  is the piecewise maximum of two linear interpolations of  $\varphi$  from  $\xi = -1$  to  $\xi = 0$  and from  $\xi = 0$  to  $\xi = 1$ . This reasoning implies that  $\mathbb{P}_\xi$  second-order stochastically dominates  $\mathbb{P}_\xi$  and that  $\bar{\mathbb{P}}_\xi$  second-order stochastically dominates  $\mathbb{P}_\xi$ . Formally,

$$\varphi(\xi) \leq \varphi(\xi) \leq \bar{\varphi}(\xi) \quad \forall \xi \in \mathbb{R}. \quad (3.5)$$

We now define the asymptotic sensitivities  $\underline{m}$  and  $\bar{m}$  as the solutions to the nonlinear algebraic equations  $\underline{m} = (1 - \eta^+ \eta^-) \varphi(\underline{m})$  and  $\bar{m} = (1 - \eta^+ \eta^-) \bar{\varphi}(\bar{m})$ , respectively, which exist and are unique by Proposition 3.4. These equations admit the closed-form solutions

$$\underline{m} = \frac{1 - \eta^+ \eta^-}{1 + \eta^+ \eta^-} \Delta \quad \text{and} \quad \bar{m} = 1 - \frac{1}{1 + (\frac{1}{\eta^+ \eta^-} - 1) \frac{\Delta}{2}}.$$

**Lemma 3.5.** We have  $\underline{m} \leq m \leq \bar{m}$ .

The discrete distributions  $\mathbb{P}_\xi$  and  $\bar{\mathbb{P}}_\xi$  provide not only explicit bounds on the asymptotic slope  $m$  of the implicit function  $g(x^r)$  but also on  $g(x^r)$  itself. These bounds, which are denoted by  $\underline{g}$  and  $\bar{g}$ , are obtained by solving the differential equation (3.3) for  $\mathbb{P}_\xi$  and  $\bar{\mathbb{P}}_\xi$ , respectively. Concretely, as  $\varphi$  and  $\bar{\varphi}$  are piecewise linear, the differential equation can be solved separately for each linear piece. Combining the results for the different pieces yields

$$\begin{aligned} g(x^r) &= \max \left\{ g(0), \underline{m} x^r + g(0) - \frac{1 - \eta^+ \eta^-}{1 + \eta^+ \eta^-} |g(0)| \right\} \\ \text{and} \quad \bar{g}(x^r) &= \max \left\{ g(0), \frac{(1 - \eta^+ \eta^-) \varphi(0) x^r - [g(0)]^-}{\eta^+ \eta^- + (1 - \eta^+ \eta^-)(1 - \varphi(0))}, \bar{m} x^r + \frac{\eta^+ \eta^- [g(0)]^+ - [g(0)]^-}{\eta^+ \eta^- + (1 - \eta^+ \eta^-) \varphi(0)} \right\}. \end{aligned}$$

## The Economics of Frequency Regulation through Electricity Storage: An Analytical Solution

---

**Lemma 3.6.** We have  $\underline{g}(x^r) \leq g(x^r) \leq \bar{g}(x^r)$  for all  $x^r \in \mathbb{R}_+$ .

In order to calculate the optimal solutions under  $\mathbb{P}_\xi$  and  $\bar{\mathbb{P}}_\xi$ , we need to calculate the boundary points of and the smallest stationary points, if they exist, in the corresponding feasible sets  $\mathcal{X}$  and  $\bar{\mathcal{X}}$ . The left boundary points of the feasible sets are both 0, as under  $\mathbb{P}_\xi$ . The right boundary points are  $\min\{\underline{x}_\ell^r, \bar{x}_u^r\}$  and  $\min\{\bar{x}_\ell^r, \underline{x}_u^r\}$ , respectively, where  $\underline{x}_\ell^r$ ,  $\bar{x}_u^r$ ,  $\bar{x}_\ell^r$ , and  $\underline{x}_u^r$  are the unique points such that  $\underline{g}(\underline{x}_\ell^r) = \ell(\underline{x}_\ell^r)$ ,  $\underline{g}(\bar{x}_u^r) = u(\bar{x}_u^r)$ ,  $\bar{g}(\bar{x}_\ell^r) = \ell(\bar{x}_\ell^r)$ , and  $\bar{g}(\underline{x}_u^r) = u(\underline{x}_u^r)$ . Lemma 3.6 implies that

$$\underline{x}_\ell^r \leq x_\ell^r \leq \bar{x}_\ell^r \quad \text{and} \quad \underline{x}_u^r \leq x_u^r \leq \bar{x}_u^r.$$

The points  $\underline{x}_\ell^r$ ,  $\bar{x}_u^r$ ,  $\bar{x}_\ell^r$ , and  $\underline{x}_u^r$  can be computed in closed form by evaluating the intersections of the affine functions  $\ell$  and  $u$  with the affine functions that compose  $\underline{g}$  and  $\bar{g}$ . The right boundary points  $\min\{\underline{x}_\ell^r, \bar{x}_u^r\}$  and  $\min\{\bar{x}_\ell^r, \underline{x}_u^r\}$  are then given by the minimum of six and eight rational functions of the problem parameters  $y_0$ ,  $\dot{y}^*$ ,  $\bar{y}$ ,  $\bar{y}^+$ ,  $\bar{y}^-$ ,  $\eta^+$ ,  $\eta^-$ ,  $\Delta$ ,  $\gamma$ , and  $T$ , respectively. The boundary points admit thus closed-form expressions, but the expressions are not very insightful. The smallest stationary points, on the other hand, are more intuitive. Since  $\underline{g}$  and  $\bar{g}$  are piecewise linear, the smallest stationary points occur, if they exist, either at kinks of the piecewise linear objective functions  $c^b \underline{g}(x^r) - c^r x^r$  and  $c^b \bar{g}(x^r) - c^r x^r$  or at  $x^r = 0$ . Nevertheless, as the expressions for the boundary points of the feasible set are too complicated to be insightful in the general case, we assume that  $y_0 = y^*$  in the subsequent analysis. In this special case, the losses due to frequency regulation are higher than for any other value of  $y_0$  as explained in the discussion of Proposition 3.4. If it is profitable to provide frequency regulation in this special case, it will thus also be profitable to provide frequency regulation in any other case. As  $\dot{y}^* = \frac{y^* - y_0}{T} = 0$ , Lemma 3.3 implies that  $\underline{g}(x^r) = \underline{m}x^r$ ,  $\bar{g}(x^r) = \bar{m}x^r$ , and  $\bar{g}(x^r) = \bar{m}x^r$ . Under any frequency deviation distribution  $\mathbb{P}_\xi$ , the optimal solution to problem (P) then satisfies  $x_*^r = \bar{x}^r$  if  $m < \frac{c^r}{c^b}$  and  $x_*^r = 0$  otherwise. Since  $\ell$  and  $u$  are piecewise linear functions with two pieces each, the right boundary point  $\bar{x}^r$  of the feasible set can be expressed as the minimum of only four rational functions of the problem parameters, and will admit an intuitive interpretation.

**Proposition 3.5.** If  $y_0 = y^*$ , then

$$\bar{x}^r = \min \left\{ \frac{\bar{y}^-}{1-m}, \frac{\bar{y}^+}{1+m}, \frac{\eta^- y_0}{\gamma(1-m)}, \frac{\bar{y} - y_0}{\eta^+(\gamma + mT)} \right\}. \quad (3.6)$$

The first two terms in formula (3.6) for  $x^r$  depend on the charging capacity  $\bar{y}^+$  and the discharging capacity  $\bar{y}^-$ , while the last two terms depend on the battery capacity  $\bar{y}$  and the initial state-of-charge  $y_0$ . We say that the battery is *power-constrained* if  $\bar{x}^r$  is equal to one of the first two terms. Otherwise, we say that the battery is *energy-constrained*. We now state the analytical solution.

**Theorem 3.3** (Analytical solution). *If  $y_0 = y^*$ , then an optimal solution to problem (P) is*

$$x_*^r = \begin{cases} 0 & \text{if } m \geq \frac{c^r}{c^b}, \\ \bar{x}^r & \text{otherwise,} \end{cases}$$

*under any frequency deviation distribution  $\mathbb{P}_\xi$ . If  $\mathbb{P}_\xi = \underline{\mathbb{P}}_\xi$ , then  $m = \underline{m}$ . If  $\mathbb{P}_\xi = \bar{\mathbb{P}}_\xi$ , then  $m = \bar{m}$ .*

As a direct consequence of Theorem 3.3, if  $\bar{m} < \frac{c^r}{c^b}$ , it is optimal to set  $x^r = \bar{x}^r$  for any frequency deviation distribution with mean absolute deviation  $\Delta$ , regardless of the shape of the distribution, because  $\bar{m} \geq m$ . In the following, we describe the maximum amount  $\bar{x}^r$  of regulation power that can be offered by power- and energy-constrained batteries, for the case  $y_0 = y^*$ .

If the battery is power-constrained, then  $\bar{x}^r$  depends on the charging and discharging efficiencies only through the marginal increase  $m$  in the expected power loss which, in turn, depends on these efficiencies only through their product, that is, the roundtrip efficiency  $\eta^+ \eta^-$ . Due to charging and discharging losses, the battery operator expects to lose energy while delivering frequency regulation and compensates the expected loss by purchasing the power  $m x^r$  from an electricity market, which decreases the effective charging capacity and increases the effective discharging capacity of the battery. Accounting for the effective charging and discharging capacities, the battery operator may dimension the discharging capacity  $\bar{y}^-$  as a fraction  $\frac{1-m}{1+m}$  of the charging capacity  $\bar{y}^+$  without restricting  $\bar{x}^r$ .

If the battery is energy-constrained, then  $\bar{x}^r$  depends not only on the roundtrip efficiency  $\eta^+ \eta^-$ , through  $m$ , but also on the individual charging and discharging efficiencies. Charging losses increase the amount of energy that the battery can consume from the grid and therefore increase the effective storage capacity. Conversely, discharging losses decrease the amount of energy that the battery can deliver to the grid and therefore decrease the effective storage capacity. For given charging and discharging efficiencies, the initial state-of-charge  $y_0$  determines how much energy the battery can consume from and deliver to the grid. As the battery operator must be able to both consume and deliver regulation power,  $\bar{x}^r$  is maximized if the battery can absorb as much energy from the grid as it can deliver to the grid. This occurs at an initial state-of-charge of  $y_0^*$  and results in the maximum amount  $\bar{x}_*^r$  of regulation power that can be offered by energy-constrained batteries, where

$$\bar{x}_*^r = \min \left\{ \frac{\bar{y}^-}{1-m}, \frac{\bar{y}^+}{1+m}, \frac{\eta^-}{\frac{\gamma}{T}(1+\eta^+ \eta^- - m) + \eta^+ \eta^- m} \frac{\bar{y}}{T} \right\} \text{ and } y_0^* = \frac{(1-m)\bar{y}}{1+\eta^+ \eta^- + (\eta^+ \eta^- \frac{T}{\gamma} - 1)m}.$$

Assuming that  $\bar{y}^- = \frac{1-m}{1+m} \bar{y}^+$ , the battery is thus energy constrained if  $\frac{\bar{y}^+}{1+m} > \bar{x}_*^r$ , which occurs if the battery's charge rate  $C = \frac{\bar{y}^+}{y}$  (C-rate) is at least as large as

$$\underline{C} = \frac{1}{T} \cdot \frac{(1+m)\eta^-}{\frac{\gamma}{T}(1+\eta^+ \eta^- - m) + \eta^+ \eta^- m}.$$



## The Economics of Frequency Regulation through Electricity Storage: An Analytical Solution

---

Note that the C-rate expresses the percentage of the battery's storage capacity that can be consumed from the grid within one hour.

The initial state-of-charge  $y_0^*$ , which maximizes the amount of regulation power that energy-constrained batteries can provide, depends on the charging and discharging efficiencies only through the roundtrip efficiency  $\eta^+ \eta^-$ . It increases from  $\frac{\bar{y}}{2}$  to  $\bar{y}$  as the roundtrip efficiency decreases from 1 to 0. The maximum amount  $\bar{x}_\star^r$  of regulation power that can be provided by energy-constrained batteries is equal to  $\frac{\bar{y}}{2\gamma}$  in the absence of charging and discharging losses. The storage capacity  $\bar{y}$  is divided by  $2\gamma$  because the storage operator must be able to both consume and deliver all of the regulation power she promised for a total time of at least  $\gamma$ .

### 3.6 Applications

In the following, we compare the profits that storage operators can earn by providing frequency regulation against the expected investment costs of lithium-ion batteries. After describing the parameters of our case study, we analyze the marginal cost and profit of providing frequency regulation as well as the maximum amount of regulation power that storage operators can provide. Last, we discuss the profits that storage operators can earn over the planning horizon  $\mathcal{T}$  and, for the specific case of lithium-ion batteries, under what conditions on the total activation period  $\gamma$  and the length of the planning horizon  $T$  it can be profitable to invest in electricity storage for frequency regulation.

#### 3.6.1 Model Parametrization

We focus on storage operators who provide frequency regulation to the French grid operator and compute their profits based on historic data on frequency deviations, availability and delivery prices, and on wholesale and retail market prices. Frequency measurements, availability prices, and delivery prices are published by the French grid operator Réseau de Transport d'Électricité (RTE).<sup>I</sup> Wholesale market prices depend on how long before delivery electricity is traded. Since frequency regulation is traded up to one day before delivery, we consider the prices of the day-ahead market, which are equal to the delivery prices published by RTE (Réseau de transport d'électricité, 2017a, p. 68). Retail market prices vary from one electric utility company to another. We use the base tariff of Electricité de France, the largest French electric utility company. The French government regulates this particular tariff and publishes the corresponding prices.<sup>II</sup> We will compare the operating costs of storage technologies with different roundtrip efficiencies, namely hydrogen, redox flow batteries, vehicle-to-grid, pumped hydro, and stationary lithium-ion batteries. In assigning roundtrip efficiencies to storage technologies, we follow Apostolaki-Iosifidou et al. (2017) for vehicle-to-grid and the World Energy Council (World Energy Council, 2020, p. 9) for all other storage technologies. Table 1 lists the roundtrip efficiencies of the storage technologies. In order to judge whether it

---

<sup>I</sup><https://clients.rte-france.com>

<sup>II</sup>Journal Officiel de la République Française: <https://legifrance.gouv.fr>

Table 1: Roundtrip efficiencies of storage technologies.

Storage Technology	Hydrogen	Redox Flow	Vehicle-to-Grid	Pumped Hydro	Li-Ion
Roundtrip Efficiency (%)	35–55	60–85	70–85	75–85	85–95

is profitable to invest in lithium-ion batteries for frequency regulation, we follow Comello and Reichelstein (2019) and assume investment costs in the year 2023 between US\$85 and US\$165 per kWh of storage capacity with a lifetime of 10 years and between US\$710 and US\$860 per kW of charging and discharging capacity with a lifetime of 30 years. We assume an exchange rate of  $1 \text{ €} = \text{US\$}1.15$  and annualize the investment costs with a yearly discount rate of 2%, which equals the long-term inflation target of the European Central Bank (2021).

The technical term for the type of frequency regulation we consider is *frequency containment reserves* (FCR). France participates in a common European market for frequency containment reserves with a daily planning horizon.<sup>III</sup> We thus set  $T = 24$  hours. In its regulation on frequency containment reserves the European Commission specifies that the “*minimum activation period to be ensured by FCR providers* [is not to be] *greater than 30 or smaller than 15 minutes*” and that storage operators “*shall ensure the recovery of [their] energy reservoirs as soon as possible, within 2 hours after the end of the alert state*” (European Commission, 2017, art. 156(10, 13)), where an *activation period* designates a period of consecutive extreme frequency deviations  $\delta(t) \in \{-1, 1\}$ . The total activation period  $\gamma$  to be ensured over a period of 24 hours is thus between 2.75 hours and 5 hours. The uncertainty set  $\mathcal{D}$  contains all frequency deviation signals that correspond to a given total activation period  $\gamma$ . Some of these signals may exhibit activation periods that are longer than the minimum activation period prescribed by the European Commission. The uncertainty set  $\mathcal{D}$  is therefore a conservative approximation of the regulation by the European Commission. The strength of the delivery guarantee required by the European Commission can nevertheless be measured by the *activation ratio*  $\gamma/T$ , that is, the fraction of time during which a storage operator must be able to provide all the regulation power she promised. When studying the profits a storage operator can reap from frequency regulation over the lifetime of an electricity storage device, we will vary the length of the planning horizon  $T$  while keeping the activation ratio constant. In line with the regulation by the European Commission, we will consider activation ratios of 0.1 and 0.2.

The desired charging rate  $y^*$  for meeting the terminal state-of-charge target influences the quantity and the price of regulation power that a storage operator can offer. Ideally, the storage operator would be able to meet the terminal state-of-charge target  $y^*$  not just in expectation but exactly. In the following, we assume that this is the case and that the terminal state-of-charge target stays constant from one planning horizon to another. The desired charging rate vanishes therefore during any given planning horizon. In this case, the implicit function  $g$  is the linear function  $g(x^r) = mx^r$  by Proposition 3.4. The marginal cost of providing frequency regulation is thus  $Tmc^b$ . If the desired charging rate was nonzero, then the marginal cost would

<sup>III</sup>[https://entsoe.eu/network\\_codes/eb/fcr](https://entsoe.eu/network_codes/eb/fcr)

## The Economics of Frequency Regulation through Electricity Storage: An Analytical Solution

---

be lower as the slope of  $g$  would converge to  $m$  only asymptotically. We thus overestimate the marginal cost of providing frequency regulation when assuming that  $\dot{y}^* = 0$ . Regardless of the particular value of  $\dot{y}^*$ , it is therefore always profitable for the storage operator to sell as much regulation power as possible if the marginal revenue,  $Tc^r$ , of providing frequency regulation is higher than the marginal cost,  $Tmc^b$ , given  $\dot{y}^* = 0$ , *i.e.*, if  $\frac{c^r}{c^b} > m$ .

In the year 2019, the expected average price of regulation power was the same as the expected average availability price because  $\mathbb{E} \frac{1}{T} \int_{\mathcal{T}} \tilde{\delta}(t) \tilde{p}^d(t) dt$  vanished. In fact, the average value of  $\frac{1}{T} \int_{\mathcal{T}} \delta(t) p^d(t) dt$  over all days was  $-8.77 \cdot 10^{-5}$ . The minimum availability, wholesale market, and retail market prices in any half-hour interval were  $0.41 \frac{\text{cts}}{\text{kWh}}$ ,  $-2.49 \frac{\text{cts}}{\text{kWh}}$ , and  $14.5 \frac{\text{cts}}{\text{kWh}}$ , respectively. Averaged over each day, the minimum daily average availability, wholesale market, and retail market prices were  $0.41 \frac{\text{cts}}{\text{kWh}}$ ,  $0.37 \frac{\text{cts}}{\text{kWh}}$ , and  $14.5 \frac{\text{cts}}{\text{kWh}}$ , respectively, which are all strictly positive. The ratio of daily average availability prices to daily average market prices of electricity was between 0.070 and 2.168 with an average of 0.251 for wholesale market prices, and between 0.026 and 0.133 with an average of 0.059 for retail market prices. Figure 3.A.2 in Appendix 3.A shows the empirical cumulative distribution function of this ratio for wholesale and retail market prices. When studying the profits from frequency regulation over the planning horizon  $\mathcal{T}$  and over the lifetimes of electricity storage devices, we will set the ratio of the expected average price of regulation power  $c^r$  to the expected average market price of electricity  $c^b$  to  $\frac{c^r}{c^b} = 0.251$  for wholesale market prices and to  $\frac{c^r}{c^b} = 0.059$  for retail market prices.

Over the years 2017 to 2019, the cumulative distribution function  $F$  corresponding to  $\mathbb{P}_{\xi}$  can be approximated by a symmetric logistic function with a maximum error of 0.018 with respect to the empirical cumulative distribution function constructed from about 9.5 million frequency recordings with a 10 second resolution. This justifies Assumption 3.1. Based on the logistic approximation, the cumulative distribution function and the characteristic function are given by  $F(\xi) = \frac{1}{1+\exp(-\theta\xi)}$  and  $\varphi(\xi) = \frac{\ln(1+\exp(\theta\xi))}{\theta}$ , respectively, where  $\theta = \frac{2\ln(2)}{\Delta}$  and  $\Delta = 2\varphi(0) = 0.0816$ , which satisfies the condition  $\Delta \leq \frac{\gamma}{T}$  in Assumption 3.2 as  $\frac{\gamma}{T} \geq 0.1$ . The coefficient  $\theta$  was chosen such that frequency deviations have the same mean absolute deviation  $\Delta$  under the logistic distribution as under the empirical distribution. In principle,  $F$  should be a truncated logistic function as the support of  $\mathbb{P}_{\xi}$ ,  $\Xi = [-1, 1]$ , is bounded. The truncation error, however, is just  $2.5 \cdot 10^{-8}$ , which we deem to be negligible. We find that the mean absolute deviation of the frequency recordings is smaller than 0.1 on 96.7% of all days. If the uncertainty set  $\mathcal{D}$  is parametrized by  $\gamma = 0.1T$ , the empirical frequency deviation signals fall thus outside of  $\mathcal{D}$  on 3.3% of all days. On these days, the storage operator may stop delivering regulation power once the total absolute deviation  $\int_0^t |\delta(t')| dt'$  of the frequency deviation signal exceeds  $\gamma$ . In principle, the frequency deviation distribution should thus be estimated based on past frequency deviation signals with mean absolute deviation capped at the activation ratio  $\gamma/T$ . The distribution estimated directly on past frequency deviation signals will differ most from the distribution estimated on capped past frequency deviation signals if the activation ratio is equal to 0.1 rather than 0.2. In this case, the maximum difference between the two distributions is less than 0.001, which we consider negligible compared to the

maximum difference of 0.018 between the empirical cumulative distribution function and the logistic function  $F$ . Figure 3.A.1 in Appendix 3.A shows the empirical cumulative distribution function and its logistic approximation.

We provide all code and data at [www.github.com/lauinger/cost-of-frequency-regulation-through-electricity-storage](https://www.github.com/lauinger/cost-of-frequency-regulation-through-electricity-storage).

### 3.6.2 Marginal Cost and Maximum Regulation Bid

The marginal cost of providing frequency regulation is the marginal increase in the expected power loss multiplied by the market price of electricity and the length of the planning horizon. Formally, the marginal cost is  $g'(x^r)c^bT$  for a fixed amount of regulation power  $x^r$ . In our case study,  $g'(x^r) = m$  as we consider that  $y^\star = 0$ . It is profitable to use a storage device at its full potential if the marginal cost is lower than the marginal revenue,  $Tc^r$ , which is the case if and only if the ratio  $\frac{c^r}{c^b}$  of the expected average price of regulation power to the expected average market price of electricity exceeds the marginal increase  $m$  in the expected power loss. Proposition 3.4 states that  $m$  is convex and nonincreasing in the roundtrip efficiency  $\eta^+\eta^-$  and nondecreasing in the mean absolute deviation of the frequency deviations  $\Delta$ . Figure 2 displays  $m$  as a function of roundtrip efficiency for the estimated logistic distribution of frequency deviations, together with its lower bound  $\underline{m}$  and its upper bound  $\overline{m}$ , both parametrized by the same mean absolute deviation as the logistic distribution. The bounds are tight when the roundtrip efficiency equals one and loosen as the roundtrip efficiency decreases. The upper bound loosens faster than the lower bound. For roundtrip efficiencies higher than 0.60, the lower bound,  $\underline{m} = \frac{1-\eta^+\eta^-}{1+\eta^+\eta^-} \Delta$ , underestimates  $m$  by less than  $4.59 \cdot 10^{-4}$ . At a roundtrip efficiency of 0.35, typical for inefficient hydrogen storage,  $m$  is 4.30%. For inefficient redox flow batteries, with a roundtrip efficiency of 0.60,  $m$  decreases to 2.09%. For inefficient lithium-ion batteries, with a roundtrip efficiency of 0.85,  $m$  decreases further to 0.66%. Unsurprisingly,  $m$  vanishes for perfectly efficient storage devices. For storage operators buying electricity at retail prices, the ratio  $\frac{c^r}{c^b}$  was greater than 0.026 on all days in 2019. It would have therefore been profitable for them to use any of the storage technologies we consider at their full potential for frequency regulation, except for hydrogen storage. For storage operators buying electricity at wholesale prices, the ratio  $\frac{c^r}{c^b}$  was greater than 0.07 on all days in 2019, which means that it would have been profitable for them to use a hydrogen storage device at its full potential, too.

Although charging and discharging losses may not cause storage operators to withhold regulation power from the market, they still reduce the profit  $c^r - mc^b$  per unit of regulation power. Figure 3 shows the average profit per unit of regulation power as a function of roundtrip efficiency for storage operators buying electricity at wholesale and retail prices in the year 2019. Losses reduce the profit by 19% from  $0.90 \frac{\text{cts}}{\text{kW}\cdot\text{h}}$  to  $0.73 \frac{\text{cts}}{\text{kW}\cdot\text{h}}$  for the most inefficient storage devices if electricity is bought at wholesale prices. If electricity is bought at retail prices, losses reduce the profit by 72% to  $0.24 \frac{\text{cts}}{\text{kW}\cdot\text{h}}$ . The reduction is thus four times higher at retail than at wholesale prices. A hydrogen tank with a roundtrip efficiency of 0.4 buying electricity at

## The Economics of Frequency Regulation through Electricity Storage: An Analytical Solution

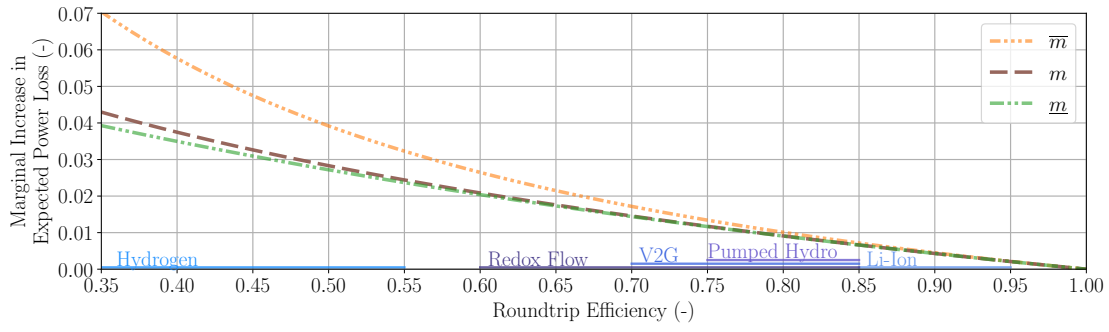


Figure 2: Marginal increase in expected power loss for different roundtrip efficiencies.

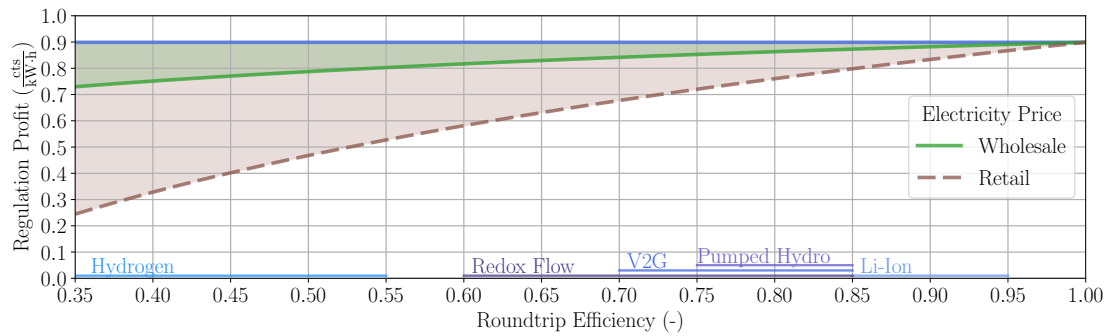


Figure 3: Profit per unit of regulation power for wholesale and retail electricity prices.

wholesale prices and an electric vehicle with a roundtrip efficiency of 0.8 buying electricity at retail prices achieve the same profit per unit of regulation power. In its recent regulation, the Federal Energy Regulatory Commission (2018) has made it easier for storage devices to access the wholesale electricity market. Such regulation is most beneficial to storage devices with low and moderate roundtrip efficiencies. Overall, the regulation may make electricity storage more competitive with fossil-fuel-based power plants in the frequency regulation market. Nevertheless, even if electricity is bought at wholesale prices, charging and discharging losses should be carefully considered as they reduce the profit per unit of regulation power by up to 19%.

Losses reduce not only the profit per unit of regulation power, but may also reduce the amount of regulation power  $\bar{x}^r$  a storage device can provide. We have seen in Section 3.5 that the storage device may be either energy-constrained or power-constrained if  $\dot{y}^* = 0$ .

If the storage device is power-constrained, then the storage operator can account for the roundtrip efficiency by dimensioning the discharging capacity  $\bar{y}^-$  as a fraction  $\frac{1-m}{1+m}$  of the charging capacity  $\bar{y}^+$  without restricting  $\bar{x}^r$ . The fraction is 1 at a roundtrip efficiency of 1, and decreases to 0.92 as the roundtrip efficiency decreases to 0.35.

If the storage device is energy-constrained, then charging losses increase the amount of energy that the storage device can consume from the grid, while discharging losses decrease the

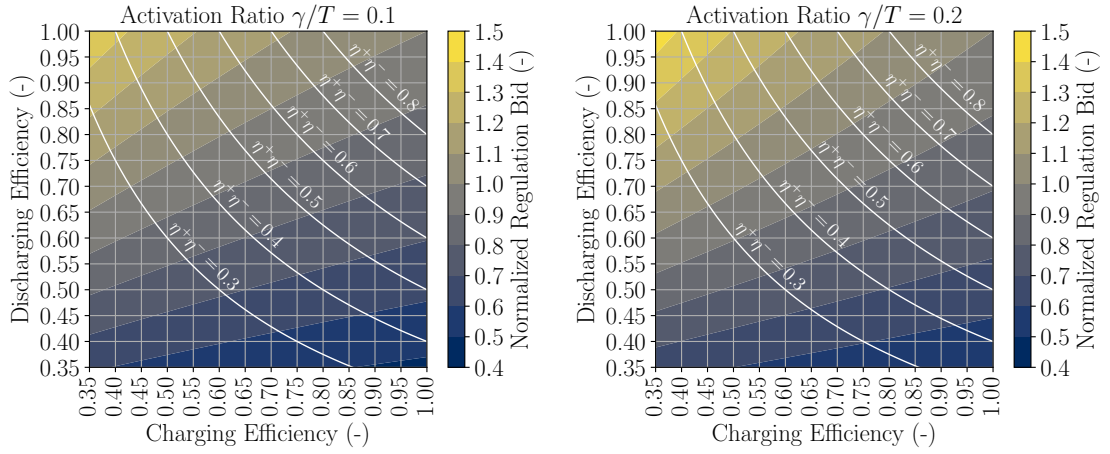


Figure 4: Maximum regulation power normalized by  $\frac{\bar{y}}{2\gamma}$ .

amount of energy that the storage device can deliver to the grid. The storage operator can offer most regulation power,  $\bar{x}_\star^r$ , to the grid operator if the initial state-of-charge is such that she can consume as much energy from the grid as she can provide to the grid. For roundtrip efficiencies in  $(0, 1)$ , the optimal initial state-of-charge,  $y_0^\star$ , is nondecreasing in the activation ratio. Given activation ratios between 0.1 and 0.2,  $\frac{y_0^\star}{\bar{y}}$  is between 0.52 and 0.53 for lithium-ion batteries with a roundtrip efficiency of 0.85, between 0.57 and 0.60 for redox flow batteries with a roundtrip efficiency of 0.60, and between 0.66 and 0.69 for hydrogen storage with a roundtrip efficiency of 0.35.

Figure 4 shows that the normalized regulation power  $\bar{x}_\star^r / \frac{\bar{y}}{2\gamma}$  is indeed nonincreasing in the charging efficiency  $\eta^+$  and nondecreasing in the discharging efficiency  $\eta^-$ . The decrease in  $\eta^+$  is more pronounced and the increase in  $\eta^-$  is less pronounced if the activation ratio is 0.2 rather than 0.1. Starting from a roundtrip efficiency of 1 and an activation ratio of 0.2, the normalized regulation power increases from 1 to 1.45 as the charging efficiency decreases from 1 to 0.35, and decreases from 1 to 0.51 as the discharging efficiency decreases from 1 to 0.35. At an activation ratio of 0.1, the normalized regulation power increases to only 1.37 as the charging efficiency decreases to 0.35, and decreases slightly further to 0.48 as the discharging efficiency decreases to 0.35. Although the normalized regulation power is lower, the absolute regulation power is considerably higher at an activation ratio of 0.1 rather than 0.2, because the normalization constant  $\frac{\bar{y}}{2\gamma}$  is inversely proportional to  $\gamma$ .

In principle, charging losses may outweigh discharging losses and increase the normalized regulation bid compared to storage devices with no losses. In practice, however, discharging losses usually outweigh charging losses. As examples, we consider lithium-ion batteries, vehicle-to-grid, and hydrogen storage, all of them operating at an activation ratio of 0.2. Hydrogen storage is unlikely to be energy-constrained because hydrogen can be stored at low cost in steel tanks, or at even lower cost in salt caverns (Victoria et al., 2019). Nevertheless, we include hydrogen in our comparison as an example of storage devices with low roundtrip

## The Economics of Frequency Regulation through Electricity Storage: An Analytical Solution

---

efficiencies. For lithium-ion batteries with charging and discharging efficiencies of 0.92 each, losses reduce the normalized regulation bid from 1 to 0.98. For vehicle-to-grid with a charging efficiency of 0.88 and a discharging efficiency of 0.79, loosely based on Apostolaki-Iosifidou et al. (2017), losses reduce the normalized regulation bid to 0.91. For hydrogen storage with a charging efficiency of 0.80 and a discharging efficiency of 0.58, based on Victoria et al. (2019), losses reduce the normalized regulation bid to 0.77. In practice, charging and discharging losses thus reduce the amount of regulation power  $\bar{x}^r$  that energy-constrained storage devices can provide by up to 23%, even at high activation ratios, and should therefore be carefully considered.

### 3.6.3 Economics

We will now consider the profit that an energy-constrained storage device may earn per unit of storage capacity. First, we describe the *operating* profit made over the planning horizon  $\mathcal{T}$  of length  $T$ . For the case of a lithium-ion battery, we then calculate the *effective yearly* profit as the difference between the operating profits made over one year and the annualized investments costs of the battery.

The operating profit is the product of the profit per unit of regulation power and the amount of regulation power the storage device can deliver. Formally, the operating profit is thus equal to

$$\frac{(c^r - c^b m) \eta^- \bar{y}}{\frac{\gamma}{T} (1 + \eta^+ \eta^- - m) + \eta^+ \eta^- m}.$$

It may be somewhat surprising that the operating profit depends on the length of the planning horizon  $T$  only through the activation ratio  $\gamma/T$ . Intuitively, one may expect the operating profit to increase linearly with the length of the planning horizon because a longer planning horizon should allow the storage operator to sell the same amount of regulation power for a longer period of time. This reasoning is correct if the storage device is power-constrained. For an energy-constrained storage device, however, the storage operator can only deliver a fixed amount of regulation energy. The length of the period over which the regulation energy is delivered does therefore not influence the operating profit.

We have established in Section 3.6.2 that the profit per unit of regulation power increases with the roundtrip efficiency, while the maximum amount of regulation power increases with the discharging efficiency but decreases with the charging efficiency. The operating profit will therefore increase with the discharging efficiency, but it is unclear how it depends on the charging efficiency. Intuitively, the higher the market price of electricity, the more pronounced the increase of the profit per unit of regulation power in the charging efficiency. Similarly, the higher the activation ratio, the more pronounced the decrease of the maximum amount of regulation power in the charging efficiency. Figure 5 and Figure 3.A.4 in Appendix 3.A show that, for activation ratios of 0.2 and 0.1, the operating profit increases with the charging efficiency at retail electricity prices but not at wholesale electricity prices. In practice, however,

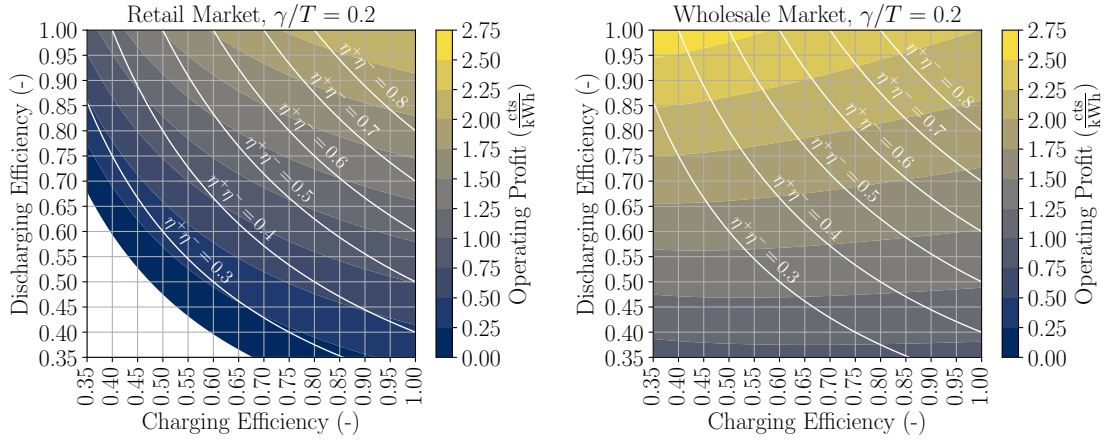


Figure 5: Operating profit per kWh of storage capacity on wholesale and retail markets.

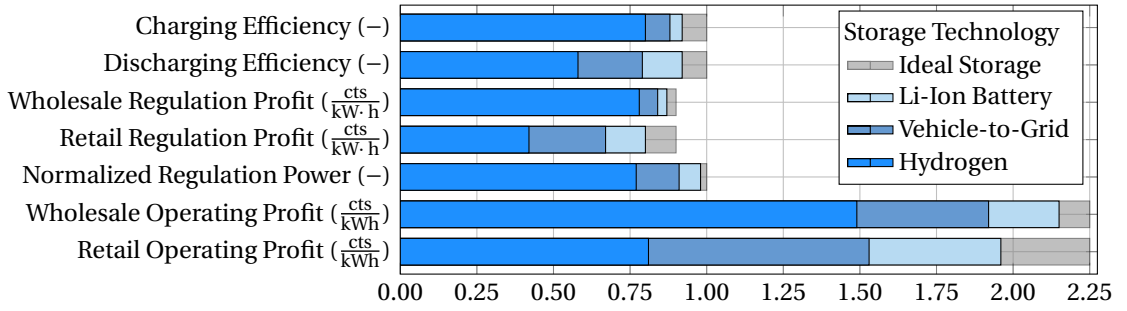


Figure 6: The impact of charging and discharging losses on regulation power and profits.

the combined effect of charging and discharging losses is usually a decrease in the operating profit, even at wholesale prices. As examples, we consider again lithium-ion batteries, vehicle-to-grid, and hydrogen storage, with the same charging and discharging efficiencies as in Section 3.6.2. At an activation ratio of 0.2, the operating profit is  $2.25 \frac{\text{cts}}{\text{kWh}}$  in the absence of charging and discharging losses, regardless of the market price of electricity. For lithium-ion batteries, the operating profit reduces to  $2.15 \frac{\text{cts}}{\text{kWh}}$  at wholesale prices and to  $1.96 \frac{\text{cts}}{\text{kWh}}$  at retail prices. For vehicle-to-grid, the operating profit decreases further to  $1.92 \frac{\text{cts}}{\text{kWh}}$  at wholesale prices and to  $1.53 \frac{\text{cts}}{\text{kWh}}$  at retail prices. For hydrogen, finally, the operating profit falls to  $1.49 \frac{\text{cts}}{\text{kWh}}$  at wholesale prices and to  $0.81 \frac{\text{cts}}{\text{kWh}}$  at retail prices. If the activation ratio halves from 0.2 to 0.1, the operating profits roughly double. Overall, charging and discharging losses should be carefully considered because they reduce the operating profit from selling frequency regulation by over 33% at wholesale prices and over 70% at retail prices. Figure 6 summarizes the impact of losses on the profits per unit of regulation power, on the maximum normalized regulation power, and on operating profits at wholesale and retail electricity prices.

The effective yearly profit determines whether it is worthwhile for a storage operator to invest into a storage device for frequency regulation. The European Network of Transmission System Operators for Gas and Electricity (2021) estimates that the need for electricity storage



## The Economics of Frequency Regulation through Electricity Storage: An Analytical Solution

---

will increase in the future as the electricity grid becomes more weather-dependent, due to more electric heating and more wind and solar power plants, while the weather itself becomes more variable, due to climate change. Batteries are to provide between 10GW to 40GW of flexible power by 2030, 75GW to 100GW by 2040, and 90GW to 100GW by 2050, to ensure that the European electricity grids can meet peak electricity demand without load shedding, the technical term for rolling black-outs. Based on the cost and lifetime data of lithium-ion batteries in Section 3.6.1, we estimate the annualized costs of lithium-ion batteries in the near future, specifically, in the year 2023, to range from  $8.2 \frac{\text{€}}{\text{kWh}}$  to  $16.0 \frac{\text{€}}{\text{kWh}}$  for energy storage capacity and from  $27.6 \frac{\text{€}}{\text{kW}}$  to  $33.4 \frac{\text{€}}{\text{kW}}$  for charging and discharging capacity. For an energy-constrained battery, we have seen that the operating profit depends on the length of the planning horizon  $T$  only through the activation ratio  $\gamma/T$ . The operating profits accrued over a one-year period are thus inversely proportional to the length of the planning horizon. Similarly, the minimum C-rate required for the battery to be energy-constrained is also inversely proportional to the length of the planning horizon, and so are the costs of the charging and discharging capacity of the battery. In fact, Figure 3.A.3 in Appendix 3.A shows that, at an activation ratio of 0.2, the minimum required C-rate increases from  $0.1\text{h}^{-1}$  to  $0.6\text{h}^{-1}$  if the planning horizon decreases from 24h to 4h. At an activation ratio of 0.1, the minimum required C-rates are about twice as high. Conversely, the costs of the energy storage capacity of the battery are independent of the length of the planning horizon.

Figure 7 shows the effective yearly profit for lithium-ion batteries with charging and discharging efficiencies of 0.92, buying electricity at wholesale prices, as a function of the length of the planning horizon, for activation ratios of 0.1 and 0.2, for low annualized investment costs of  $8.2 \frac{\text{€}}{\text{kWh}}$  and  $27.6 \frac{\text{€}}{\text{kW}}$ , and for high annualized investment costs of  $16.0 \frac{\text{€}}{\text{kWh}}$  and  $33.4 \frac{\text{€}}{\text{kW}}$ . At the current 24 hour planning horizon, lithium-ion batteries are profitable only at an activation ratio of 0.1 and low investment costs. Given that we have only considered the cost of the battery itself but no additional costs related to installation, maintenance, administration, or land lease, investing in lithium-ion batteries for frequency regulation does not seem to be profitable in the near future. In the medium term, lithium-ion batteries may become sufficiently low-cost (Ziegler and Trancik, 2021) to be used for frequency regulation. Besides falling battery prices, grid operators might opt for an activation ratio of 0.1 rather than 0.2 to make the use of energy storage for frequency regulation more profitable. This would roughly double the operating profits from frequency regulation, but it would also shrink the uncertainty set  $\mathcal{D}$  and therefore make grid operators more vulnerable to extreme frequency deviations that could cause black-outs.

Alternatively, grid operators might reduce the length of the planning horizon  $T$ . If the planning horizon were to be reduced from 24 hours to 4 hours, for example, the operating profits accrued over a one-year period would increase by a factor 6. Lithium-ion batteries could then achieve an effective yearly profit of 10p€/er kWh of storage capacity, even at high investment costs and high activation ratios. A shorter planning horizon for frequency regulation does not necessarily make grid operators more vulnerable to extreme frequency deviations. In fact, grid operators already use intraday markets with 15 minute bidding blocks for the wholesale of

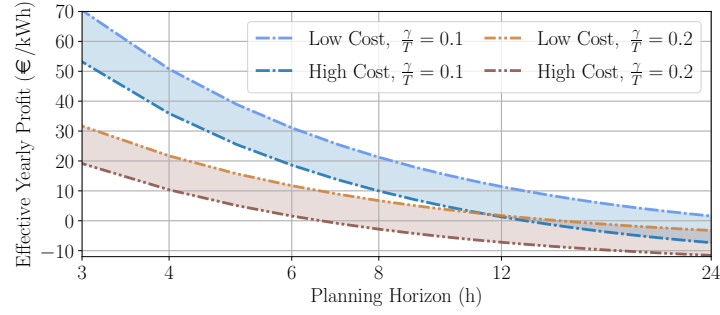


Figure 7: Effective yearly profit per kWh of storage capacity after investment costs.

electricity.<sup>IV</sup> Adopting intraday markets for frequency regulation as well would make energy-constrained storage devices more competitive with power-constrained flexibility providers, such as thermal power plants and pumped hydro storage. The latter may not welcome this competition and lobby grid operators and policy makers to keep the current planning horizons for frequency regulation. Increased competition, however, may decrease the total cost of frequency regulation, which is ultimately borne by the public since grid operators are public entities.

Finally, if battery costs decline slower than projected, vehicle-to-grid may be a viable alternative to newly built batteries as it would use existing batteries in electric vehicles for frequency regulation when the vehicles are parked. Lauinger et al. (2022) suggest, however, that the value of vehicle-to-grid under current market conditions may not be high enough to convince vehicle owners, aggregators, and equipment manufacturers to invest in this technology. Vehicle-to-grid, too, would thus benefit from a shorter planning horizon for frequency regulation.

### 3.7 Conclusions

We analyze the decision problem of an electricity storage operator offering frequency regulation, or, more precisely, frequency containment reserves, under a reliability guarantee that captures effective EU regulations. We show that although frequency deviations vanish on average, the average power flow entering the storage device is nonincreasing in the amount of regulation power offered. The lower the roundtrip efficiency of the storage device and the higher the mean absolute deviation of the frequency deviations, the higher the dissipative losses incurred by the provision of regulation power. We assume that the storage operator purchases power to compensate these losses. There is therefore a nonzero marginal cost of providing frequency regulation. The higher the market price of electricity, the higher the marginal cost. To our best knowledge, we are the first to quantify the marginal cost of providing frequency regulation through electricity storage and to study its dependence on both the roundtrip

<sup>IV</sup>[https://www.entsoe.eu/network\\_codes/cacm/implementation/sidc/](https://www.entsoe.eu/network_codes/cacm/implementation/sidc/)

## **The Economics of Frequency Regulation through Electricity Storage: An Analytical Solution**

---

efficiency of the storage device and on the dispersion of the frequency deviations. In particular, we provide closed-form lower and upper bounds on the marginal cost, which are tight for some extremal frequency deviation distributions.

In a numerical case-study based on frequency measurements in the continental European electricity grid, we find that storage operators need to purchase between 0.6% and 4.3% of the regulation power they offer in order to compensate charging and discharging losses. Since the average wholesale and retail market prices of electricity are about five and fifteen times higher, respectively, than the average price for regulation power, even small losses can increase the marginal cost of frequency regulation significantly. In fact, for inefficient storage devices, such as hydrogen tanks with a roundtrip efficiency of 35%, we find that charging and discharging losses reduce the expected profits per unit of regulation power by up to 19% at wholesale prices and by up to 72% at retail prices. For more efficient storage devices, such as lithium-ion batteries with a roundtrip efficiency of 85%, the reductions are still up to 3% at wholesale prices and up to 11% at retail prices.

In order to balance electricity demand and supply in the future, European grid operators estimate that they may need to store electricity in batteries with a total power of up to 100GW by the year 2050. Lithium-ion batteries, in particular, are considered a promising source of frequency regulation, thanks to their fast dynamics. The investment costs of lithium-ion batteries have declined sharply in recent years, but we find that they are not yet low enough for lithium-ion batteries to be profitable in the frequency regulation market. Since Europe plans to increasingly rely on batteries in the future, however, their use should become profitable.

We identify two policy options that make electricity storage in general and battery storage in particular more profitable. First, regulators can decrease the marginal costs of frequency regulation by making it easier for small and medium-sized storage devices to access wholesale electricity markets. This is one of the aims of Order 845 from the year 2018 by the US Federal Energy Regulatory Commission. Second, regulators can decrease the length of the planning horizon, which is currently one day in the common European frequency regulation market. In fact, we show that the amount of regulation power that storage devices can provide may be constrained not by their charging and discharging capacities but rather by their storage capacity and their initial state-of-charge. In this case, the profits from frequency regulation over the lifetime of the storage devices are inversely proportional to the length of the planning horizon. The planning horizon could, for example, be shortened by adopting intraday markets for frequency regulation. In fact, such markets already exist for the wholesale of electricity. In general, regulations that make electricity storage more profitable also make it more competitive. The increased competition may not be welcome by traditional frequency regulation providers such as thermal power plants and pumped hydro storage plants. Their operators may lobby against new regulations. Nevertheless, a more competitive frequency regulation market may lead to a higher security of supply, especially in electricity grids with high shares of intermittent wind and solar power, and to lower public costs of frequency regulations, which are borne by all electricity consumers alike.

# Appendices

## 3.A Additional Figures

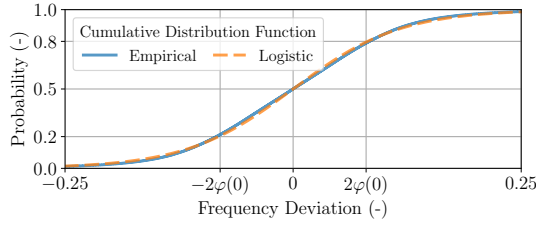


Figure 3.A.1: Distribution of frequency deviations in 2017–19.

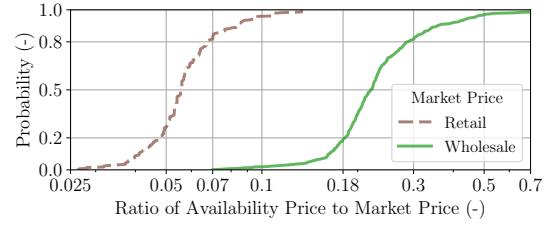


Figure 3.A.2: Distribution of daily average electricity prices in 2019.

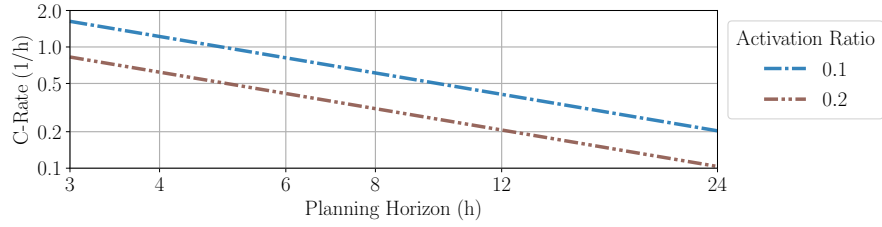


Figure 3.A.3: Minimum C-rate for a lithium-ion battery to be energy-constrained.

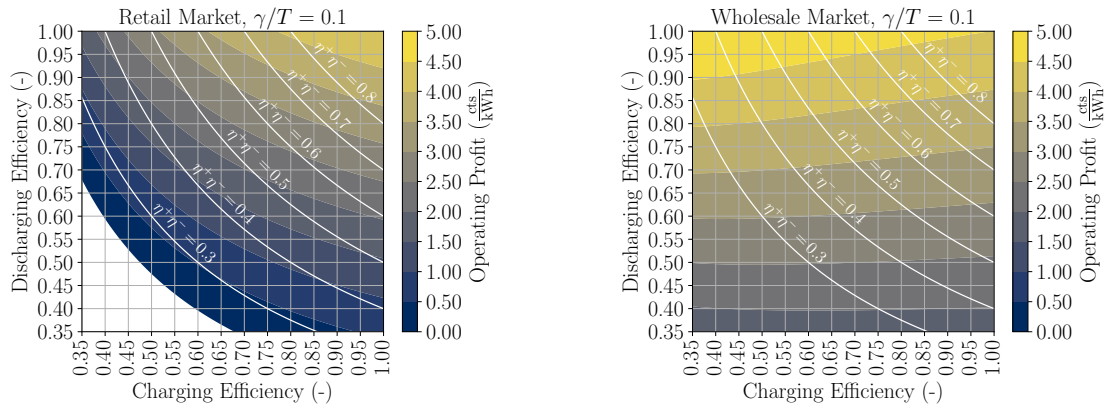


Figure 3.A.4: Operating profit on wholesale and retail markets for  $\frac{\gamma}{T} = 0.1$ .

### 3.B Proofs

This appendix contains the proofs of all theorems, propositions, and lemmas in the main text.

*Proof of Proposition 3.1.* The proof is similar to the one of Proposition 1 by Lauinger et al. (2022), which analyzes the state-of-charge of an electric vehicle battery providing frequency regulation. The difference is that we do not model any electricity consumption for driving. By definition,

$$\begin{aligned} y(x^b, x^r, \delta, y_0, t) &= y_0 + \int_0^t \eta^+ [x^b + \delta(t')x^r]^+ - \frac{1}{\eta^-} [x^b + \delta(t')x^r]^- dt' \\ &= y_0 + \int_0^t \min \left\{ \eta^+ (x^b + \delta(t')x^r), \frac{1}{\eta^-} (x^b + \delta(t')x^r) \right\} dt', \end{aligned}$$

where the second equality holds because  $\eta^+ < 1/\eta^-$ . As  $\eta^+ > 0$ ,  $\eta^- > 0$ , and  $x^r \geq 0$ , both  $\eta^+ (x^b + \delta(t')x^r)$  and  $\frac{1}{\eta^-} (x^b + \delta(t')x^r)$  are nondecreasing in  $\delta(t')$  and strictly increasing in  $x^b$ . The minimum of two (nondecreasing/strictly increasing) affine functions is a concave (nondecreasing/strictly increasing) function (Boyd and Vandenberghe, 2004, p. 73). The function  $y$  is thus concave strictly increasing in  $x^b$ , concave in  $x^r$ , concave nondecreasing in  $\delta$ , and affine nondecreasing in  $y_0$ .  $\square$

*Proof of Lemma 3.1.* The claim follows immediately from the definition of  $\mathcal{D}$  and is thus omitted.  $\square$

*Proof of Proposition 3.2.* We first show that the upper bound on the charging power and the upper bound on the state-of-charge are valid for all frequency deviation trajectories  $\delta \in \mathcal{D}$  and all time instants  $t \in \mathcal{T}$  if and only if they are valid for the particular frequency deviation trajectory  $\delta^{(+)}$ , defined through  $\delta^{(+)}(t) = 1$  if  $t \leq \gamma$  and  $\delta^{(+)} = 0$  otherwise, and all time instants  $t \in \{\gamma, T\}$ .

The upper bound on the charging power is valid for all  $\delta \in \mathcal{D}$  and all  $t \in \mathcal{T}$  if and only if it is valid for the maximum charging power that can be achieved by any  $\delta \in \mathcal{D}$  and any  $t \in \mathcal{T}$ . We have

$$\max_{\delta \in \mathcal{D}, t \in \mathcal{T}} y^+(x^b, x^r, \delta(t)) = \max_{\delta \in \mathcal{D}^+, t \in \mathcal{T}} y^+(x^b, x^r, \delta(t)) = \max_{\delta \in \mathcal{D}^+, t \in \mathcal{T}} x^b + \delta(t)x^r = x^b + x^r,$$

where the first equality holds because  $y^+$  is nondecreasing in  $\delta(t)$  and because  $\mathcal{D}$  is symmetric. In fact, for any  $\delta \in \mathcal{D}$ , we have  $|\delta| \in \mathcal{D}$ , and the maximum charging power for  $|\delta|$  will be at least as high as the one for  $\delta$ . The second equality holds because  $y^+$  is linear in  $\delta(t)$  whenever  $\delta(t) \geq 0$ . The last equality holds because  $\delta(t) \leq 1$  for all  $\delta \in \mathcal{D}^+$  and  $t \in \mathcal{T}$ , and because the upper bound is attained at  $\delta = \delta^{(+)}$  and  $t = \gamma$ , for example. Thus, assertion (i) follows.

The state-of-charge at a given time instant  $t$  for a given frequency deviation trajectory  $\delta$  is

given by the integral of the difference between the instantaneous charging and discharging power weighted by  $\eta^+$  and  $\frac{1}{\eta^-}$ , respectively. This integral does not depend on the order of the frequency deviations within the interval  $[0, t]$ . We can thus assume without loss of generality that  $\delta$  is sorted in decreasing order within this interval. Next, define the effective charging time  $t^c = \max_{t' \in [0, t]} \{t' : x^b + \delta(t')x^r \geq 0\}$ . In addition, denote the average frequency deviations during charging and discharging by  $\delta^c$  and  $\delta^d$ , respectively, which we define through  $\delta^c = \frac{1}{t^c} \int_0^{t^c} \delta(t') dt'$  if  $t^c > 0$  and  $= 0$  otherwise, and  $\delta^d = \frac{1}{t-t^c} \int_{t^c}^t \delta(t') dt'$  if  $t^c < t$  and  $= 0$  otherwise. Recalling that  $-1 \leq \delta(t) \leq 1$  for all  $\delta \in \mathcal{D}$  and all  $t \in \mathcal{T}$ , we now address two special cases. First, if  $-x^b > x^r$ , then  $t^c = 0$  and the battery is discharging at all times, regardless of the frequency deviation trajectory. The maximum state-of-charge is thus the initial state-of-charge, which we assumed to satisfy the upper bound for consistency. Second, if  $x^b > x^r$ , then  $t^c = t$  and the battery is charging at all times, regardless of the frequency deviation trajectory. The maximum state-of-charge is thus attained at time  $t = T$  by any nonnegative frequency deviation trajectory that exhausts the uncertainty budget such as  $\delta^{(+)}$ . For the case  $|x^b| \leq x^r$ , we now prove that

$$\begin{aligned} \max_{\delta \in \mathcal{D}, t \in \mathcal{T}} y(x^b, x^r, \delta, y_0, t) &= \max_{t, t^c, \delta^c, \delta^d} y_0 + t^c \eta^+ (x^b + \delta^c x^r) + \frac{t-t^c}{\eta^-} (x^b + \delta^d x^r) \\ \text{s.t.} \quad &x^b + \delta^c x^r \geq 0, \quad x^b + \delta^d x^r < 0, \\ &t^c \delta^c + (t-t^c) \delta^d \leq \gamma, \\ &0 \leq \delta^c, \delta^d \leq 1, \quad 0 \leq t^c \leq t \leq T. \end{aligned} \quad (3.7)$$

First, we note that  $\mathcal{D}$  can be replaced with  $\mathcal{D}^+$  on the left-hand side of equation (3.7) because  $y$  is nondecreasing in  $\delta$  by Proposition 3.1 and because  $\mathcal{D}$  is symmetric by Lemma 3.1. Next,  $\mathcal{D}^+$  can be further restricted to  $\mathcal{D}_{\triangleright}^+$  of all  $\delta \in \mathcal{D}^+$  that are nonincreasing because  $y$  depends only on the integral of  $\delta$  over the interval  $[0, t]$ . In fact, for  $t = T$ ,  $y(x^b, x^r, \delta, y_0, T)$  does not depend on the order of  $\delta$ . For  $t < T$ , Proposition 3.1 implies that  $y(x^b, x^r, \delta, y_0, t)$  is maximized if  $\delta$  is sorted in nonincreasing order. If  $\delta \in \mathcal{D}^+$ , then the sorted  $\delta \in \mathcal{D}^+$  because the order of  $\delta$  matters neither for the budget constraint  $\int_{\mathcal{T}} \delta(t) dt \leq \gamma$  nor for the box constraints  $\delta \in \mathcal{L}(\mathcal{T}, [0, 1])$  which define  $\mathcal{D}^+$ . We thus have

$$\max_{\delta \in \mathcal{D}, t \in \mathcal{T}} y(x^b, x^r, \delta, y_0, t) = \max_{\delta \in \mathcal{D}_{\triangleright}^+, t \in \mathcal{T}} y(x^b, x^r, \delta, y_0, t).$$

We now show that  $\max_{\delta \in \mathcal{D}_{\triangleright}^+, t \in \mathcal{T}} y(x^b, x^r, \delta, y_0, t)$  is equal to the right-hand side of equation 3.7. Select  $\delta \in \mathcal{D}_{\triangleright}^+$  and  $t \in \mathcal{T}$ , then we have

$$\begin{aligned} y(x^b, x^r, \delta, y_0, t) &= y_0 + \int_0^t \eta^+ [x^b + \delta(t')x^r]^+ - \frac{1}{\eta^-} [x^b + \delta(t')x^r]^- dt' \\ &= y_0 + \int_0^{t^c} \eta^+ (x^b + \delta(t')x^r) dt' + \int_{t^c}^t \frac{1}{\eta^-} (x^b + \delta(t')x^r) dt' \\ &= y_0 + t^c \eta^+ (x^b + \delta^c x^r) + \frac{t-t^c}{\eta^-} (x^b + \delta^d x^r), \end{aligned}$$

## The Economics of Frequency Regulation through Electricity Storage: An Analytical Solution

---

where  $\delta^c$ ,  $\delta^d$ , and  $t^c$  are as defined above. The new variables  $\delta^c$ ,  $\delta^d$ , and  $t^c$  correspond to feasible frequency deviation trajectories  $\delta \in \mathcal{D}_{\triangleright}^+$  and to feasible time instants  $t \in \mathcal{T}$  if and only if they satisfy the constraints of the optimization problem on the right-hand side of equation (3.7). In fact, we have

$$\int_0^t \delta(t') dt' = \int_0^{t^c} \delta(t') dt' + \int_{t^c}^t \delta(t') dt' = t^c \delta^c + (t - t^c) \delta^d \leq \gamma.$$

All other constraints are valid by construction. We now solve the optimization problem on the right-hand side of equation (3.7) analytically. It is optimal to set  $t - t^c = 0$  since the negative term  $x^b + \delta^d x^r$  is multiplied by the nonnegative term  $t - t^c$  in the objective function. The budget constraint  $t^c \delta^c + (t - t^c) \delta^d \leq \gamma$  thus reduces to  $t^c \delta^c \leq \gamma$  and the objective function reduces to  $y_0 + t^c \eta^+(x^b + \delta^c x^r)$ . As  $x^r$  is nonnegative, it is also optimal to set  $t^c \delta^c = \gamma$ , which restricts  $t$  to be no smaller than  $\gamma$  as  $\delta^c$  must be no greater than 1. This restriction, however, does not affect optimality because the objective function is nondecreasing in  $t$  as  $x^b + \delta^c x^r$  is nonnegative. We obtain the equivalent problem

$$\begin{aligned} \max_t \quad & y_0 + \eta^+(tx^b + \gamma x^r) \\ \text{s.t.} \quad & x^b + \frac{\gamma}{t} x^r \geq 0, \quad \gamma \leq t \leq T. \end{aligned}$$

If  $x^b \geq 0$ , then it is optimal to set  $t = T$ , which implies that  $\delta^c = \frac{\gamma}{T}$  in the earlier problem. Conversely, if  $x^b \leq 0$ , then it is optimal to set  $t = \gamma$ , which implies that  $\delta^c = 1$  in the earlier problem. The average of the frequency deviation trajectory  $\delta^{(+)}$  is  $\gamma$  on the interval  $[0, t]$  and  $\frac{\gamma}{T}$  on the interval  $[0, T]$ . The upper bound on the state-of-charge thus holds if and only if it holds for  $y(x^b, x^r, \delta^{(+)}, y_0, t)$  and  $y(x^b, x^r, \delta^{(+)}, y_0, T)$ , which leads to assertion (iii).

Using similar arguments, one can show that the upper bound on the discharging power and the lower bound on the state-of-charge hold for all frequency deviation signals  $\delta \in \mathcal{D}$  and all time instants  $t \in \mathcal{T}$  if and only if they hold for the particular frequency deviation signal  $\delta^{(-)} = -\delta^{(+)}$  and all time instants  $t \in \{\gamma, T\}$ . We omit the details for the sake of brevity.  $\square$

The proof of Proposition 3.3 relies on the following symmetry property of  $\varphi$ .

**Lemma 3.7** (Symmetry of  $\varphi$ ). For all  $z \in \mathbb{R}$ , we have  $\varphi(z) = \varphi(-z) + z$ .

*Proof of Lemma 3.7.* We first prove that the symmetry of  $\mathbb{P}_\xi$  implies that  $F(z) + F(-z) = 1 + \mathbb{P}_\xi[\{z\}]$  for all  $z \in \mathbb{R}$ . To see this, note that

$$F(z) + F(-z) = \mathbb{P}_\xi((-\infty, z]) + \mathbb{P}_\xi((-\infty, -z]) = \mathbb{P}_\xi((-\infty, z]) + \mathbb{P}_\xi([z, \infty)) = 1 + \mathbb{P}_\xi[\{z\}].$$

Thus,  $F(z) - 1/2(1 + \mathbb{P}_\xi[\{z\}]) = 1/2(1 + \mathbb{P}_\xi[\{z\}]) - F(-z) = -(F(-z) - 1/2(1 + \mathbb{P}_\xi[\{z\}]))$  is an odd

function, which implies that

$$\begin{aligned}
 \varphi(z) &= \int_{-\infty}^z F(\xi) d\xi = \int_{-\infty}^{-z} F(\xi) d\xi + \int_{-z}^z F(\xi) d\xi - \frac{1}{2}(1 + \mathbb{P}_\xi[\{z\}]) + \frac{1}{2}(1 + \mathbb{P}_\xi[\{z\}]) d\xi \\
 &= \varphi(-z) + \int_{-z}^z \frac{1}{2}(1 + \mathbb{P}_\xi[\{z\}]) d\xi = \varphi(-z) + \frac{1}{2}(z + \mathbb{P}_\xi[\{z\}] - (-z) - \mathbb{P}_\xi[\{-z\}]) \\
 &= \varphi(-z) + z + \frac{1}{2}(\mathbb{P}_\xi[z] - \mathbb{P}_\xi[z]) = \varphi(-z) + z.
 \end{aligned}$$

Hence, the claim follows.  $\square$

*Proof of Proposition 3.3.* We first prove equation (3.2). If  $x^r > 0$ , then we have

$$\begin{aligned}
 \mathbb{E} \left[ y(x^b, x^r, \tilde{\delta}, y_0, T) \right] &= y_0 + T \mathbb{E} \left[ \frac{1}{T} \int_{\mathcal{T}} \eta^+ \left[ x^b + \tilde{\delta}(t)x^r \right]^+ - \frac{1}{\eta^-} \left[ x^b + \tilde{\delta}(t)x^r \right]^- dt \right] \\
 &= y_0 + T x^r \int_{-1}^1 \eta^+ \left[ \frac{x^b}{x^r} + \xi \right]^+ - \frac{1}{\eta^-} \left[ \frac{x^b}{x^r} + \xi \right]^- \mathbb{P}_\xi(d\xi), \tag{3.8}
 \end{aligned}$$

where the second equality follows from the definitions of  $\tilde{\xi}$  and  $\mathbb{P}_\xi$ . Setting  $z = x^b/x^r$  to simplify notation, we then find

$$\begin{aligned}
 \int_{-1}^1 [z + \xi]^+ \mathbb{P}_\xi(d\xi) &= \int_{-z}^1 (z + \xi) \mathbb{P}_\xi(d\xi) = zF(\xi)|_{-z}^1 + \xi F(\xi)|_{-z}^1 - \int_{-z}^1 F(\xi) d\xi \\
 &= (z + \xi)F(\xi) - \varphi(\xi)|_{-z}^1 = (z + 1)F(1) + \varphi(-z) - \varphi(1) = z + \varphi(-z).
 \end{aligned}$$

The second equality follows from integration by parts, and the fifth equality holds because  $F(1) = \varphi(1) = 1$ . In fact, as  $\varphi(-1) = 0$  by construction, Lemma 3.7 implies that  $\varphi(1) = \varphi(-1) + 1 = 1$ . Following a similar reasoning and keeping in mind that  $F(-1) = 0$ , we obtain

$$\begin{aligned}
 \int_{-1}^1 [z + \xi]^- \mathbb{P}_\xi(d\xi) &= - \int_{-1}^{-z} (z + \xi) \mathbb{P}_\xi(d\xi) = \varphi(\xi) - (z + \xi)F(\xi)|_{-1}^{-z} \\
 &= (z - 1)F(-1) + \varphi(-z) - \varphi(-1) = \varphi(-z).
 \end{aligned}$$

Substituting these expressions into (3.8) yields equation (3.2).

If  $x^r = 0$ , then we find

$$\mathbb{E} \left[ y(x^b, 0, \tilde{\delta}, y_0, T) \right] = y_0 + T \left( \eta^+ [x^b]^+ - \frac{1}{\eta^-} [x^b]^- \right) = \lim_{x^r \rightarrow 0^+} y_0 + T \left( \eta^+ x^b - \eta_d x^r \varphi \left( -\frac{x^b}{x^r} \right) \right).$$

The second equality holds because  $x^r \varphi(-\frac{x^b}{x^r})$  is the perspective of  $\varphi(-x^b)$ , which implies that

$$\lim_{x^r \rightarrow 0^+} x^r \varphi \left( -\frac{x^b}{x^r} \right) = x^b \left( \lim_{x^r \rightarrow 0^+} \frac{\partial}{\partial x^b} x^r \varphi \left( -\frac{x^b}{x^r} \right) \right) = x^b \left( \lim_{x^r \rightarrow 0^+} -F \left( -\frac{x^b}{x^r} \right) \right) = [x^b]^- .$$



## The Economics of Frequency Regulation through Electricity Storage: An Analytical Solution

---

We now establish several useful properties of the expected terminal state-of-charge. Note first that  $\varphi$  is convex, continuous, and almost everywhere differentiable because it is a super-cumulative distribution function. The expected terminal state-of-charge is jointly concave in  $x^b$  and  $x^r$  because  $-x^r \varphi(-\frac{x^b}{x^r})$  is the negative perspective of the convex function  $\varphi(-x^b)$  and therefore concave (Boyd and Vandenberghe, 2004, p. 89). Theorem 10.1 by Rockafellar (1970) implies that any concave function is continuous on the interior of its domain. We have shown above that the expected terminal state-of-charge on the boundary of its domain, *i.e.*, for  $x^r = 0$ , is equal to its right limit. It is thus continuous. Theorem 25.5 again by Rockafellar (1970) implies that it is also differentiable almost everywhere. To see that the expected terminal state-of-charge is strictly increasing in  $x^b$ , note that

$$\frac{\partial}{\partial x^b} \mathbb{E} \left[ y(x^b, x^r, \tilde{\delta}, y_0, T) \right] = T \left( \eta^+ + \eta_d F \left( -\frac{x^b}{x^r} \right) \right) > 0 \quad \forall (x^b, x^r) \in \mathbb{R} \times \mathbb{R}_+$$

because  $\eta^+ > 0$ ,  $\eta_d \geq 0$ , and  $F$  is nonnegative. Here, we use the convention that  $F(-\frac{x^b}{0}) = 0$  if  $x^b \geq 0$  and  $F(-\frac{x^b}{0}) = 1$  if  $x^b < 0$ . Similarly, to see that the expected terminal state-of-charge is nondecreasing in  $x^r$ , we note that

$$\frac{\partial}{\partial x^r} \mathbb{E} \left[ y(x^b, x^r, \tilde{\delta}, y_0, T) \right] = -\eta_d T \left( \varphi \left( -\frac{x^b}{x^r} \right) + \frac{x^b}{x^r} F \left( -\frac{x^b}{x^r} \right) \right) \leq 0 \quad \forall (x^b, x^r) \in \mathbb{R} \times \mathbb{R}_{++}.$$

To prove the inequality, we set  $z = -x^b/x^r$  and show that the function  $-\eta_d(\varphi(z) - zF(z))$  is nonnegative. As  $\varphi(z) = 0$  for all  $z \leq -1$ , Lemma 3.7 implies that  $\varphi(z) = z$  for all  $z \geq 1$ . Thus, we have  $\varphi(z) - zF(z) = 0$  for all  $|z| \geq 1$ . If  $z \in [-1, 0]$ , then  $\varphi(z) - zF(z) \geq 0$  because  $\varphi$  and  $F$  are both nonnegative. Finally, if  $z \in [0, 1]$  then we first note that

$$\varphi(1) = \varphi(z) + \int_z^1 F(z') dz' \leq \varphi(z) + \int_z^1 F(1) dz' = \varphi(z) + F(1)(1 - z), \quad (3.9)$$

where the first and second equalities follow from the definition of  $\varphi$  and the monotonicity of  $F$ , respectively. Hence, we have for every  $z \in [0, 1]$  that

$$0 = \varphi(1) - F(1) \leq \varphi(z) + F(1)(1 - z) - F(1) = \varphi(z) - zF(1) \leq \varphi(z) - zF(z),$$

where the first and second inequalities follow from (3.9) and from the monotonicity of  $F$ , respectively.

Finally, the expected terminal state-of-charge is unbounded above in  $x^b$  because

$$\lim_{x^b \rightarrow \infty} y_0 + T \left( \eta^+ x^b - \eta_d x^r \varphi \left( -\frac{x^b}{x^r} \right) \right) = \lim_{x^b \rightarrow \infty} y_0 + T \eta^+ x^b = \infty,$$

where the first equality holds because  $\varphi(-\frac{x^b}{x^r}) = 0$  for all  $x^b \geq x^r$ . □

*Proof of Proposition 3.4.* The average expected charging rate  $\dot{y}$  is a positive affine transformation of the expected terminal state-of-charge. Proposition 3.3 thus immediately implies that  $\dot{y}$  is continuous, differentiable almost everywhere, and jointly concave in  $x^b$  and  $x^r$ . In addition,  $\dot{y}$  is strictly increasing and unbounded above in  $x^b$ , and nonincreasing in  $x^r$ . As  $\dot{y}$  is concave and strictly increasing in  $x^b$ , it is also unbounded below in  $x^b$ . Overall,  $\dot{y}$  is continuous and unbounded below and above in  $x^b$ , which means that the equation  $\dot{y}(x^b, x^r) = \dot{y}^*$  has at least one solution  $x_o^b$  for any given  $x^r \in \mathbb{R}_+$ . As  $\dot{y}$  is strictly increasing in  $x^b$ , this solution is also unique. The constraint  $\dot{y}(x^b, x^r) = \dot{y}^*$  defines therefore a unique implicit function  $g : \mathbb{R}_+ \rightarrow \mathbb{R}$  such that  $\dot{y}(g(x^r), x^r) = \dot{y}^*$  for all  $x^r \in \mathbb{R}_+$ .

As  $\dot{y}$  is nonincreasing in  $x^r$ , an increase in  $x^r$  either leaves  $\dot{y}$  unchanged or decreases  $\dot{y}$ . As  $\dot{y}$  is strictly increasing in  $x^b$ , the equality  $\dot{y}(x^b, x^r) = \dot{y}^*$  remains valid if and only if  $x_o^b$  stays unchanged in the first case and increases in the second case. The implicit function  $g$  is thus nondecreasing.

As  $\dot{y}$  is jointly concave in  $x^b$  and  $x^r$ , the superlevel set  $\mathcal{C} = \{(x^b, x^r) \in \mathbb{R} \times \mathbb{R}_+ : \dot{y}(x^b, x^r) \geq \dot{y}^*\}$  is convex. As  $\dot{y}$  is strictly increasing in  $x^b$ , a point  $(x^b, x^r)$  satisfies  $\dot{y}(x^b, x^r) \geq \dot{y}^*$  if and only if  $x^b \geq g(x^r)$ . The set  $\mathcal{C}$  thus coincides with the epigraph of  $g$ . The convexity of  $\mathcal{C}$  then implies that  $g$  is a convex function (Boyd and Vandenberghe, 2004, p. 75).

As  $\dot{y}$  is differentiable almost everywhere and continuous, so is  $g$ . By the implicit function theorem (Protter and Morrey, 1985, p. 395), the derivative of  $g$  is given by

$$g'(x^r) = -\frac{\frac{\partial \dot{y}(x^b, x^r)}{\partial x^r}}{\frac{\partial \dot{y}(x^b, x^r)}{\partial x^b}} = \eta_d \frac{\varphi(-\frac{x^b}{x^r}) + \frac{x^b}{x^r} F(-\frac{x^b}{x^r})}{\eta^+ + \eta_d F(-\frac{x^b}{x^r})}$$

wherever it exists. If  $g(0) \neq 0$ , then we have

$$\dot{y}(g(0), |g(0)|) = \eta^+ g(0) - \eta_d |g(0)| \varphi\left(-\frac{g(0)}{|g(0)|}\right) = \eta^+ g(0) - \eta_d [g(0)]^- = \dot{y}(g(0), 0),$$

where the first and third equalities follow from Proposition 3.3 and the second equality holds because  $\varphi(z) = 0$  for  $z \leq -1$  and  $\varphi(z) = z$  for  $z \geq 1$ .

As  $g$  is nondecreasing, it must be constant on the interval  $[0, |g(0)|]$ , which means that  $g'(x^r) = 0$  for all  $x^r$  in the interior of that interval.

The asymptotic slope  $m = \lim_{x^r \rightarrow \infty} g'(x^r)$  is equal to the asymptotic average slope  $\lim_{x^r \rightarrow \infty} \frac{g(x^r)}{x^r}$ , which can be found by analyzing the expression  $\lim_{x^r \rightarrow \infty} \frac{\dot{y}(g(x^r), x^r)}{x^r}$ . In fact,

$$\lim_{x^r \rightarrow \infty} \frac{\dot{y}(g(x^r), x^r)}{x^r} = \lim_{x^r \rightarrow \infty} \eta^+ \frac{g(x^r)}{x^r} - \eta_d \varphi\left(-\frac{g(x^r)}{x^r}\right) = \lim_{x^r \rightarrow \infty} \frac{\dot{y}^*}{x^r} = 0 \iff \lim_{x^r \rightarrow \infty} \frac{g(x^r)}{x^r} = m,$$

where  $m$  is the unique solution to the equation  $\eta^+ m - \eta_d \varphi(-m) = 0$ . As  $\eta_d = \frac{1}{\eta^-} - \eta^+$  and  $\varphi(-m) = \varphi(m) - m$  by Lemma 3.7, this equation is equivalent to  $m = (1 - \eta^+ \eta^-) \varphi(m)$ . It admits

## The Economics of Frequency Regulation through Electricity Storage: An Analytical Solution

---

a unique solution within the interval  $[0, 1]$ , because the function  $s(m) = m - (1 - \eta^+ \eta^-) \varphi(m)$  is nondecreasing in  $m$ , nonpositive for  $m = 0$ , and strictly positive for  $m = 1$ . Indeed,  $s$  is nondecreasing as its derivative  $1 - (1 - \eta^+ \eta^-) F(m)$  is nonnegative because  $F(m) \leq 1$  for all  $m \in \mathbb{R}$  and because  $\eta^+ \eta^- \in (0, 1]$ . The asymptotic slope of  $g$  is indeed equal to  $m$  because

$$\lim_{x^r \rightarrow \infty} g'(x^r) = \eta_d \frac{\varphi(-m) + mF(-m)}{\eta^+ + \eta_d F(-m)} = \eta_d \frac{\frac{\eta^+}{\eta_d} m + mF(-m)}{\eta^+ + \eta_d F(-m)} = m. \quad \square$$

*Proof of Lemma 3.2.* From the proof of Proposition 3.4 we know that the asymptotic slope  $m$  is the unique solution to the equation  $s(\mu) = 0$ , where  $s(\mu) = \mu - (1 - \eta^+ \eta^-) \varphi(\mu)$ . We have  $s(0) = -(1 - \eta^+ \eta^-) \varphi(0) \leq 0$  and  $s'(\mu) = 1 - (1 - \eta^+ \eta^-) F(\mu)$ . As  $F(\mu) \in [0, 1]$  for all  $\mu \in \mathbb{R}$  and as  $\eta^+ \eta^- \in (0, 1]$ ,  $s'$  is nonnegative and  $s$  is nondecreasing in  $\mu$ . An increase in  $\Delta = 2\varphi(0)$  can decrease (but not increase) the intercept  $s(0)$ , but it does not influence the slope  $s'$ . An increase in  $\eta^+ \eta^-$  can increase (but not decrease) the intercept  $s(0)$  and the slope  $s'$ . The zero-crossing of  $s$  is thus nondecreasing in  $\Delta$  and nonincreasing in  $\eta^+ \eta^-$ , and so is  $m$ .

As  $\varphi$  is a continuous convex function, it is closed. By Rockafellar's envelope representation theorem, any closed convex function is the pointwise supremum of all affine functions below it (Rockafellar, 1970, p. 102). For  $\varphi$ , specifically, we have  $\varphi(\mu) = 0$  for all  $\mu \leq -1$  and  $\varphi(\mu) = \mu$  for all  $\mu \geq 1$ . It thus suffices to consider all affine functions  $a\mu + b$  with  $a \geq 0$  and  $b \geq 0$  such that  $\varphi(\mu) \geq a\mu + b$ . The highest possible slope of any such function is the highest possible slope of  $\varphi$ , which is 1. Similarly, the highest possible intercept of any such function is the intercept of  $\varphi$ , which is  $\varphi(0)$ . Let  $\mathcal{A} = \{(a, b) \in [0, 1] \times [0, \varphi(0)] : \varphi(\mu) \geq a\mu + b \ \forall \mu \in \mathbb{R}\}$  be the set of all admissible coefficients for the affine functions. By the envelope representation theorem, we have  $\varphi(\mu) = \max_{(a,b) \in \mathcal{A}} a\mu + b$  for all  $\mu \in \mathbb{R}$ . Substituting this expression into the equation for the asymptotic slope yields

$$\mu = (1 - \eta^+ \eta^-) \left( \max_{(a,b) \in \mathcal{A}} a\mu + b \right) = \max_{(a,b) \in \mathcal{A}} (1 - \eta^+ \eta^-)(a\mu + b),$$

where the second equality holds because  $1 - \eta^+ \eta^- \geq 0$ . The asymptotic slope  $m$  is the solution to

$$\min_m m \text{ s.t. } m \geq (1 - \eta^+ \eta^-)(am + b) \ \forall (a, b) \in \mathcal{A}.$$

The constraint holds for all  $(a, b) \in \mathcal{A}$  if and only if

$$m \geq (1 - \eta^+ \eta^-)(am + b) \iff (1 - a(1 - \eta^+ \eta^-))m \geq (1 - \eta^+ \eta^-)b \iff m \geq \frac{1 - \eta^+ \eta^-}{1 - a(1 - \eta^+ \eta^-)} b,$$

where the first equivalence is valid because  $1 - a(1 - \eta^+ \eta^-) > 0$  as  $a \leq 1$  and  $\eta^+ \eta^- \in (0, 1]$ . Hence,

$$m = \max_{(a,b) \in \mathcal{A}} \zeta(a, b, \eta^+ \eta^-), \text{ where } \zeta(a, b, \eta^+ \eta^-) = \frac{1 - \eta^+ \eta^-}{1 - a(1 - \eta^+ \eta^-)} b.$$

If  $\varsigma$  is convex in  $\eta^+ \eta^-$  for all  $(a, b) \in \mathcal{A}$ , then  $m$  is also convex in  $\eta^+ \eta^-$  since the pointwise maximum of convex functions is a convex function (Boyd and Vandenberghe, 2004, p. 80). Note that  $\varsigma$  is twice differentiable in  $\eta^+ \eta^-$ . In fact,

$$\frac{\partial}{\partial \eta^+ \eta^-} \varsigma(a, b, \eta^+ \eta^-) = -\frac{b}{(1 - a(1 - \eta^+ \eta^-))^2} \quad \text{and} \quad \frac{\partial^2}{(\partial \eta^+ \eta^-)^2} \varsigma(a, b, \eta^+ \eta^-) = \frac{2ab}{(1 - a(1 - \eta^+ \eta^-))^3}.$$

As  $a \geq 0$  and  $b \geq 0$  for all  $(a, b) \in \mathcal{A}$ , the first and second derivatives are always nonpositive and nonnegative, respectively. The asymptotic slope  $m$  is thus convex and nonincreasing in  $\eta^+ \eta^-$ .  $\square$

*Proof of Lemma 3.3.* If  $\dot{y}^* = 0$ , we have for all  $x^r > 0$

$$\dot{y}(g(x^r), x^r) = 0 \iff \frac{\dot{y}(g(x^r), x^r)}{x^r} = \eta^+ \frac{g(x^r)}{x^r} - \eta_d \varphi\left(-\frac{g(x^r)}{x^r}\right) = 0 \iff g(x^r) = m x^r,$$

where the second equivalence holds because  $m$  is the unique solution to  $\eta^+ m - \eta_d \varphi(-m) = 0$ , which is equivalent to  $m = (1 - \eta^+ \eta^-) \varphi(m)$ , by Proposition 3.4. For  $x^r = 0$ , we trivially have  $g(x^r) = m x^r$ . The function  $g$  is thus linear with slope  $m$ .  $\square$

*Proof of Theorem 3.1.* The robust constraints are replaced by their deterministic counterparts in Proposition 3.2. The constraint on the expected terminal state-of-charge is modeled implicitly by expressing the decision variable  $x^b$  as the function  $g$ , characterized in Proposition 3.4, of  $x^r$ .  $\square$

*Proof of Lemma 3.4.* The feasible set  $\mathcal{X}$  is convex if the function  $s(x^r) = g(x^r) - \ell(x^r)$  is monotonic. In the following, we show that Assumption 3.2 implies that  $s$  is strictly decreasing. The slope of  $s$  is maximal when the slope of  $g$  is maximal and the slope of  $\ell$  is minimal. The maximal slope of  $g$  is  $m$ , while the minimal slope of  $\ell$  is  $\frac{\gamma}{T}$ . The function  $s$  is strictly decreasing if its maximal slope is strictly negative, which is the case if  $m < \frac{\gamma}{T}$ . As  $\varphi(m) = \varphi(-m) + m$  by Lemma 3.7, we have indeed

$$m = (1 - \eta^+ \eta^-) \varphi(m) = \left(\frac{1}{\eta^+ \eta^-} - 1\right) \varphi(-m) \leq \left(\frac{1}{\eta^+ \eta^-} - 1\right) \varphi(0) < \frac{1}{2} \left(\frac{1}{\eta^+ \eta^-} - 1\right) \frac{\gamma}{T} \leq \frac{\gamma}{T}.$$

The first inequality holds as  $\varphi$  is nondecreasing and  $m \geq 0$ . The strict inequality holds because  $\varphi(0) < \frac{\gamma}{2T}$  by Assumption 3.2. The second inequality holds because  $\eta^+ \eta^- \geq \frac{1}{3}$ , also by Assumption 3.2.  $\square$

*Proof of Theorem 3.2.* Problem (P) consists of minimizing the convex cost function  $T(c^b g(x^r) - c^r x^r)$  over the interval  $\mathcal{X} = [0, \bar{x}^r]$ . Proposition 3.4 implies that the marginal profit  $T(c^r - c^b g'(x^r))$  exists almost everywhere and is nonincreasing, since  $g$  is convex, and that  $g'(0)$  exists.

## The Economics of Frequency Regulation through Electricity Storage: An Analytical Solution

---

Problem (P) is feasible because it is equivalent to problem (R), which we assumed to be feasible for consistency. Hence,  $\bar{x}^r \geq 0$ . If  $\bar{x}^r = 0$ , the only feasible, and therefore optimal solution, is  $x_*^r = 0$ .

If  $g'(0) \geq \frac{c^r}{c^b}$ , the marginal profit is nonpositive for all feasible values of  $x^r$  and  $x_*^r = 0$  is the smallest optimal solution. Conversely, if  $\min \partial g(\bar{x}^r) < \frac{c^r}{c^b}$ , then the marginal profit is strictly positive for all feasible values of  $x^r$  and  $x_*^r = \bar{x}^r$  is the only optimal solution.

If  $g'(0) < \frac{c^r}{c^b}$  and  $\min \partial g(x^r) \geq \frac{c^r}{c^b}$ , then the marginal profit may admit roots on  $\mathcal{X}$ , any of which would be an optimal solution. We now show that the set  $\mathcal{X}_\star$  of roots, or stationary points, is nonempty and closed, which implies that  $\min \mathcal{X}_\star$  exists. In this case,  $x_*^r = \min \mathcal{X}_\star$  is the smallest optimal solution.

Let  $g'_+$  and  $g'_-$  denote the right and left derivative functions of  $g$ . We have  $g'_+(0) < \frac{c^r}{c^b}$  and  $g'_-(\bar{x}^r) \geq \frac{c^r}{c^b}$  since  $g'(0) < \frac{c^r}{c^b}$  and  $\min \partial g(x^r) \geq \frac{c^r}{c^b}$ . Theorem 24.3 by Rockafellar (1970) implies that the graph of the subdifferential mapping  $\partial g$  on  $\mathcal{X}$  is the complete nondecreasing curve segment

$$\Gamma = \left\{ (x^r, x^{b'}) \in \mathcal{X} \times \mathbb{R} : g'_-(x^r) \leq x^{b'} \leq g'_+(x^r) \right\}.$$

The subsegment  $\Gamma_\star = \{(x^r, x^{b'}) \in \Gamma : x^{b'} = \frac{c^r}{c^b}\}$  is nonempty since  $g'_+(0) < \frac{c^r}{c^b}$  and  $g'_-(\bar{x}^r) \geq \frac{c^r}{c^b}$ , closed, and bounded as a consequence of Theorem 23.4 by Rockafellar (1970). The set  $\mathcal{X}_\star$  is the projection of  $\Gamma_\star$  onto the  $x^r$ -axis and therefore also nonempty, closed, and bounded.  $\square$

*Proof of Lemma 3.5.* By Proposition 3.4, the asymptotic sensitivities  $\underline{m}$ ,  $m$ , and  $\bar{m}$  are the unique roots of the functions  $s_{\underline{\varphi}}$ ,  $s_\varphi$ , and  $s_{\bar{\varphi}}$ , respectively, where  $s_\varphi$  is defined as

$$s_\varphi(\mu) = (1 - \eta^+ \eta^-) \varphi(\mu) - \mu$$

and the functions  $s_{\underline{\varphi}}$  and  $s_{\bar{\varphi}}$  are defined similarly. Equation (3.5) implies that  $s_{\underline{\varphi}}(\mu) \leq s_\varphi(\mu) \leq s_{\bar{\varphi}}(\mu)$  for all  $\mu \in \mathbb{R}$  as  $1 - \eta^+ \eta^- \geq 0$ . In addition, the functions  $s_{\underline{\varphi}}$ ,  $s_\varphi$ , and  $s_{\bar{\varphi}}$  are nonincreasing because neither  $\underline{\varphi}$ , nor  $\varphi$ , nor  $\bar{\varphi}$  admit a subgradient that is strictly greater than 1. In fact,  $\underline{\varphi}$ ,  $\varphi$ , and  $\bar{\varphi}$  are convex since they are super-cumulative distribution functions of  $\tilde{\xi}$  and thus achieve their greatest subgradients when  $\mu$  tends to infinity. As  $\tilde{\xi}$  is supported on  $[-1, 1]$ , we have  $\underline{\varphi}(\mu) = \varphi(\mu) = \bar{\varphi}(\mu) = \mu$  for all  $\mu \geq 1$ . Hence, the greatest subgradients are equal to 1.

We have  $0 = s_{\underline{\varphi}}(\underline{m}) \leq s_\varphi(\underline{m})$ . As  $m$  is the unique root of the nonincreasing function  $s_\varphi$ , this implies that  $m \geq \underline{m}$ . A similar reasoning leads us to conclude that  $m \leq \bar{m}$ .  $\square$

*Proof of Lemma 3.6.* For any  $x^r \geq 0$ , the constraint  $\dot{y}(x^b, x^r) = \dot{y}^\star$  implies that  $\underline{g}(x^r)$ ,  $g(x^r)$ , and  $\bar{g}(x^r)$  are the unique roots of the functions  $s_{\underline{\varphi}}$ ,  $s_\varphi$ , and  $s_{\bar{\varphi}}$ , respectively, where  $s_\varphi$  is defined

as

$$s_\varphi(x^b) = \dot{y}^\star + \eta_d \varphi\left(-\frac{x^b}{x^r}\right) x^r - \eta^+ x^b$$

and the functions  $s_\varphi$  and  $s_{\bar{\varphi}}$  are defined similarly. Equation (3.5) implies that  $s_{\varphi}(\mu) \leq s_\varphi(\mu) \leq s_{\bar{\varphi}}(\mu)$  for all  $x^b \in \mathbb{R}$  since  $\eta_d x^r \geq 0$ . In addition, Proposition 3.3 implies that  $s_{\varphi}$ ,  $s_\varphi$ , and  $s_{\bar{\varphi}}$  are all strictly decreasing. The claim follows from the same arguments as at the end of the proof of Lemma 3.5.  $\square$

*Proof of Proposition 3.5.* If  $y_0 = y^\star$ , then  $\dot{y}^\star = \frac{y^\star - y_0}{T} = 0$  and so  $g(x^r) = mx^r$  by Lemma 3.3. Hence, the constraints in Problem (P) obey the following equivalences.

$$\begin{aligned} x^r + g(x^r) &\leq \bar{y}^+ &\iff x^r &\leq \frac{\bar{y}^+}{1+m} \\ x^r - g(x^r) &\leq \bar{y}^- &\iff x^r &\leq \frac{\bar{y}^-}{1-m} \\ x^r + \max\left\{\frac{T}{\gamma}g(x^r), g(x^r)\right\} &\leq \frac{\bar{y} - y_0}{\eta^+ \gamma} &\iff x^r &\leq \frac{\bar{y} - y_0}{\eta^+ (\gamma + mT)} \\ x^r - \min\left\{\frac{T}{\gamma}g(x^r), g(x^r)\right\} &\leq \frac{\eta^- y_0}{\gamma} &\iff x^r &\leq \frac{\eta^- y_0}{\gamma(1-m)} \end{aligned}$$

The last two equivalences hold because  $\frac{T}{\gamma} \geq 1$  and  $g(x^r) = mx^r \geq 0$  since any feasible  $x^r$  must be nonnegative and since  $m$  is nonnegative by Proposition 3.4.  $\square$

*Proof of Theorem 3.3.* If  $y_0 = y^\star$ , then  $\dot{y}^\star = \frac{y^\star - y_0}{T} = 0$  and so  $g(x^r) = mx^r$  by Lemma 3.3. Hence,  $g'(0) = \min \partial g(\bar{x}^r) = m$ . Theorem 3.2 implies that  $x_\star^r = 0$  if  $m \geq \frac{c^r}{c^b}$  and  $= \bar{x}^r$  otherwise.  $\square$



## Conclusions and Perspectives

In this thesis, we model the decision-making problem of electric vehicle aggregators that participate in primary frequency regulation markets subject to EU regulations. Three overarching themes emerge from this work.

First, time must be considered carefully when modeling the state-of-charge of electricity storage devices. In general, modeling the state-of-charge in discrete rather than continuous time underestimates the maximum state-of-charge and overestimates the minimum and average state-of-charge (see Example 2.1).

Second, electricity systems are physical systems and must obey the laws of thermodynamics. The first law states that energy can neither be created nor destroyed, it can only be transformed. The second law implies that energy is lost in every transformation. For storage devices, charging and discharging losses lead to nonzero marginal costs of providing frequency regulation, even if the average frequency deviation is zero.

Third, electricity systems are also political and cultural systems and thus subject to government regulations, which will be respected if the penalties for noncompliance are sufficiently high. For frequency regulation, European Union regulations specify an energy reserve that storage devices must maintain to provide a given amount of regulation power. It is natural to model such regulations through robust, as opposed to probabilistic, constraints so that compliance can be audited. Maintaining the energy reserve means that, when providing frequency regulation, electric vehicles are often constrained not by how fast they can charge and discharge but by how much energy they can store. We show that the prevailing penalties for noncompliance are too low to incentivize aggregators to maintain the energy reserve.

These three aspects may seem to complicate our decision-making problem, but, when considered together, the robust constraints pertaining to the energy reserve have a special structure that allows for a simple mathematical solution. Surprisingly, the deterministic counterpart of our decision-making problem does not have such a structure and is much harder to solve. We believe that we have discovered the first practically relevant class of optimization problems that become dramatically easier through robustification. Thanks to its simplicity, our solution can potentially be integrated into more general models, which may account for the aggregation of many electric vehicles or for the provision of multiple grid services.



## Conclusions and Perspectives

---

Without taking the three themes into account, decision makers may experience a false sense of security and run the risk of taking decisions that are infeasible in practice. For frequency regulation, this could lead to blackouts.

In practice, aggregators can use our solution to compute the amount of regulation power that each vehicle can provide by solving multiple independent linear programs. This can be done efficiently by parallel computing even for large fleets with thousands of vehicles. In a second step, aggregators may want to take advantage of economies of scale. As opposed to individual vehicle owners, aggregators can decide which cars to use to provide a given amount of regulation power. This has several advantages. First, battery degradation can be reduced by managing the state-of-charge of vehicles more precisely. Second, charging and discharging losses can be reduced by running vehicle chargers at their nominal operating points. Third, aggregators can trade electricity on intra-day markets, which allows them to balance the state-of-charge in the event of extreme frequency deviations, and hence to offer more regulation power for a given battery capacity. Fourth, the availability of individual vehicles can be estimated less conservatively because the vehicles will be somewhat independent. Extreme deviations from the expected number of parked vehicles, for example, become less likely as aggregators pool more vehicles. Finally, the fixed costs of creating and operating an aggregation platform can be spread over more vehicles. On the downside, aggregators incur transaction costs to convince vehicle owners to sign up with them. Even though the prices for frequency regulation have doubled from the year 2019 to the year 2021, due partly to higher gas prices and a wide-spread outage of French nuclear power plants, it is unclear whether frequency regulation through vehicle-to-grid will be profitable enough to outweigh these costs.

Governments could reduce the costs of vehicle-to-grid by mandating that all new electric vehicles be equipped with vehicle-to-grid technology. Such a mandate may encourage vehicle owners to participate in vehicle-to-grid, which would lower the need to import batteries for stationary electricity storage. Compared to other storage technologies, vehicle-to-grid may enjoy greater public acceptance because it is invisible to the general public. In contrast, the dams and lakes of pumped-hydro storage are quite visible and may irritate local populations, especially if they have to resettle, as well as environmental organizations. Stationary battery storage, too, requires space and may, in addition, pose fire hazards.

Finally, vehicle-to-grid will only be successful if there is a sufficient amount of underused electric vehicles. The global electric vehicle fleet has increased rapidly in the last decade and, given global efforts in mitigating climate change and air pollution, it seems reasonable to expect that the fleet will continue to expand in the coming decades. It is less clear how the utilization of electric vehicles will evolve. On the one hand, the number of vehicles per capita has increased by about 10% in the US and by about 5% in Western Europe over the last decade, which points to a decreasing utilization. On the other hand, the deployment of car-sharing, ride-sharing, and ride-hailing services, possibly facilitated by self-driving cars, points to an increasing utilization, which may hamper the potential of vehicle-to-grid.

# Bibliography

- E. J. Anderson, P. Nash, and A. F. Perold. Some properties of a class of continuous linear programs. *SIAM Journal on Control and Optimization*, 21(5):758–765, 1983.
- C. Andrey, P. Barberi, L. Lacombe, L. van Nuffel, F. Gérard, J. Gorenstein Dedecca, K. Rademaekers, Y. El Idrissi, and M. Crenes. *Study on Energy Storage – Contribution to the Security of the Electricity Supply in Europe*. Publications Office of the European Union, 2020.
- M. Anvari, L. R. Gorjão, M. Timme, D. Witthaut, B. Schäfer, and H. Kantz. Stochastic properties of the frequency dynamics in real and synthetic power grids. *Physical Review Research*, 2(1):013339, 2020.
- E. Apostolaki-Iosifidou, P. Codani, and W. Kempton. Measurement of power loss during electric vehicle charging and discharging. *Energy*, 127:730–742, 2017.
- S. Awerbuch and A. Preston, editors. *The Virtual Utility: Accounting, Technology & Competitive Aspects of the Emerging Industry*. Kluwer Academic Publishers, 1997.
- G. A. Bakke. *The Grid: The Fraying Wires between Americans and our Energy Future*. Bloomsbury, 2016.
- S. Beer, T. Gómez, D. Dallinger, I. Momber, C. Marnay, M. Stadler, and J. Lai. An economic analysis of used electric vehicle batteries integrated into commercial building microgrids. *IEEE Transactions on Smart Grid*, 3(1):517–525, 2012.
- A. Ben-Tal, A. Goryashko, E. Guslitzer, and A. Nemirovski. Adjustable robust solutions of uncertain linear programs. *Mathematical Programming*, Ser. A 99(2):351–376, 2004.
- A. Ben-Tal, L. El Ghaoui, and A. Nemirovski. *Robust Optimization*. Princeton University Press, 2009.
- D. Bertsimas and M. Sim. The price of robustness. *Operations Research*, 52(1):35–53, 2004.
- D. Bertsimas and J. N. Tsitsiklis. *Introduction to Linear Optimization*. Athena Scientific & Dynamic Ideas, 1997.
- O. Borne. *Vehicle-to-Grid and Flexibility for Electricity Systems: From Technical Solutions to Design of Business Models*. PhD thesis, Université Paris-Saclay, 2019.

## Bibliography

---

- O. Borne, Y. Perez, and M. Petit. Market integration or bids granularity to enhance flexibility provision by batteries of electric vehicles. *Energy Policy*, 119:140–148, 2018.
- S. P. Boyd and L. Vandenberghe. *Convex Optimization*. Cambridge University Press, 2004.
- G. Broneske and D. Wozabal. How do contract parameters influence the economics of vehicle-to-grid? *Manufacturing & Service Operations Management*, 19(1):150–164, 2017.
- A. Brooks. Vehicle-to-grid project: Grid regulation ancillary service with a battery electric vehicle. Technical report, AC Propulsion Inc., 2002.
- Bundesnetzagentur and Bundeskartellamt. Monitoringbericht 2021, 2021.
- P. Carpentier, J.-P. Chancelier, M. de Lara, and T. Rigaut. Algorithms for two-time scales stochastic optimization with applications to long term management of energy storage. Preprint available from <http://hal.archives-ouvertes.fr/hal-02013963>, 2019.
- P. Codani, M. Petit, and Y. Perez. Participation of an electric vehicle fleet to primary frequency control in France. *International Journal of Electric and Hybrid Vehicles*, 7(3):233–249, 2015.
- S. Comello and S. Reichelstein. The emergence of cost effective battery storage. *Nature Communications*, 10(2038), 2019.
- Commissariat général au développement durable. La mobilité des Français. *La Revue du CGDD*, 2010.
- J. Donadee and M. D. Ilić. Stochastic optimization of grid to vehicle frequency regulation capacity bids. *IEEE Transactions on Smart Grid*, 5(2), 2014.
- M. Dubarry, A. Devie, and K. McKenzie. Durability and reliability of electric vehicle batteries under electric utility grid operations: Bidirectional charging impact analysis. *Journal of Power Sources*, 358:39–49, 2017.
- European Central Bank. An overview of the ECB’s monetary policy strategy. Technical report, 2021.
- European Commission. Commission Regulation (EU) 2017/1485 of 2 August 2017 establishing a guideline on electricity transmission system operation. *Official Journal of the European Union*, 60, 2017.
- European Commission. A Clean Planet for all, 2018. In-depth analysis in support of the Commission Communication COM(2018) 773.
- European Commission. Stepping up Europe’s 2030 climate ambition, 2020. Communication from the Commission to the European Parliament, the Council, the European Economic and Social Committee and the Committee of the Regions.
- European Network of Transmission System Operators for Gas and Electricity. TYNDP 2022 Draft scenario report. Technical report, 2021.

- Eurostat. Passenger cars, by type of motor energy, 2021. Retrieved 3 December 2021 from <http://ec.europa.eu/eurostat/web/transport/data/database>.
- Everoze and EVConsult. V2G global roadtrip: Around the world in 50 projects, 2018. Retrieved 4 December 2021 from [http://go.epfl.ch/v2g\\_global\\_roadtrip](http://go.epfl.ch/v2g_global_roadtrip).
- Federal Energy Regulatory Commission. Reform of generator interconnection procedures and agreements. *Federal Register*, 83(90):21342–21414, 2018.
- Federal Highway Administration. 2017 National Household Travel Survey. Technical report, United States Department of Transportation, 2017. URL <http://nhts.ornl.gov>.
- A. Georghiou, A. Tsoukalas, and W. Wiesemann. Robust dual dynamic programming. *Operations Research*, 67(3):813–830, 2019.
- J. Geske and D. Schumann. Willing to participate in vehicle-to-grid (V2G)? Why not! *Energy Policy*, 120:392–401, 2018.
- Gestionnaire du Réseau de Transport d’Electricité. Documentation Technique de Référence, Chapitre 4—Contribution des utilisateurs aux performances du RPT, Article 4.1—Réglage Fréquence/Puissance. Technical report, 2009.
- A. Ghathe. Robust continuous linear programs. *Optimization Letters*, 14:1627–1642, 2020.
- J. D. Glover, M. S. Sarma, and T. J. Overbye. *Power Systems Analysis and Design*. Cengage Learning, 2010.
- R. Gough, C. Dickerson, P. Rowley, and C. Walsh. Vehicle-to-grid feasibility: A techno-economic analysis of EV-based energy storage. *Applied Energy*, 192:12–23, 2017.
- C. Guille. A conceptual framework for the vehicle-to-grid (V2G) implementation. Master’s thesis, University of Illinois at Urbana-Champaign, 2009.
- C. Guille and G. Gross. A conceptual framework for the *vehicle-to-grid* (V2G) implementation. *Energy Policy*, 37:4379–4390, 2009.
- S. Habib, M. Kamran, and U. Rashid. Impact analysis of vehicle-to-grid technology and charging strategies of electric vehicles on distribution networks—A review. *Journal of Power Sources*, 277:205–214, 2015.
- V. Halleux. New EU regulatory framework for batteries, 2021. European Parliamentary Research Service Briefing.
- S. Han, S. Han, and K. Sezaki. Development of an optimal vehicle-to-grid aggregator for frequency regulation. *IEEE Transactions on Smart Grid*, 1(1):65–72, 2010.
- S. Han, S. Han, and K. Sezaki. Estimation of achievable power capacity from plug-in electric vehicles for V2G frequency regulation: Case studies for market participation. *IEEE Transactions on Smart Grid*, 2(4):632–641, 2011.

## Bibliography

---

- G. He, Q. Chen, C. Kang, P. Pinson, and Q. Xia. Optimal bidding strategy of battery storage in power markets considering performance-based regulation and battery cycle life. *IEEE Transactions on Smart Grid*, 7(5):2359–2367, 2016.
- B. Houska. *Robust Optimization of Dynamic Systems*. PhD thesis, KU Leuven, 2011.
- International Energy Agency. Global EV Outlook 2021. Technical report, 2021.
- W. Kempton and S. E. Letendre. Electric vehicles as a new power source for electric utilities. *Transportation Research Part D: Transport and Environment*, 2(3):157–175, 1997.
- W. Kempton and J. Tomić. Vehicle-to-grid power fundamentals: Calculating capacity and net revenue. *Journal of Power Sources*, 144(1):268–279, 2005a.
- W. Kempton and J. Tomić. Vehicle-to-grid power implementation: From stabilizing the grid to supporting large-scale renewable energy. *Journal of Power Sources*, 144(1):280–294, 2005b.
- D. Lauinger, F. Vuille, and D. Kuhn. A review of the state of research on vehicle-to-grid (V2G): Progress and barriers to deployment. In *European Battery, Hybrid and Fuel Cell Electric Vehicle Congress*, Geneva, 2017.
- D. Lauinger, F. Vuille, and D. Kuhn. Reliable frequency regulation through vehicle-to-grid: Encoding legislation with robust constraints, 2022. arXiv:2005.06042v3[math.OC].
- T. Lehtola and A. Zahedi. Electric vehicle to grid for power regulation: A review. In *IEEE International Conference on Power System Technology*, 2016.
- N. Löhdorf, D. Wozabal, and S. Minner. Optimizing trading decisions for hydro storage systems using approximate dual dynamic programming. *Operations Research*, 61(4):810–823, 2013.
- A. Malhotra, B. Battke, M. Beuse, A. Stephan, and T. Schmidt. Use cases for stationary battery technologies: A review of the literature and existing projects. *Renewable and Sustainable Energy Reviews*, 56:705–721, 2016.
- C. Marnay, T. Chan, N. DeForest, J. Lai, J. MacDonald, M. Stadler, T. Erdmann, A. Hoheisel, M. Müller, S. Scott, E. Koch, P. Lipkin, R. W. Anderson, S. Gerber, and E. Reid. Los Angeles Air Force base vehicle to grid project. In *ECREEE 2013 Summer Study on Energy Efficiency*, 2013.
- D. Q. Mayne, J. B. Rawlings, C. V. Rao, and P. O. M. Scokaert. Constrained model predictive control: Stability and optimality. *Automatica*, 36:789–814, 2000.
- P. Mercier, R. Cherkaoui, and A. Oudalov. Optimizing a battery energy storage system for frequency control application in an isolated power system. *IEEE Transactions on Power Systems*, 24(3):1469–1477, 2009.
- F. Mwasliu, J. J. Justo, E.-K. Kim, T. D. Do, and J.-W. Jung. Electric vehicles and smart grid interaction: A review on vehicle to grid and renewable energy sources integration. *Renewable and Sustainable Energy Reviews*, 34:501–516, 2014.

- S. Nadarajah, F. Margot, and N. Secomandi. Relaxations of approximate linear programs for the real option management of commodity storage. *Management Science*, 61(12):3054–3076, 2015.
- E. Namor, F. Sossan, R. Cherkaoui, and M. Paolone. Control of battery storage systems for the simultaneous provision of multiple services. *IEEE Transactions on Smart Grid*, 10(3):2799–2808, 2019.
- G. L. Nemhauser and L. A. Wolsey. *Integer and Combinatorial Optimization Part III*. John Wiley & Sons, 1999.
- L. Noel, G. Z. de Rubens, J. Kester, and B. K. Sovacool. *Vehicle-to-Grid: A Sociotechnical Transition Beyond Electric Mobility*. Palgrave Macmillan, 2019.
- A. Nursimulu. Demand-side flexibility for energy transitions: Policy recommendations for developing demand response. 2016. Policy Brief. EPFL Energy Center.
- C. Ozansoy, T. S. Ustun, and A. Zayegh. Experiences and Applications of Electric and Plug-In Hybrid Vehicles in Power System Networks. In O. Veneri, editor, *Technologies and Applications for Smart Charging of Electric and Plug-In Hybrid Vehicles*, chapter 7, pages 243–280. Springer, 2017.
- P. Palensky and D. Dietrich. Demand side management: Demand response, intelligent energy systems, and smart loads. *IEEE Transactions on Industrial Informatics*, 7(3), 2011.
- G. R. Parsons, M. K. Hidrue, W. Kempton, and M. P. Gardner. Willingness to pay for vehicle-to-grid (V2G) electric vehicles and their contract terms. *Energy Economics*, 42:313–324, 2014.
- M. V. F. Pereira and L. M. V. G. Pinto. Multi-stage stochastic optimization applied to energy planning. *Mathematical Programming*, 52(2):359–375, 1991.
- S. B. Peterson, J. Whitacre, and J. Apt. The economics of using plug-in hybrid electric vehicle battery packs for grid storage. *Journal of Power Sources*, 195:2377–2384, 2010.
- G. Pritchard, A. Philpott, and P. Neame. Hydroelectric reservoir optimization in a pool market. *Mathematical Programming*, Ser. A 103(3):445–461, 2005.
- M. H. Protter and C. B. Morrey, Jr. *Intermediate Calculus*. Springer, 2nd edition, 1985.
- D. Pudjianto, C. Ramsay, and G. Strbac. Virtual power plant and system integration of distributed energy resources. *IET Renewable Power Generation*, 1(1):10–16, 2007.
- M. C. Pullan. Forms of optimal solutions for separated continuous linear programs. *SIAM Journal on Control and Optimization*, 33(6):1952–1977, 1995.
- Y. G. Rebours, D. S. Kirschen, M. Trotignon, and S. Rossignol. A survey of frequency and voltage control ancillary services—Part I: Technical features. *IEEE Transactions on Power Systems*, 22(1):350–357, 2007.

## Bibliography

---

- Réseau de transport d'électricité. Règles Service Système Fréquence. Technical report, 2017a.
- Réseau de transport d'électricité. Bilan prévisionnel de l'équilibre offre-demande d'électricité en France. Technical report, 2017b.
- Réseau de transport d'électricité. Electricity Report 2017. Technical report, 2017c.
- R. T. Rockafellar. *Convex Analysis*. Princeton University Press, 1970.
- E. Roos, D. den Hertog, A. Ben-Tal, F. de Ruiter, and J. Zhen. Tractable approximation of hard uncertain convex optimization problems. *Available from Optimization Online*, 2020.
- N. Secomandi. Optimal commodity trading with a capacitated storage asset. *Management Science*, 56(3):449–467, 2010.
- E. Sortomme and M. A. El-Sharkawi. Optimal scheduling of vehicle-to-grid energy and ancillary services. *IEEE Transactions on Smart Grid*, 3(1):351–359, 2012.
- B. K. Sovacool, L. Noel, J. Axsen, and W. Kempton. The neglected social dimensions to a vehicle-to-grid (V2G) transition: A critical and systematic review. *Environmental Research Letters*, 13:013001, 2018.
- D. Sperling. *Future Drive: Electric Vehicles and Sustainable Transportation*. Island Press, Washington, D.C. & Covelo, California, 1994.
- Statistics Norway. Table 11823: Registered vehicles, by euro classes and type of fuel (M) 2016–2020, 2021. Retrieved 2 December 2021 from <http://www.ssb.no/en/statbank/table/11823/>.
- N. Sunar and J. R. Birge. Strategic commitment to a production schedule with uncertain supply and demand: Renewable energy in day-ahead electricity markets. *Management Science*, 65(2):714–734, 2019.
- T. M. Sweda, I. S. Dolinskaya, and D. Klabjan. Optimal recharging policies for electric vehicles. *Transportation Science*, 51(2):457–479, 2017.
- J. A. Taylor. *Convex Optimization of Power Systems*. Cambridge University Press, 2015.
- A. Thompson. Economic implications of lithium ion battery degradation for vehicle-to-grid (V2X) services. *Journal of Power Sources*, 396:691–709, 2018.
- R. Thorne, F. A. Lopez, E. Figenbaum, L. Fridstrøm, and D. B. Müller. Estimating stocks and flows of electric passenger vehicle batteries in the Norwegian fleet from 2011 to 2030. *Journal of Industrial Ecology*, 25(6):1529–1542, 2021.
- K. Uddin, T. Jackson, W. D. Widanage, G. Chouchelamane, P. A. Jennings, and J. Marco. On the possibility of extending the lifetime of lithium-ion batteries through optimal V2G facilitated by an integrated vehicle and smart-grid system. *Energy*, 133:710–722, 2017.

- K. Uddin, M. Dubarry, and M. B. Glick. The viability of vehicle-to-grid operations from a battery technology and policy perspective. *Energy Policy*, 113:342–347, 2018.
- United States Department of Energy. Benefits of demand response in electricity markets and recommendations for achieving them. Technical report, 2006.
- United States Senate. Examining Enron: Developments Regarding Electricity Price Manipulation in California: US Senate Committee on Commerce, Science, and Transportation, 2002. Testimony of S. David Freeman.
- S. Vandael, T. Holvoet, G. Deconinck, S. Kamboj, and W. Kempton. A comparison of two GIV mechanisms for providing ancillary services at the University of Delaware. In *IEEE SmartGridComm 2013 Symposium–Demand Side Management, Demand Response, Dynamic Pricing*, 2013.
- S. Vandael, T. Holvoet, G. Deconinck, H. Nakano, and W. Kempton. A scalable control approach for providing regulation services with grid-integrated electric vehicles. In T. Suzuki, S. Inagaki, Y. Susuki, and A. T. Tran, editors, *Design and Analysis of Distributed Energy Management Systems*, chapter 6, pages 107–128. Springer, 2020.
- M. Victoria, K. Zhu, T. Brown, G. B. Andresen, and M. Greiner. The role of storage technologies throughout the decarbonisation of the sector-coupled European energy system. *Energy Conversion and Management*, 201(111977), 2019.
- D. Wang, J. Coignard, T. Zeng, C. Zhang, and S. Saxena. Quantifying electric vehicle battery degradation from driving vs. vehicle-to-grid services. *Journal of Power Sources*, 332:193–203, 2016.
- J. Warrington, P. Goulart, S. Mariethoz, and M. Morari. Policy-based reserves for power systems. *IEEE Transactions on Power Systems*, 20(4):4427–4437, 2013.
- G. Wenzel, M. Negrete-Pincetic, D. E. Olivares, J. MacDonald, and D. S. Callaway. Real-time charging strategies for an electric vehicle aggregator to provide ancillary services. *IEEE Transactions on Smart Grid*, 9(5):5141–5151, 2018.
- World Energy Council. Five steps to energy storage. Technical report, 2020.
- F. Wu and R. Sioshansi. A stochastic operational model for controlling electric vehicle charging to provide frequency regulation. *Transportation Research Part D*, 67:475–490, 2019.
- E. Yao, V. W. S. Wong, and R. Schober. Robust frequency regulation capacity scheduling algorithm for electric vehicles. *IEEE Transactions on Smart Grid*, 8(2):984–997, 2017.
- W. W.-G. Yeh. Reservoir management and operations models: A state-of-the-art review. *Water Resources Research*, 21(12):1797–1818, 1985.



## Bibliography

---

- M. Yilmaz and P. T. Krein. Review of the impact of vehicle-to-grid technologies on distribution systems and utility interfaces. *IEEE Transactions on Power Electronics*, 28(12):5673–5689, 2013.
- X. Zhang, M. Kamgarpour, A. Georghiou, P. Goulart, and J. Lygeros. Robust optimal control with adjustable uncertainty sets. *Automatica*, 75:249–259, 2017.
- Y. Zhang, M. Lu, and S. Shen. On the values of vehicle-to-grid electricity selling in electric vehicle sharing. *Manufacturing & Service Operations Management*, 23(2):488–507, 2021.
- Y. H. Zhou, A. Scheller-Wolf, N. Secomandi, and S. Smith. Electricity trading and negative prices: Storage vs. disposal. *Management Science*, 62(3):880–898, 2016.
- M. S. Ziegler and J. E. Trancik. Re-examining rates of lithium-ion battery technology improvement and cost decline. *Energy & Environmental Science*, 14(4):1635–1651, 2021.
- S. Zymler, B. Rustem, and D. Kuhn. Robust portfolio optimization with derivative insurance guarantees. *European Journal of Operational Research*, 210(2):410–424, 2011.

**Dirk Lauinger** investigates how electricity demand and supply can be balanced through storage. Electricity networks should work properly at all points in time even when they experience disturbances. Mathematically, this requirement is captured by robust optimization problems with functional uncertain parameters. I have found that, for electricity storage devices, some of these robust and possibly nonconvex optimization problems are equivalent to finite-dimensional deterministic linear programs.

## Employment

- 2017 – 2022 **Doctoral Assistant**, Risk Analytics and Optimization Chair, Ecole polytechnique fédérale de Lausanne.
- 2016 – 2016 **Research Assistant**, Industrial Ecology Program, Norwegian University of Technology and Science.
- 2015 – 2016 **Research Assistant**, Energy Materials Group, Ecole polytechnique fédérale de Lausanne.
- 2008 – 2010 **Cofounder**, Scolaire, Germany: Set up a high school student company to install a 55kWp solar PV system.

## Education

- 2017 – 2022 **Ph.D. Management of Technology**, Ecole polytechnique fédérale de Lausanne  
Thesis title: *Vehicle-to-Grid for Reliable Frequency Regulation*, Advisors: Daniel Kuhn and François Vuille.
- 2013 – 2015 **M.Sc. Energy Management and Sustainability**, Ecole polytechnique fédérale de Lausanne  
Thesis title: *Optimization of Residential Energy Systems*, Advisors: Jan Van Herle and Daniel Kuhn.  
Minor in Area and Cultural Studies, Thesis title: *The Environmental Impact of Offshoring in China*.
- 2010 – 2013 **B.Sc. Electrical and Electronics Engineering**, Ecole polytechnique fédérale de Lausanne  
Thesis title: *Transmission Expansion beyond the La Grande Complex*, Advisor: François Bouffard.  
Exchange year at McGill University, Canada.

## Selected Publications and Preprints

- 1 **Lauinger, D.**, Vuille, F., & Kuhn, D. (2022). Reliable frequency regulation through vehicle-to-grid: Encoding legislation with robust constraints. *arXiv:2005.06042v3[math.OC]*.
- 2 **Lauinger, D.**, Billy, R. G., Vásquez, F., & Müller, D. B. (2021). A general framework for stock dynamics of populations and built and natural environments. *Journal of Industrial Ecology*, 25(5), 1136–1146.
- 3 **Lauinger, D.**, Vuille, F., & Kuhn, D. (2017). A review of the state of research on vehicle-to-grid (V2G): Progress and barriers to deployment. In *European Battery, Hybrid and Fuel Cell Electric Vehicle Congress*, Geneva.
- 4 **Lauinger, D.**, Caliandro, P., Van herle, J., & Kuhn, D. (2016). A linear programming approach to the optimization of residential energy systems. *Journal of Energy Storage*, 7, 24–37.




## Teaching Experience

- Convex Optimization    Design of course materials from linear programs to semidefinite programs and conjugate duality; Applications in machine learning, statistics, energy, and optimization under uncertainty.
- Optimal Decision Making    Preparation of course materials on (mixed-integer) linear programs and the Simplex algorithm.

## Awards

Incubator award from “The Ark”, Prize for having the highest GPA in my Master’s cohort, EPFL Excellence Scholarship

## Side Projects

- Swiss National Park    Organized a visit to the Swiss National Park for the Swiss Study Foundation.  
 <https://go.epfl.ch/wildnis-schaffen>
- My Thesis in 180s    Presented my doctoral research to a general audience in under 3 minutes.  
 [https://go.epfl.ch/mt180s\\_dirk\\_lauinger](https://go.epfl.ch/mt180s_dirk_lauinger)
- Swiss Train Challenge    Solved an optimization problem to visit all Swiss Cantons as fast as possible using only public transport.  
 <https://go.epfl.ch/swiss-train-challenge>